



Durham E-Theses

The development of muscle spindles in the rat

Milburn, Alice

How to cite:

Milburn, Alice (1973) *The development of muscle spindles in the rat*, Durham theses, Durham University. Available at Durham E-Theses Online: <http://etheses.dur.ac.uk/8583/>

Use policy

The full-text may be used and/or reproduced, and given to third parties in any format or medium, without prior permission or charge, for personal research or study, educational, or not-for-profit purposes provided that:

- a full bibliographic reference is made to the original source
- a [link](#) is made to the metadata record in Durham E-Theses
- the full-text is not changed in any way

The full-text must not be sold in any format or medium without the formal permission of the copyright holders.

Please consult the [full Durham E-Theses policy](#) for further details.

THE DEVELOPMENT OF MUSCLE SPINDLES

IN THE RAT.

VOL. II. PLATES.

A thesis presented in candidature for the

degree of

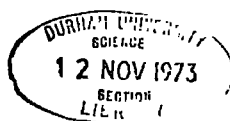
Doctor of Philosophy

by

Alice Milburn, B.Sc. (Dunelm),

Department of Zoology, University of Durham.

Durham, September 1973



ABBREVIATIONS ON PLATES

DF	days foetal
DPN	days postnatal
EDL	extensor digitorum longus
Ef	extrafusal
FDL	flexor digitorum longus
FHL	flexor hallucis longus
Fib	fibula
F1	first formed nuclear-bag fibre
F2	second formed nuclear-bag fibre
F3	first formed nuclear-chain fibre
F4	second formed nuclear-chain fibre
F5	third formed nuclear-chain fibre
F6	fourth formed nuclear-chain fibre
Go	Golgi complex
H	H zone
Iff	intrafusal muscle fibre
IO	interosseous
M	M line
Mb	myoblast
Mf	muscle fibre
Mt	myotube
Mt'	motor terminal
Mt1	primary generation extrafusal myotube
Mt2	secondary generation extrafusal myotube
PL	peroneus longus
St	sensory terminal
Tib	tibia
TP	tibialis posterior
Z	Z band

a nerve axon
bc blood capillary
bm basement membrane
c collagen fibrils
cc capsule cell
cg cytoplasmic granule
cj close junction
cl cilium
cn centriole
csc capsular sheet cell
cv coated vesicle
dcv dense-cored vesicle
e elastic fibrils
ec endomysial cell
fb fibroblast
g glycogen granules
ger granular endoplasmic reticulum
ib intermediate bag fibre
icc inner capsule cell
li lipid droplet
m mitochondrion
mb myoblast
mf myofibril
mfl myofilament
ms muscle spindle
mt motor terminal

mv micropinocytotic vesicle
mvb multivesicular body
n nucleus
nb nuclear-bag fibre
nc nuclear-chain fibre
occ outer capsule cell
p pseudopodial extension
pas periaxial space
pc Pacinian corpuscle
pjf postjunctional folds
pv pinocytotic vacuoles
rbc red blood corpuscle
sc Schwann cell
sg sarcoplasmic granule
snt spindle nerve trunk
sp sole-plate
spn sole-plate nucleus
sr tubule of sarcoplasmic reticulum
sst secondary sensory terminal
st sensory terminal
sv smooth vesicle
t triad
tb typical bag fibre
tmt trail motor terminal
tt transverse tubule
vc vacuolated cell

FIGURE 1. Schematic diagrams illustrating the main ultra-structural features of muscle cells, as used in this study.

- A. Myoblast. Note the abundance of free ribosomes and paucity of other cell organelles.
- B. Fibroblast. Note its elongate shape and the abundance of granular endoplasmic reticulum (ger) cisternae.
- C. Myotube. Note the presence of myofibrils in the peripheral sarcoplasm, the central nuclei and sarcoplasm, the appearance of basement membrane and the immaturity of the sarcotubular system.
- D. Muscle fibre. Myonuclei are peripheral in position. Myofibrils occupy both peripheral and central regions of the fibre.
- E. Satellite cell. Note its distinctive location, beneath the basement membrane of the "parent" muscle fibre.



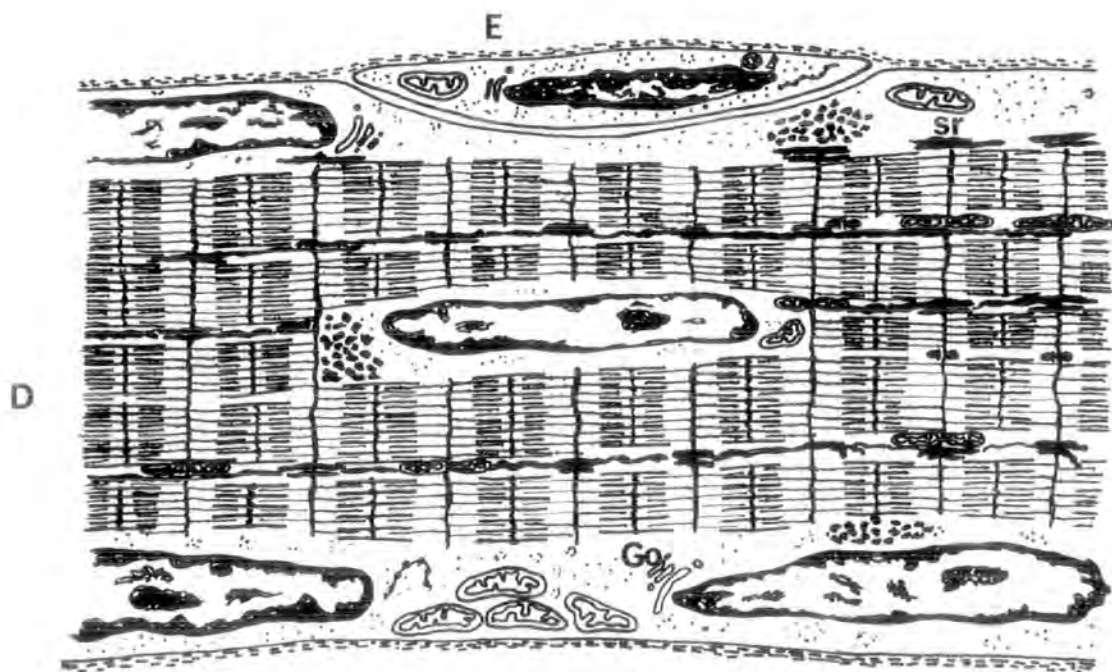
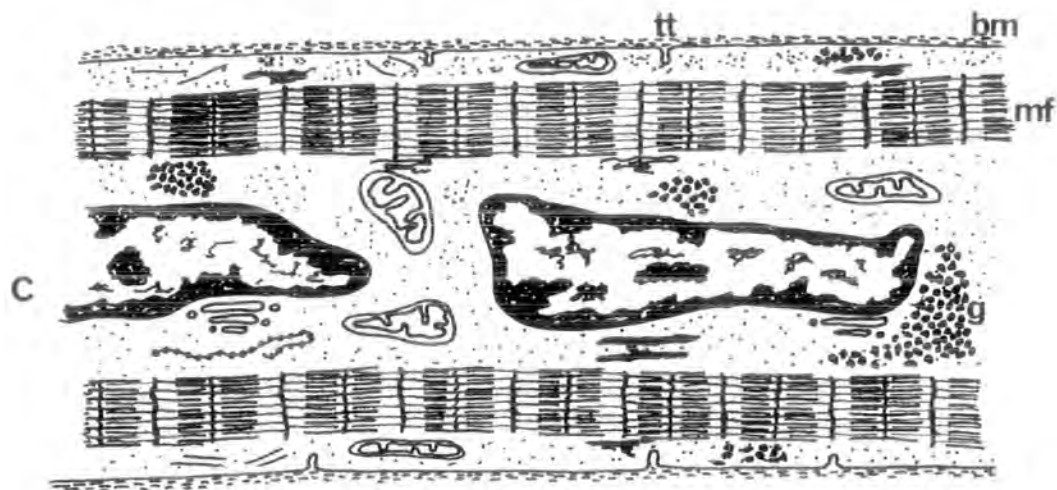
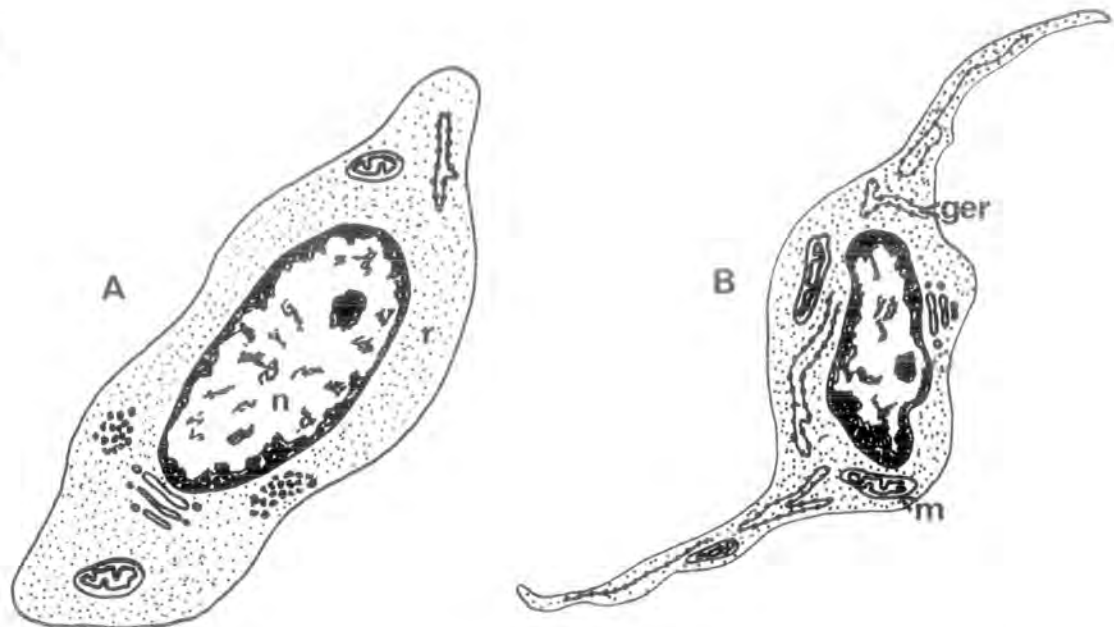


FIGURE 2. Drawing of the innervation of FHL muscle of adult rat, from osmium teasing and silver impregnation. Left limb, medial aspect.

Tibialis posterior and FDL muscles have been removed. Flexor hallucis longus is cut at its insertion, freed from the interosseous membrane (cross-hatched) and deflected backwards to expose the terminations of the interosseous nerve.

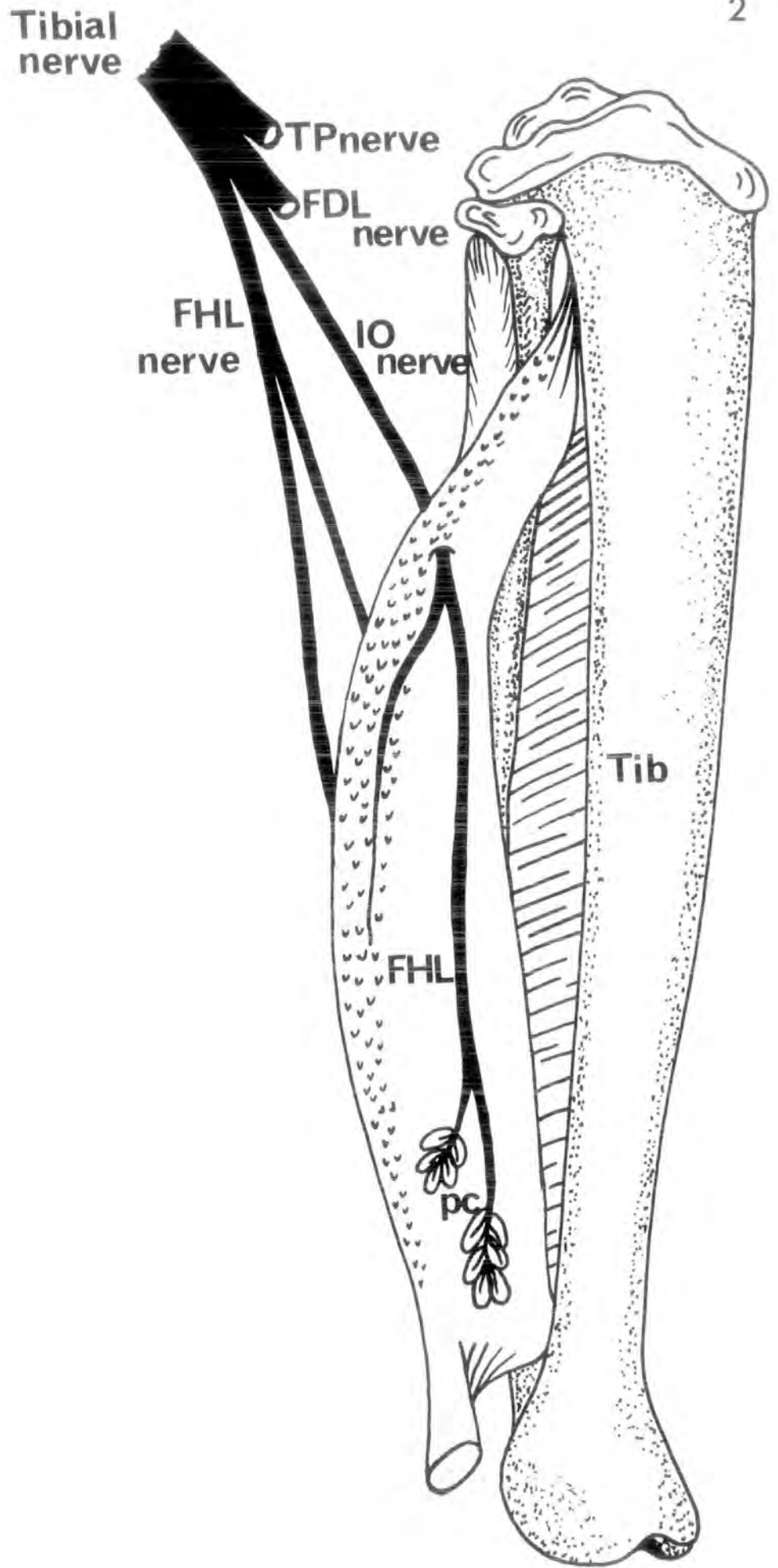


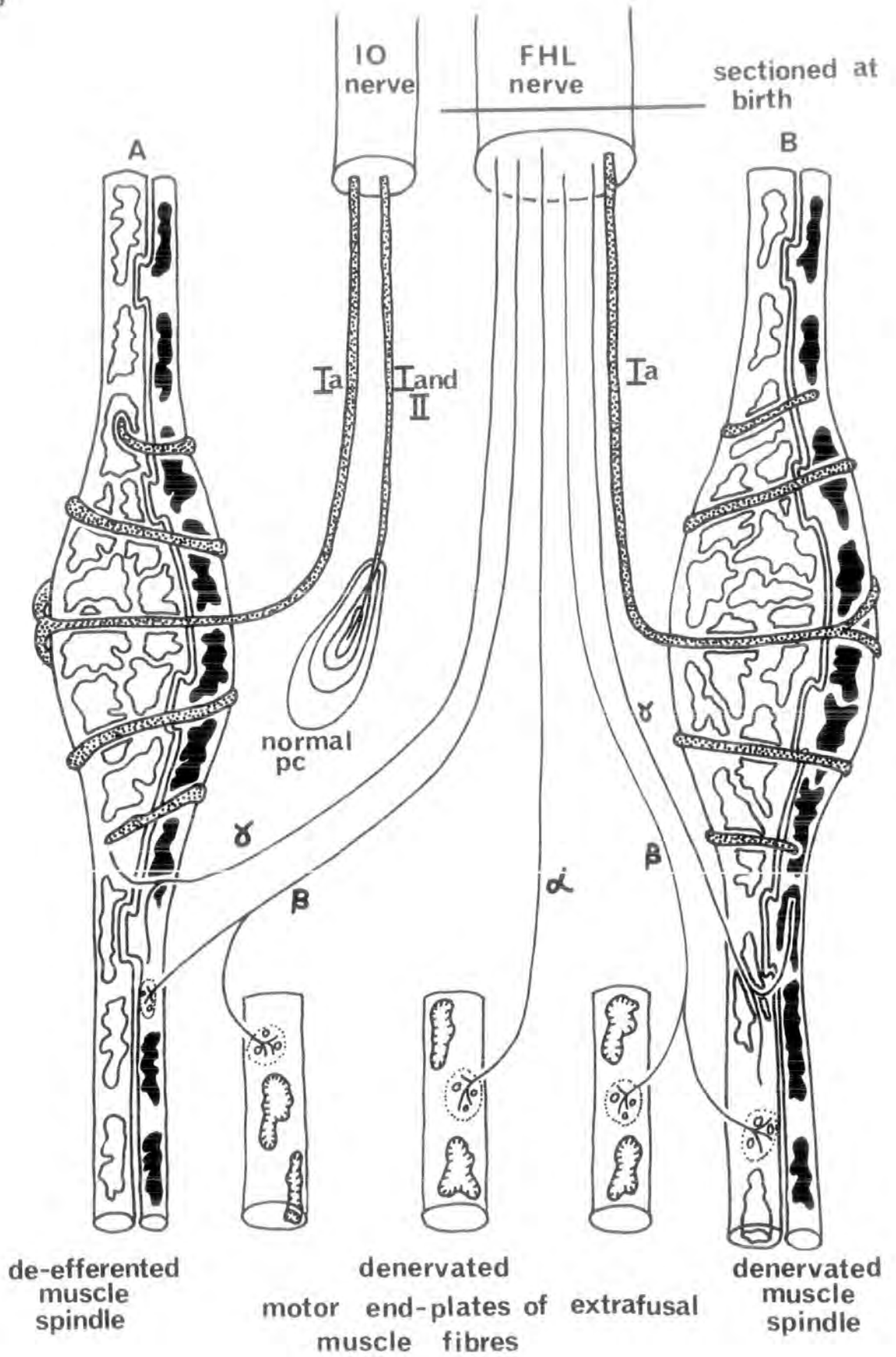
FIGURE 3. Experimental model for the peripheral de-efferentation of FHL muscle in newborn rats.

It is assumed that some spindles (eg. A), as in adult cat (Barker, 1962) receive their sensory nerve component from the interosseous nerve, while their motor innervation is supplied by the FHL nerve. All other spindles (eg. B) receive both their sensory and motor nerve components from the FHL nerve.

Motor terminals on extrafusal muscle fibres are supplied by axons of the FHL nerve.

Sectioning of the FHL nerve at birth should therefore deprive spindle A of its motor innervation only (de-efferented spindle), and spindle B of both sensory and motor innervation (denervated spindle). All extrafusal motor end-plates are thus denervated, while Pacinian corpuscles innervated by the interosseous nerve are unaffected.

Nuclei in the large diameter bag fibre are unshaded and those of the smaller bag fibre, black. Sensory axons are stippled. Motor and fusimotor axons are unbroken lines.



de-efferented muscle spindle

denervated motor end-plates of extrafusal muscle fibres

denervated muscle spindle

FIGURE 4. Transverse sections of lower hindlimb of 18.5 DF rat, illustrating the positions of the main muscles used in this study.

A. Transverse section of whole lower hindlimb.

Note the cartilagenous nature of the limb bones and the absence of hair follicles in the dermis.

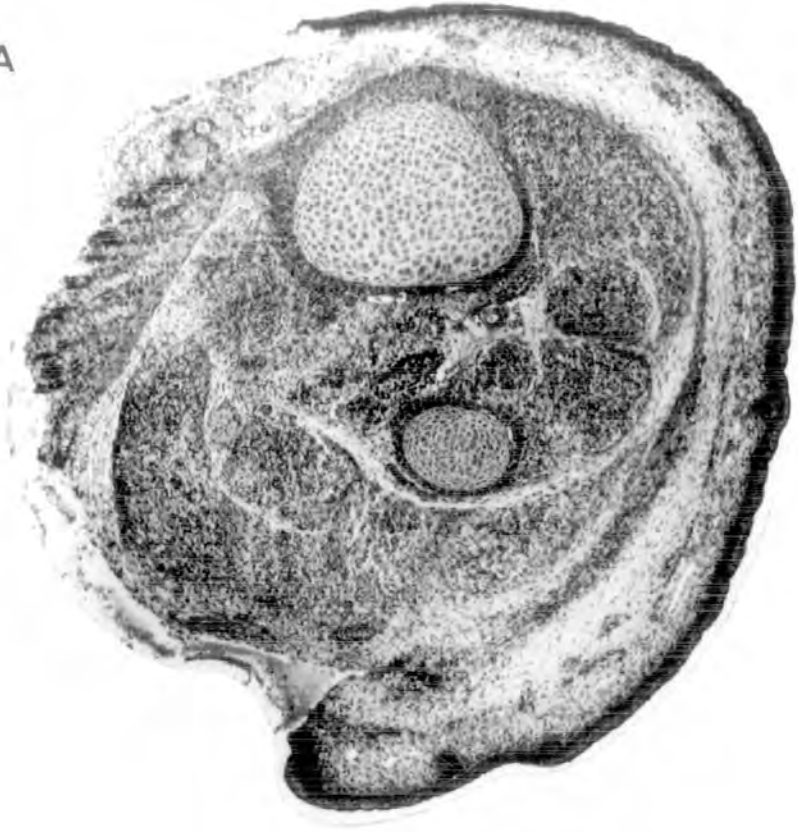
10 μ m thick section. Haemalum & eosin.

x 45

B. Line drawing of (A), illustrating the

position of individual muscles. x 45

4A



0.625mm

4B

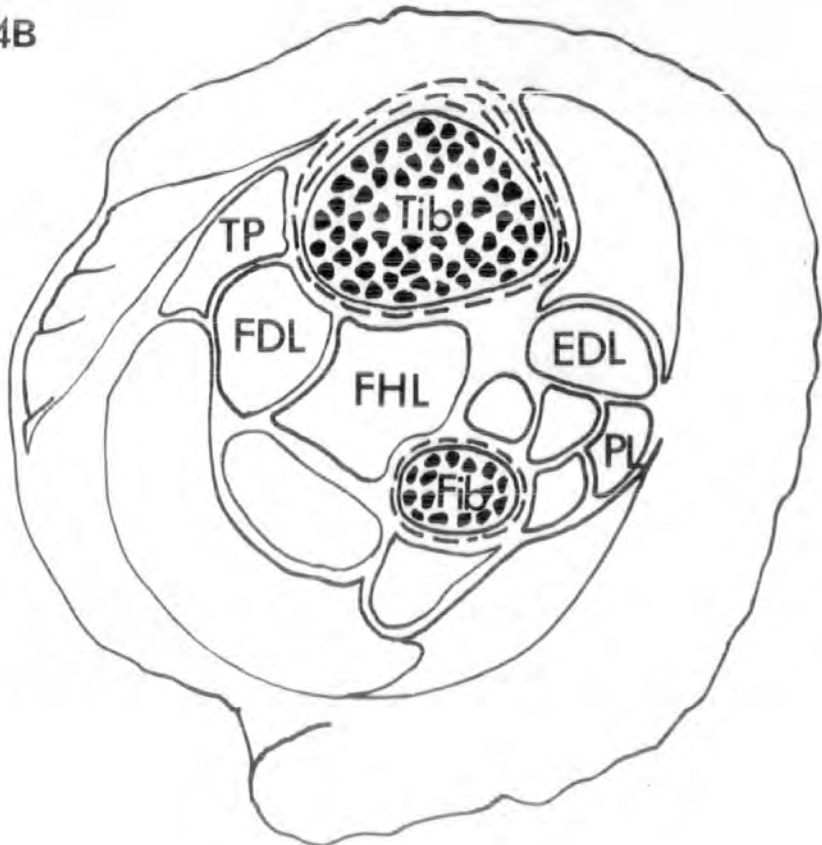
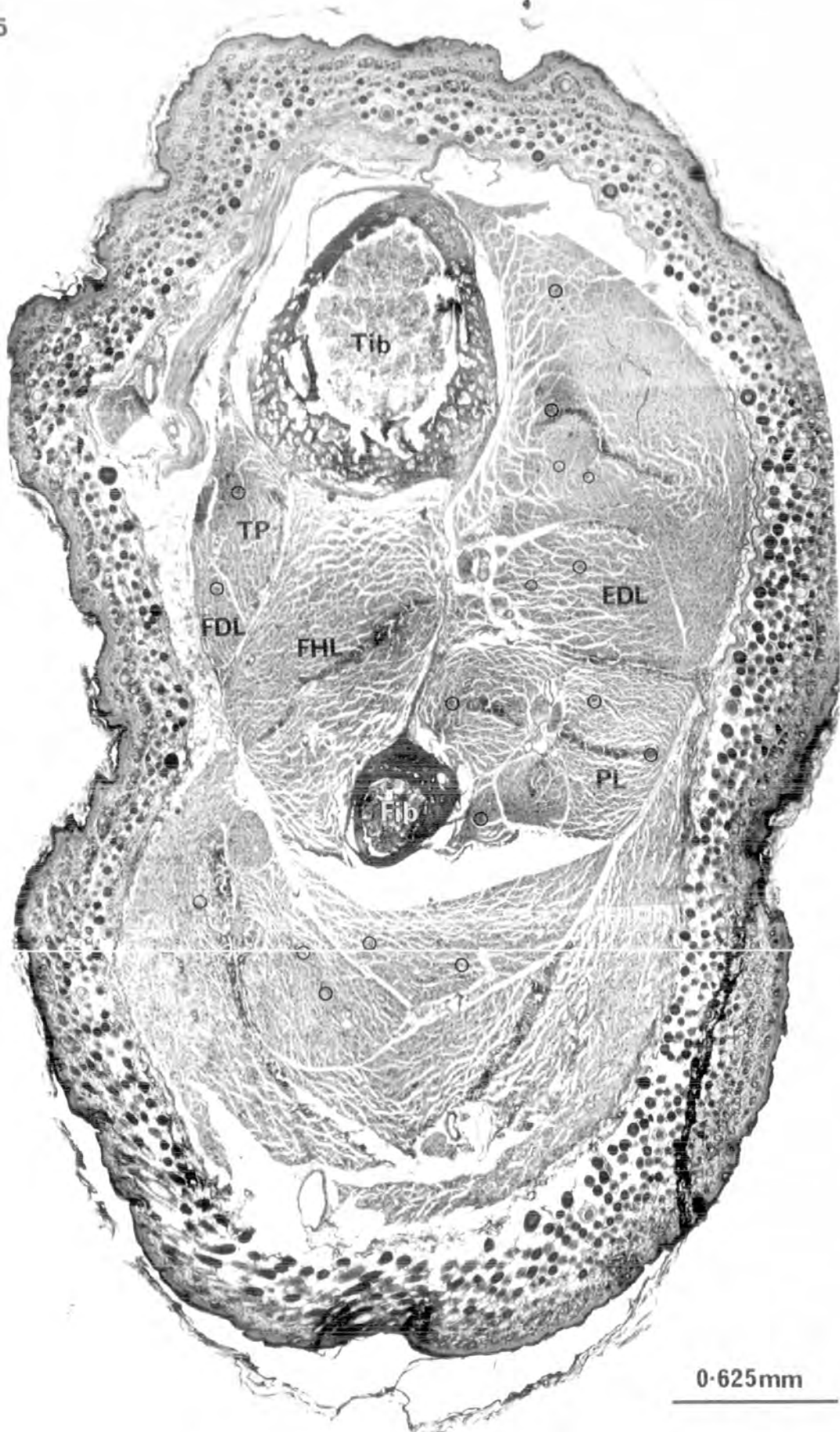


FIGURE 5. Transverse section of lower hindlimb of 12 DPN rat.

Note the ossified tibia and fibula, the fascicular nature of individual muscles, the presence of hair follicles in the dermis and the appearance of muscle spindles, some of which are ringed.

10 μ m thick section. Haemalum & eosin.

x 45



0.625mm

FIGURES 6-11. Transverse sections of lower hindlimb shank muscle of rats at various stages of development, used to locate spindles for electron microscopy.

6. 19.5 DF rat.
7. 20 DF rat.
8. newborn rat.
9. 4 DPN rat.
10. 12 DPN rat.
11. Peroneus longus of adult rat.

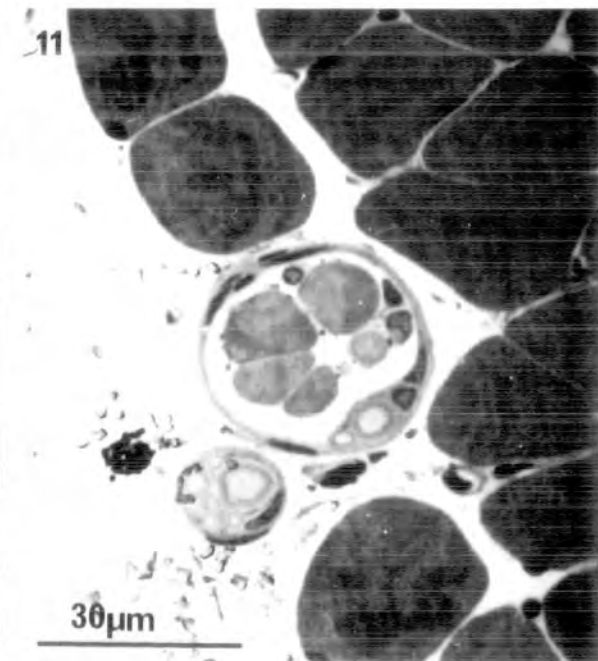
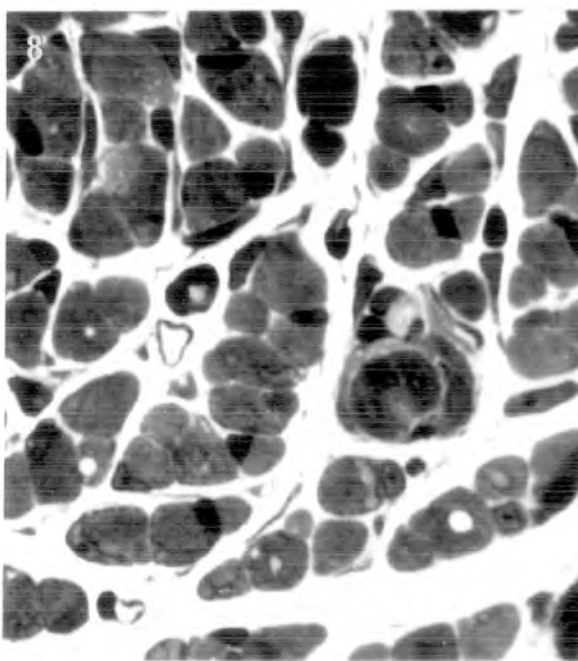
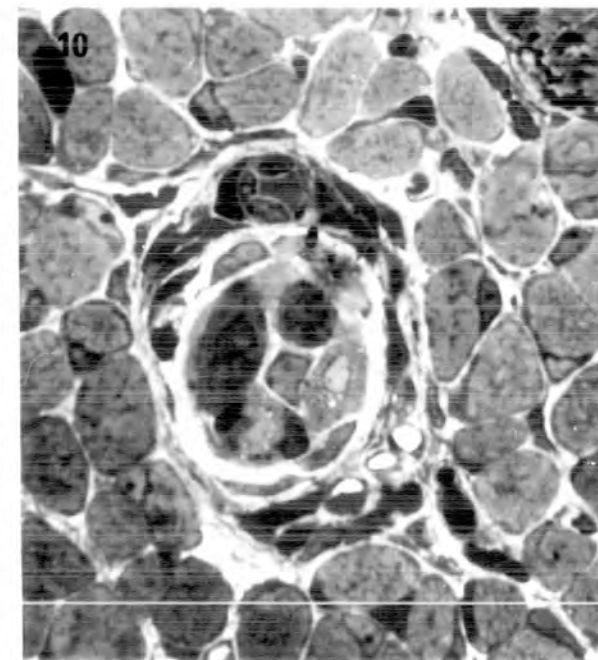
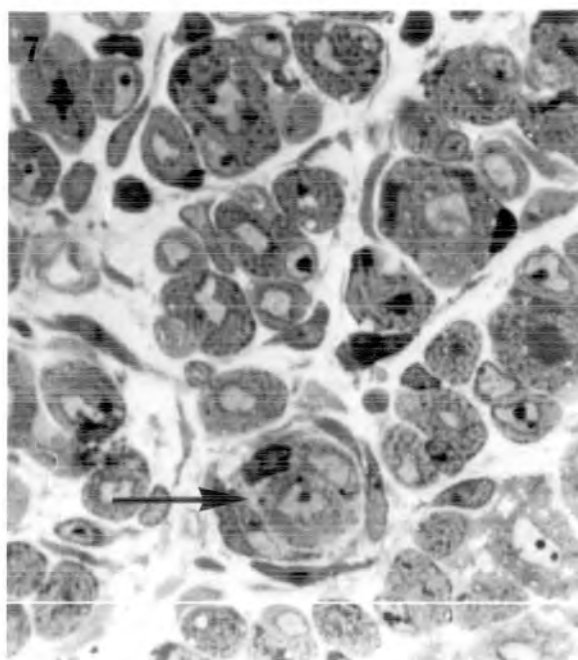
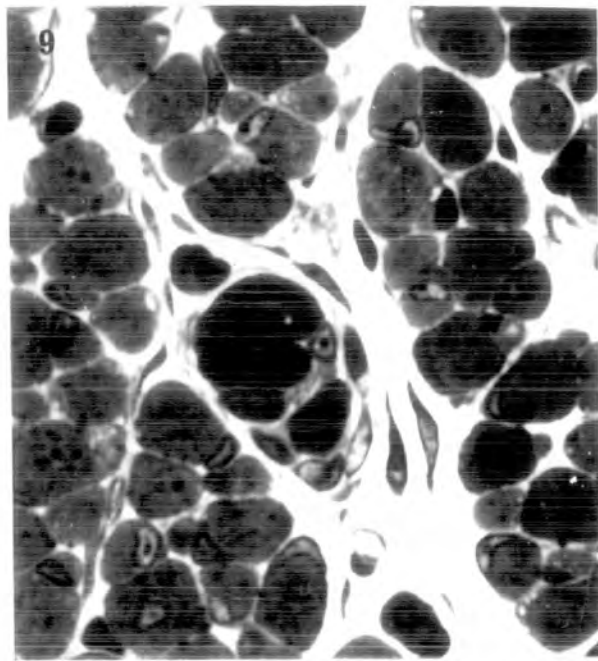
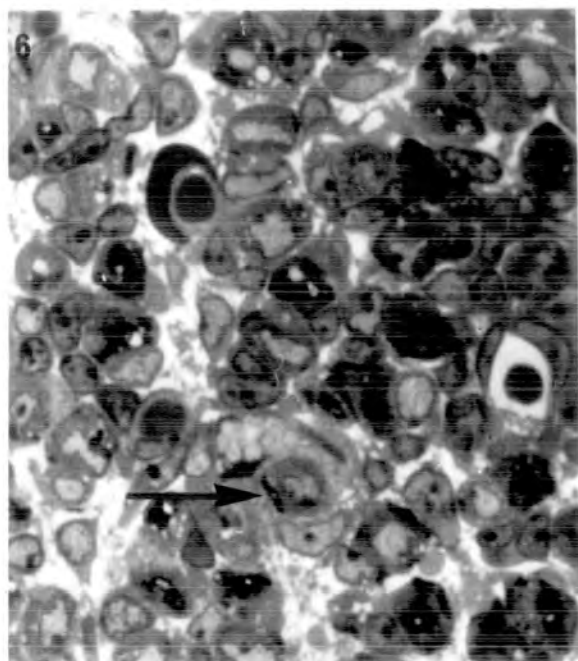
Note the similarity in the size of intrafusal and extrafusal muscle fibres in 6, 7 and 8; the progressive increase in size of extrafusal muscle fibres in the post-natal stages; the development of the spindle capsule and the decrease in the number of myotubes with increasing maturity.

Arrows point to muscle spindles in foetal muscle.

Scale on fig. 11 refers to all figures.

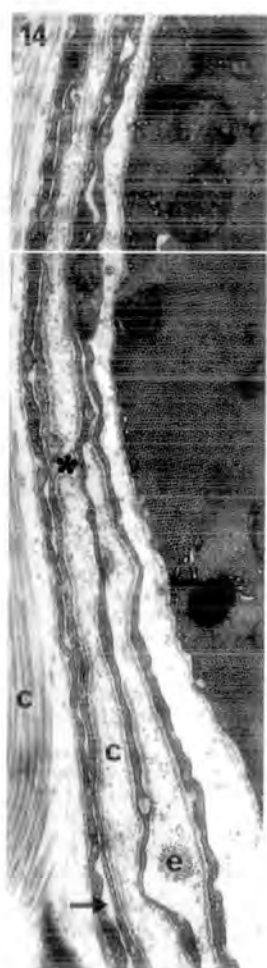
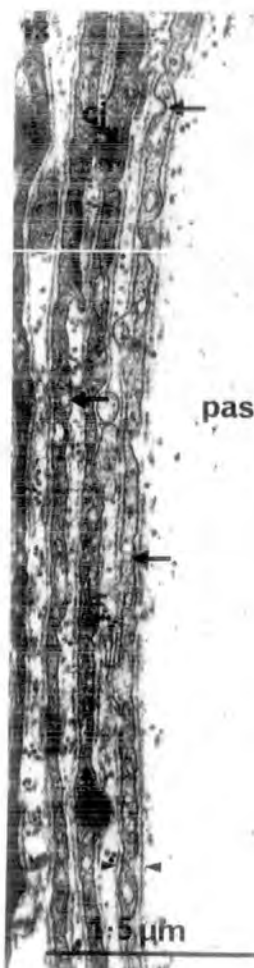
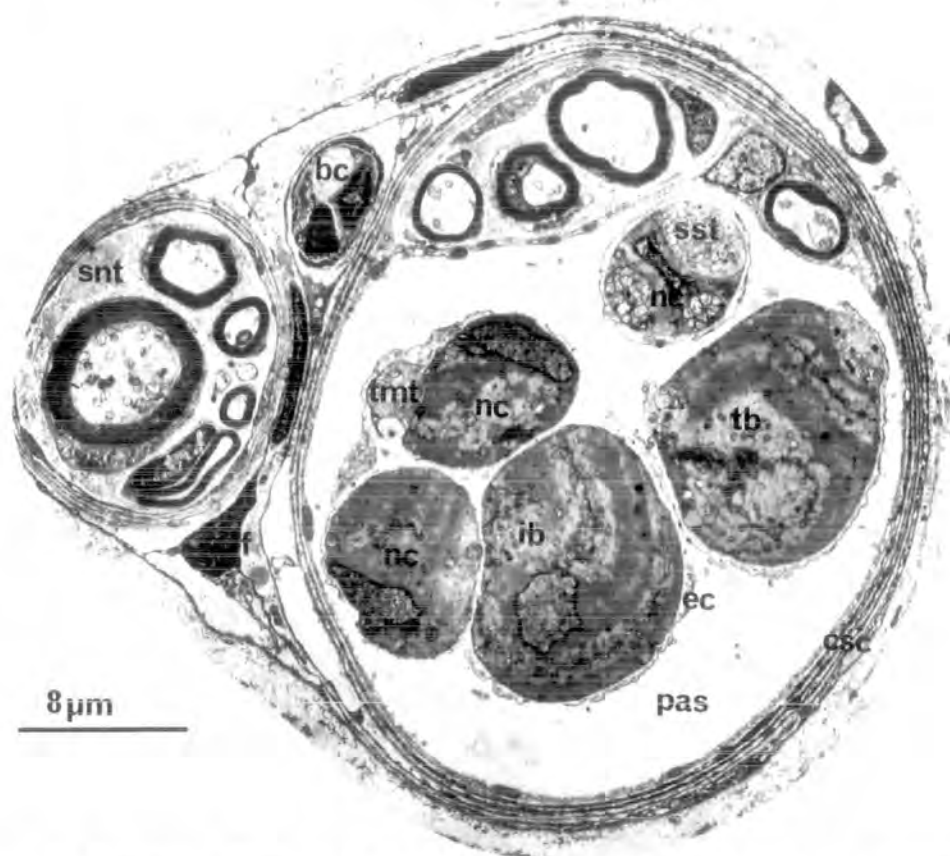
c.1 μ m thick section. Toudine blue.

x 900



FIGURES 12-16. The fine structure of muscle spindles in PL of adult rat; details of the capsule.

12. Transverse section through the juxta-equatorial region of a spindle.
x 3,000
13. Transverse section of capsular sheet cells. Small arrowheads point to basement membrane that borders both sides of each cell. Arrows point to micropinocytotic vesicles. x 20,000
14. Transverse section of capsular sheet cells to illustrate their pairing to form channels (arrow). Asterisk marks associated cells of neighbouring layers. Scale as in fig. 13.
x 20,000
15. Transverse section of an endomysial cell of the axial sheath. Note the electron density of the cytoplasm, the absence of basement membrane and lateral overlap with a neighbouring cell (asterisk). Scale as in fig. 13.
x 20,000
16. Transverse section of convoluted basement membrane associated with a nuclear-bag fibre. Scale as in fig. 13.
x 20,000

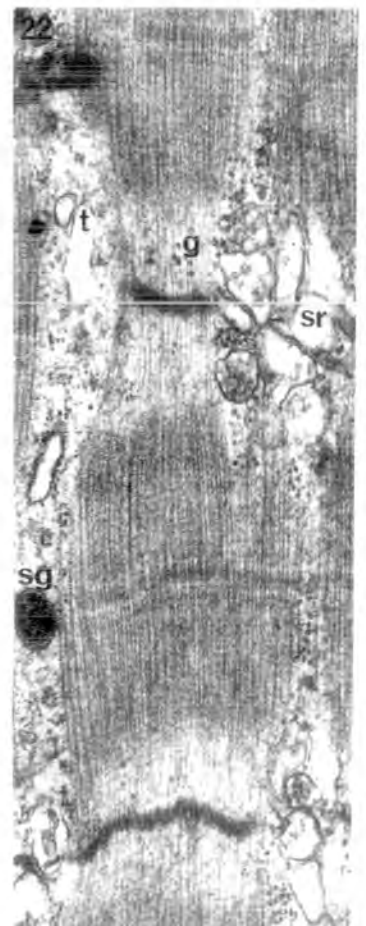
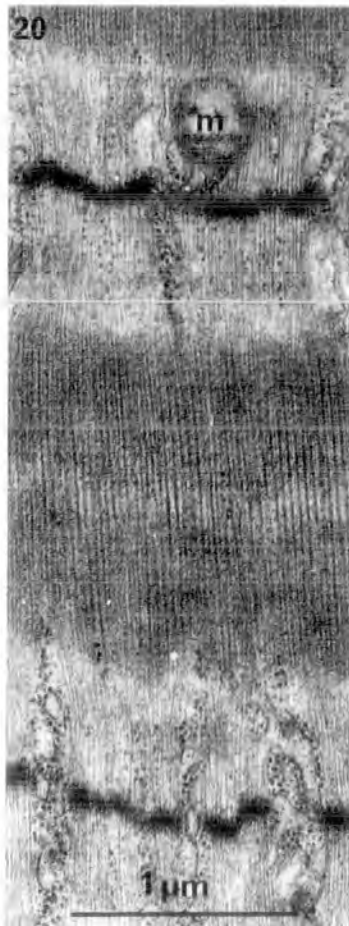
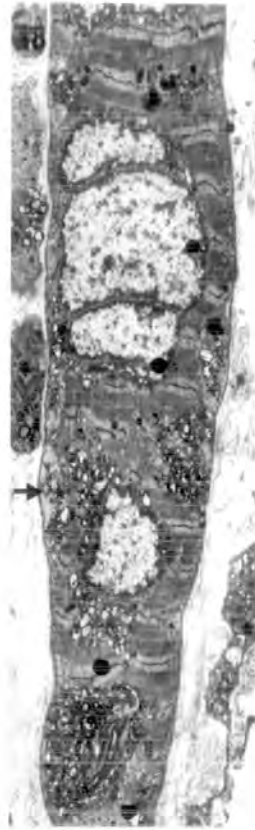
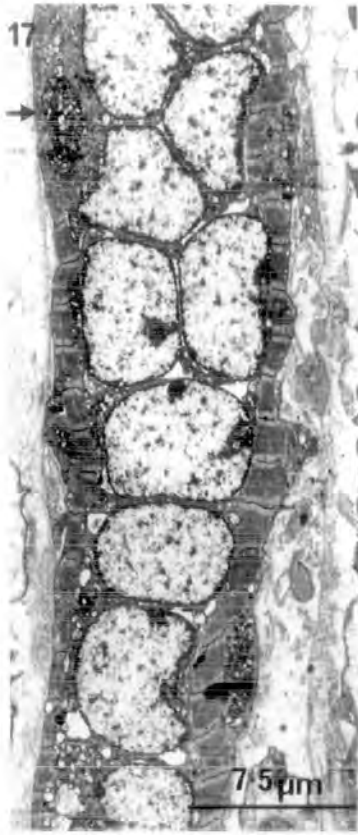


FIGURES 17-22. The fine structure of muscle spindles in PL of adult rat; details of intrafusal muscle fibres.

17. Longitudinal section through the equatorial region of a typical bag fibre. Note the central rounded nuclei of the myotube region and the aggregated nuclei of the nuclear bag. x 3,200
18. Longitudinal section through the myotube region of an intermediate bag fibre. Note the rounded nuclei. Scale as in fig. 17. x 3,200
19. Longitudinal section through the equatorial region of a nuclear-chain fibre. Note the single column of elongate nuclei. Scale as in fig. 17. x 3,200

Arrows in 17, 18 and 19 point to primary sensory terminals.

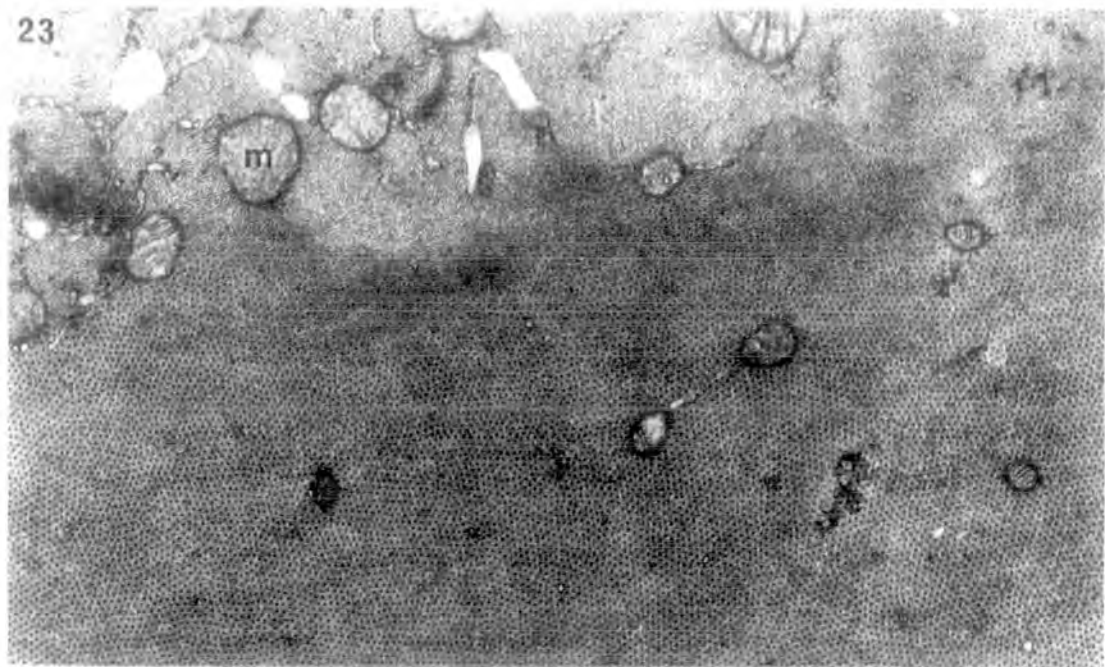
20. Longitudinal section through the polar region of a typical bag fibre. Note the small mitochondria confined to the I-band region; the poorly developed sarcotubular system and the absence of a distinct M line from the H zone. x 32,000
21. Longitudinal section through the polar region of an intermediate bag fibre. Note the well developed sarcotubular system and the central M line. Scale as in fig. 20. x 32,000
22. Longitudinal section through the polar region of a nuclear-chain fibre. Note the abundant interfibrillar sarcoplasm and SR tubules; the distinct M line and glycogen granules associated with the I-band filaments. Scale as in fig. 20. x 32,000



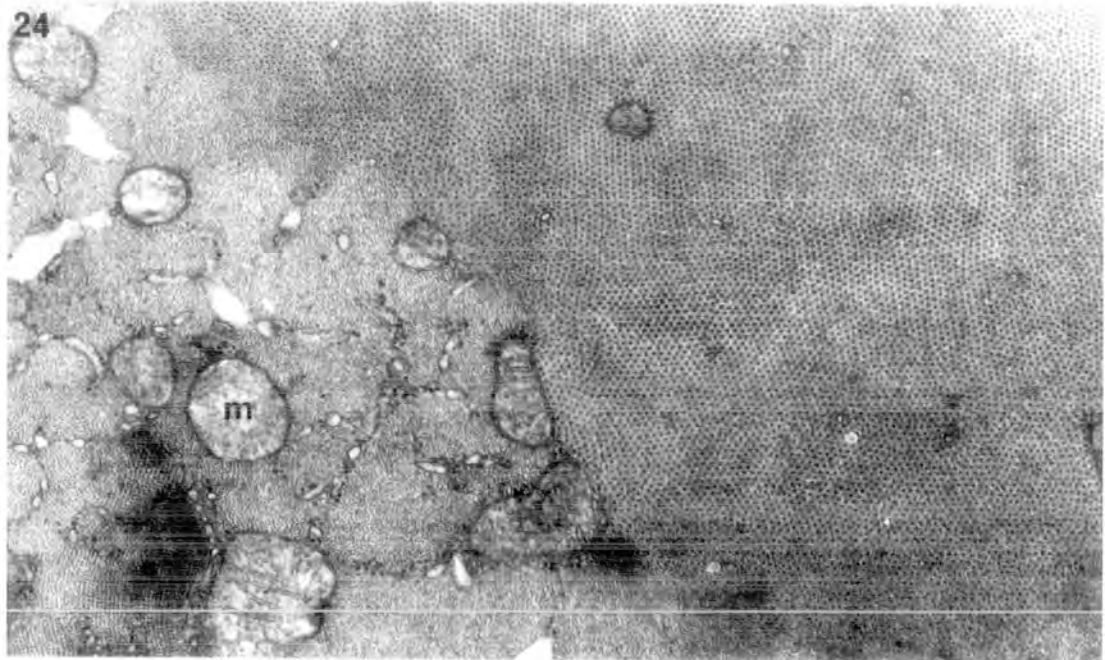
FIGURES 23-25. The fine structure of muscle spindles in PL of adult rat; details of the intrafusal muscle fibres.

23. Transverse section through the polar region of a typical bag fibre. Note the small mitochondria that are largely confined to the I-band region and the paucity of interfibrillar sarcoplasm and SR tubules at all levels of the myofibrils. Scale as in fig. 25. x 32,000
24. Transverse section through the polar region of an intermediate bag fibre. Note the small mitochondria that are largely confined to the I-band region and the absence of interfibrillar sarcoplasm at the A-band level. SR tubules are more abundant in the I-band region compared to the typical bag fibre. Scale as in fig. 25. x 32,000
25. Transverse section through the polar region of a nuclear-chain fibre. Note the numerous large mitochondria present at both the A and I-band levels of the myofibrils and the double layer of SR tubules encircling each myofibril at the I-band region (arrow). Triads are more numerous than in bag fibres. x 32,000

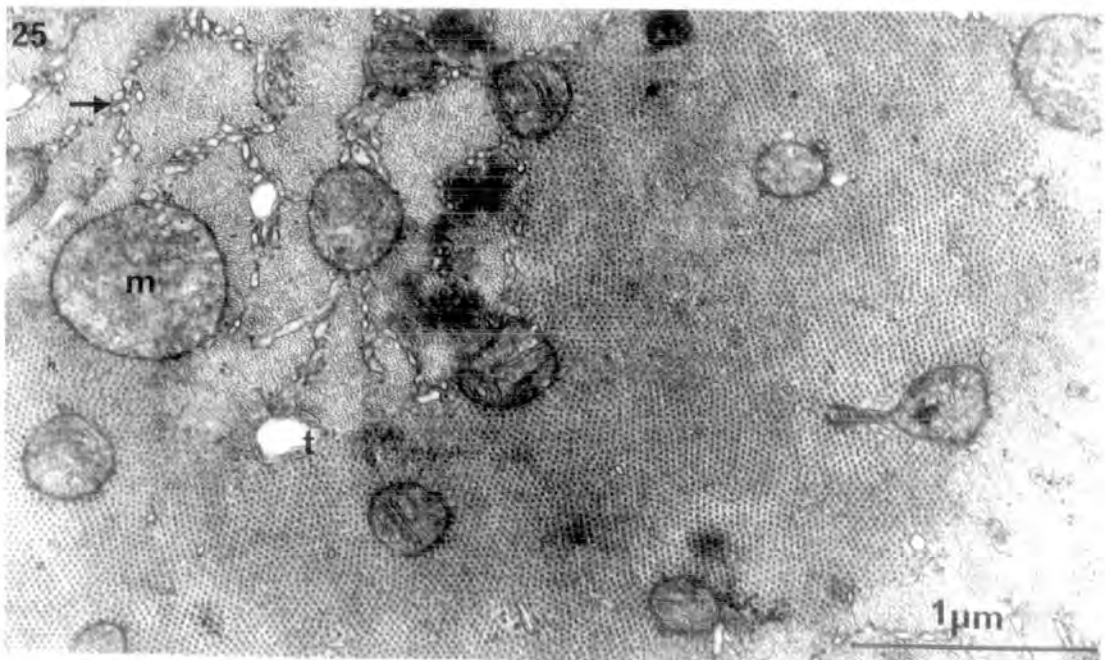
23



24



25

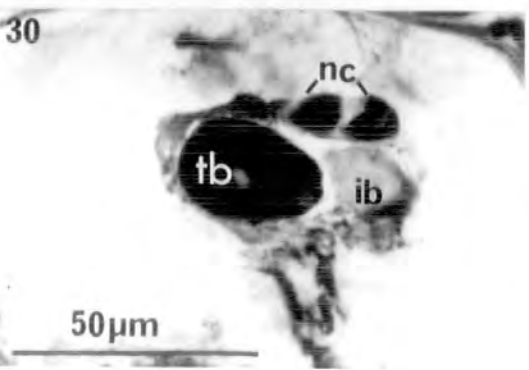
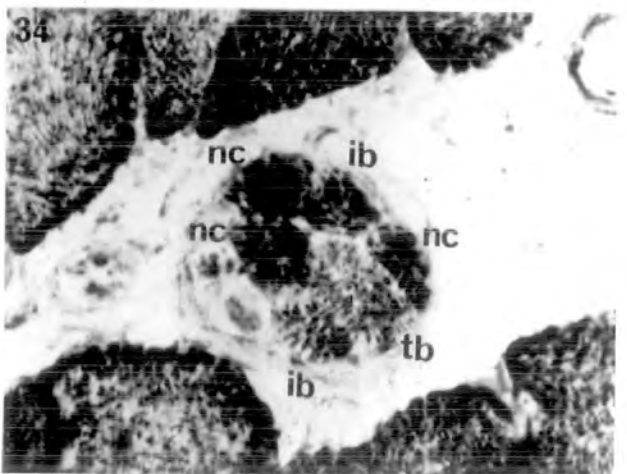
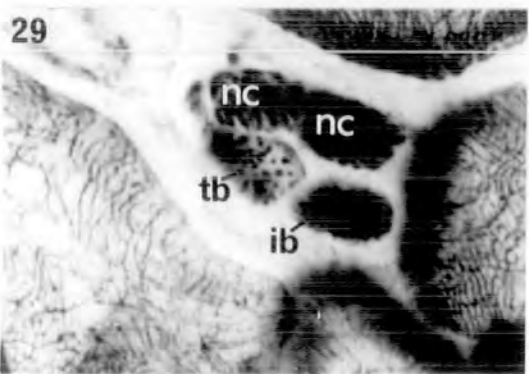
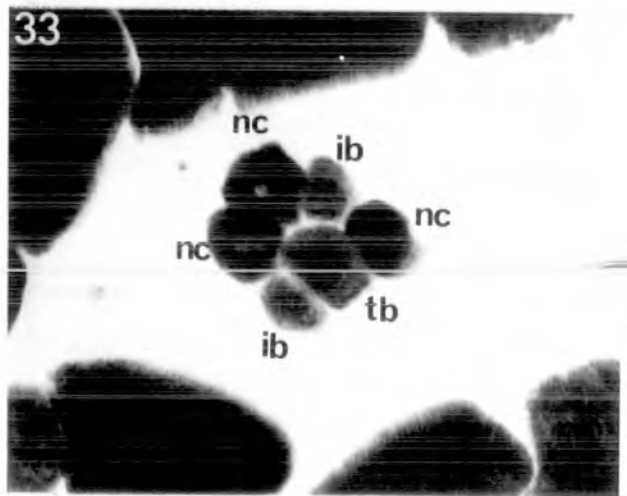
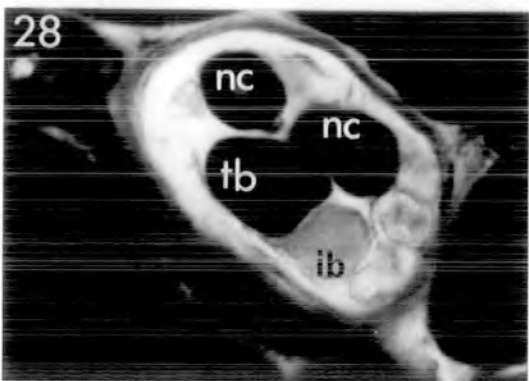
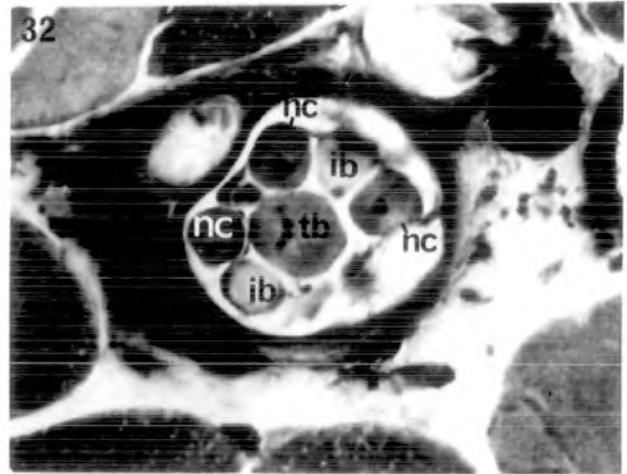
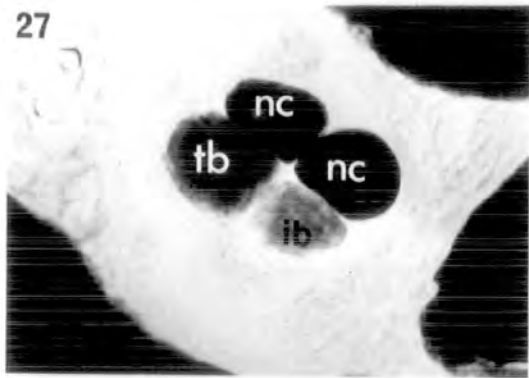
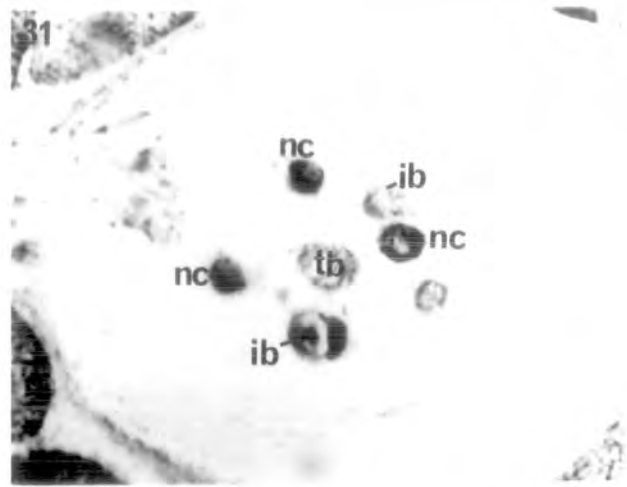
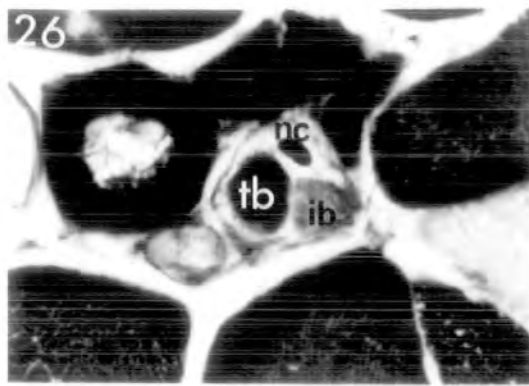


FIGURES 26-34. The histochemistry of intrafusal muscle fibres in PL of adult rat.

26. Transverse section through the polar region of spindle A. Alkali pre-incubated ATPase. Note the single nuclear-chain fibre and the differences in diameter between the muscle fibres.
27. Transverse section through the mid-polar region of spindle A. P'ase. Two nuclear-chain fibres are now present. Note their high activity compared to that of the typical and intermediate bag fibres.
28. Transverse section through the mid-polar region of spindle A. Alkali pre-incubated ATPase.
29. Transverse section through the mid-polar region of spindle A. SDH.
30. Transverse section through the juxta-equatorial region of spindle A. Alkali pre-incubated ATPase.
31. Transverse section through the equatorial region of spindle B. SDH. Three nuclear-bag and three nuclear-chain fibres are present.
32. Transverse section through the mid-polar region of spindle B. Alkali pre-incubated ATPase.
33. Transverse section through the mid-polar region of spindle B. P'ase.
34. Transverse section through the mid-polar region of spindle B. SDH.

Scale in fig. 30 refers to all figures.

x 720

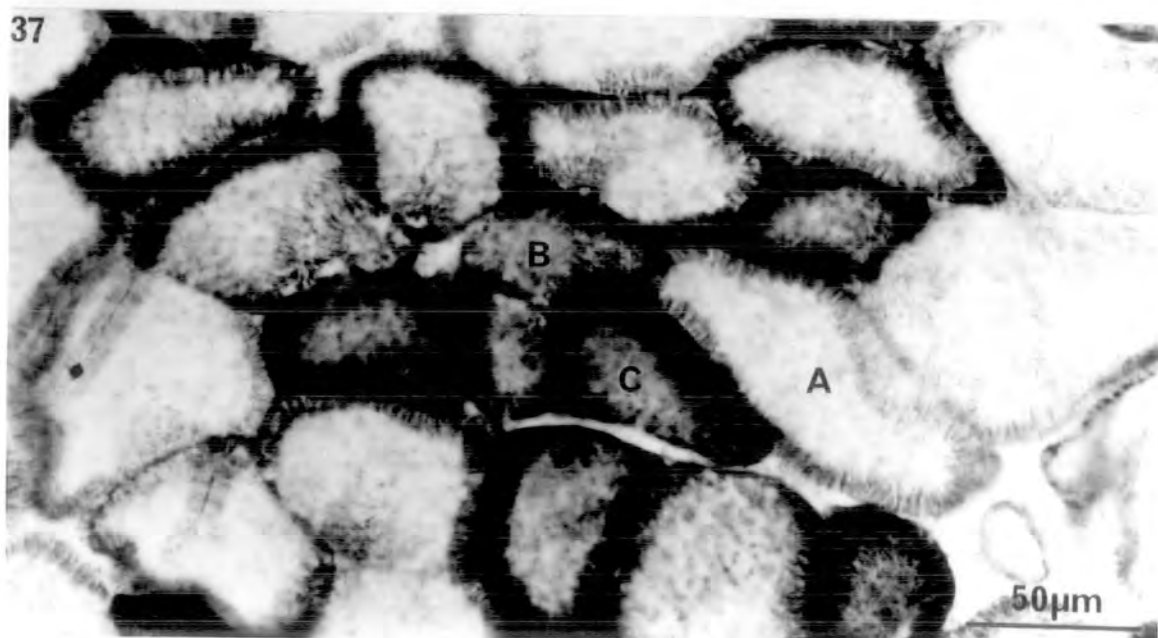
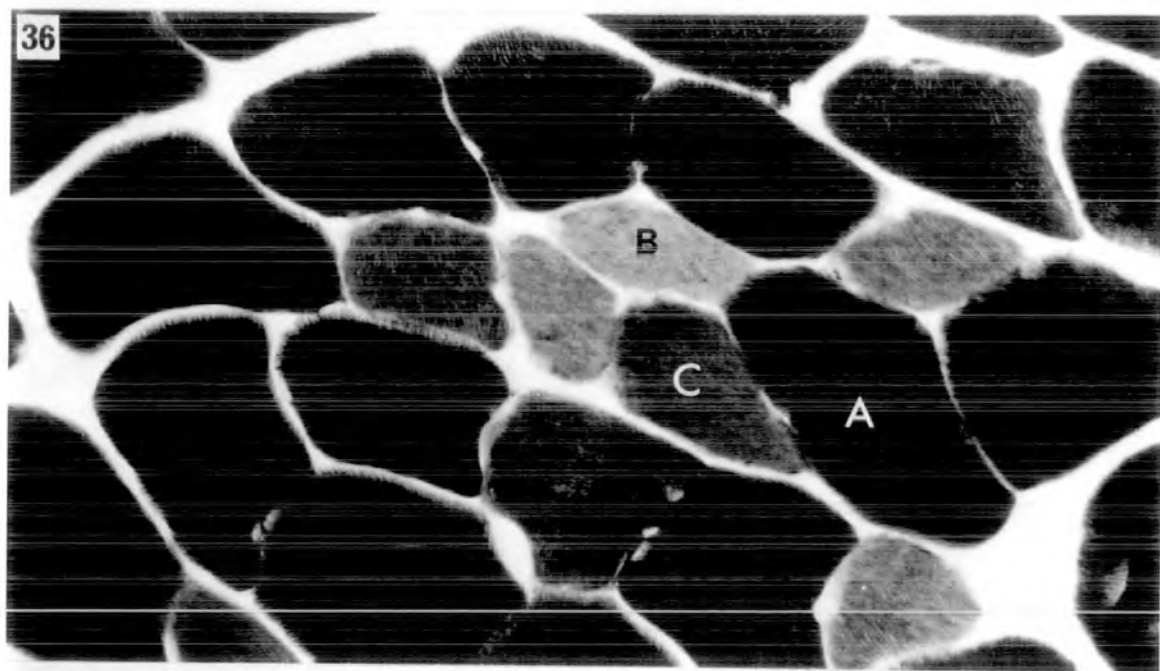
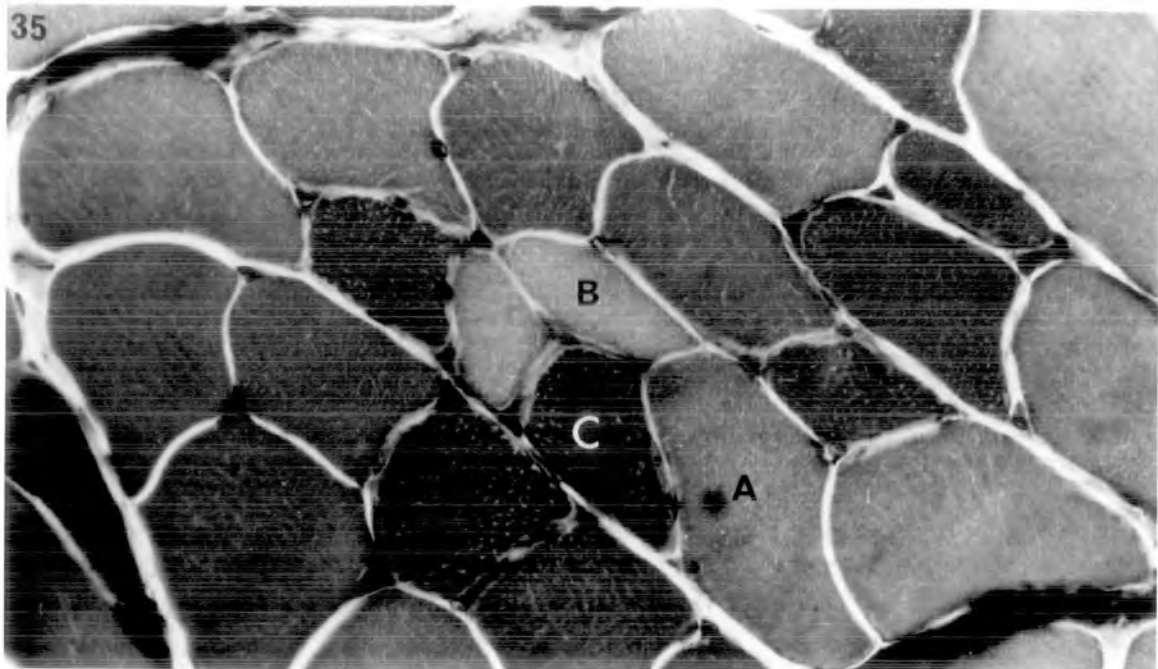


FIGURES 35-37. Serial transverse sections illustrating the histochemistry of extrafusal muscle fibres in EDL of adult rat.

35. Alkali pre-incubated ATPase. Type A fibres exhibit intermediate activity, type B fibres low activity and type C, high activity.
36. P'ase. Type A fibres exhibit high activity, type B fibres low activity and type C, intermediate activity.
37. SDH. Type A fibres exhibit low activity and type B and C fibres high activity. Note particularly the large subsarcolemmal accumulations of diformazan granules in type C fibres.

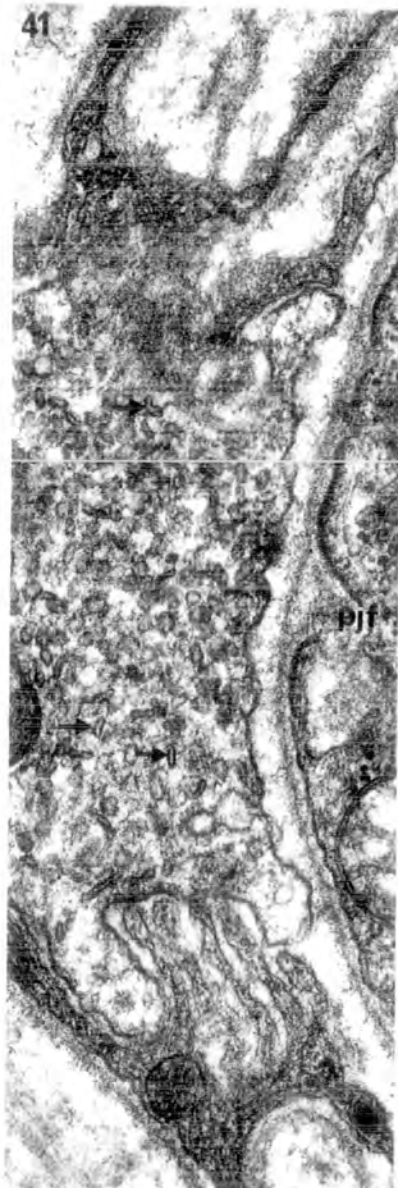
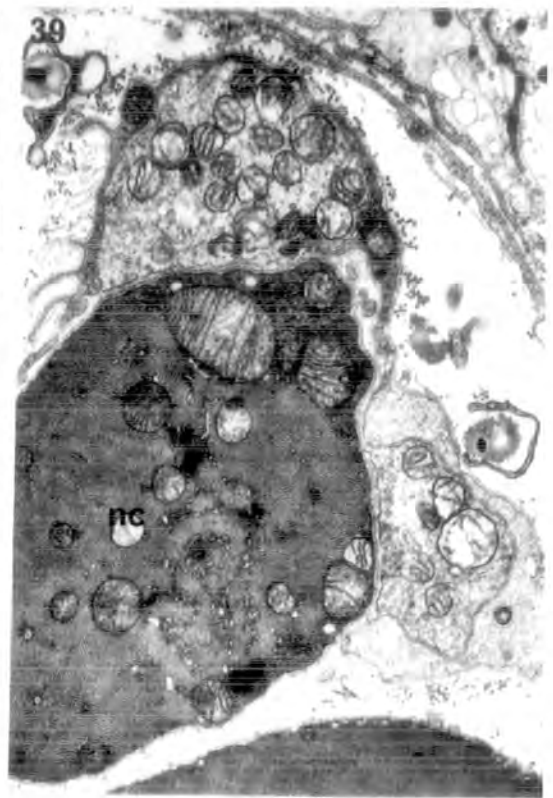
Scale in fig. 37 refers to all figures.

x 450



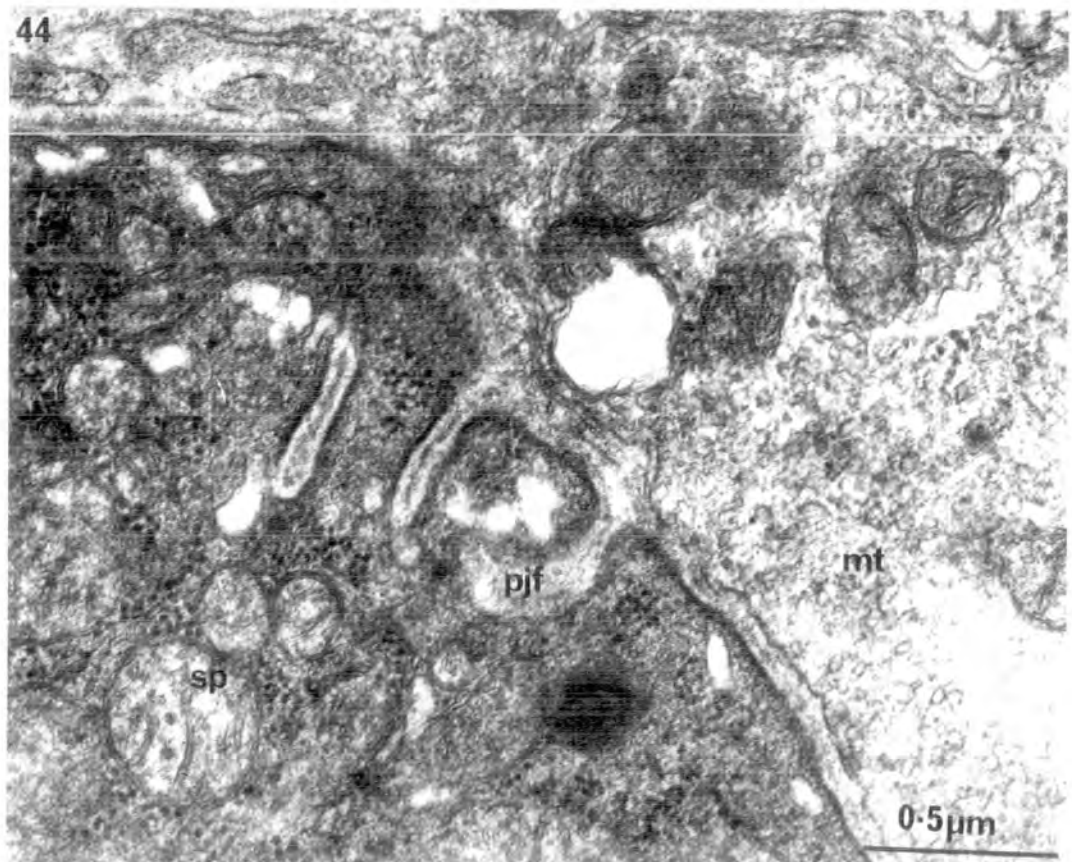
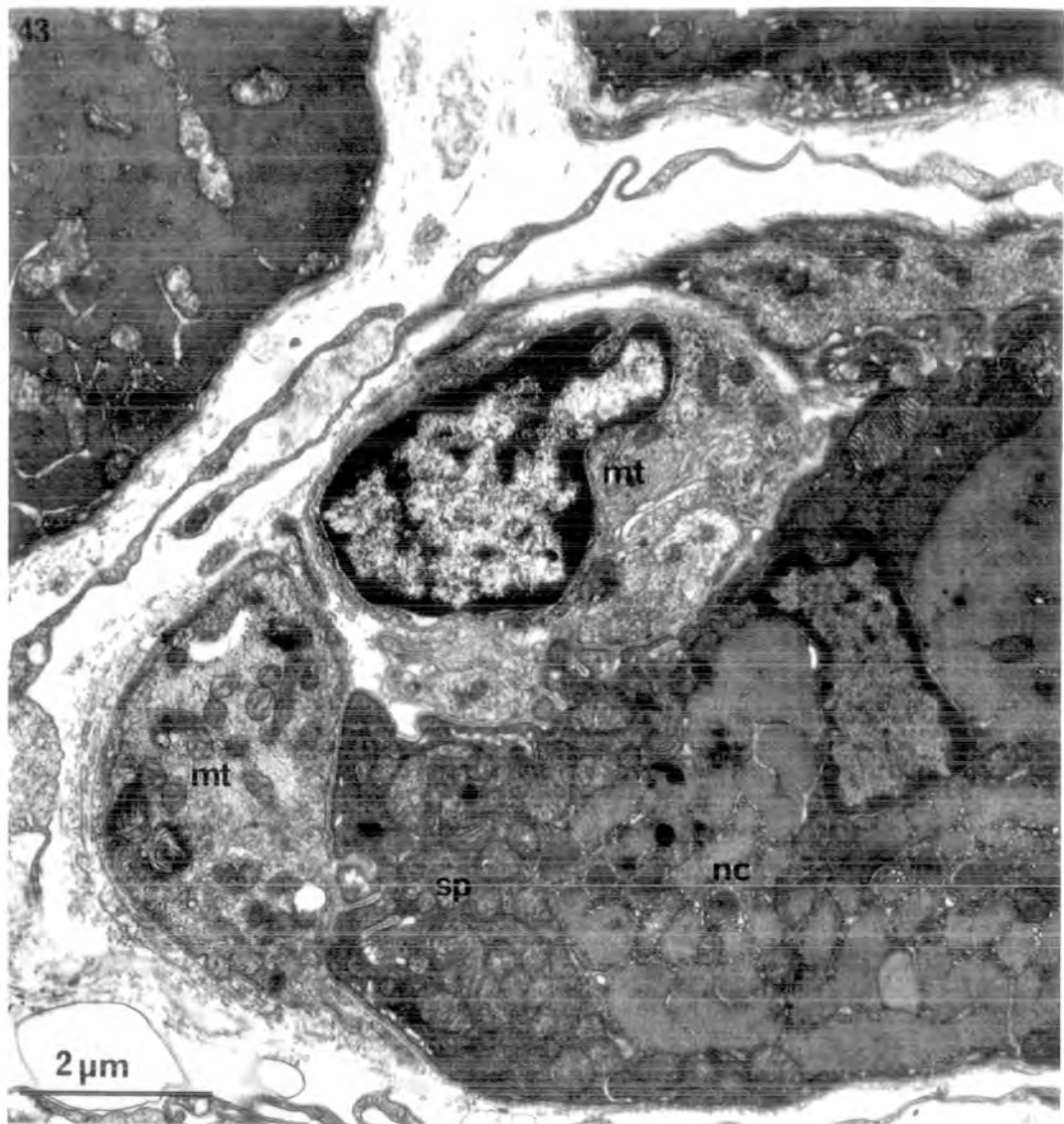
FIGURES 38-42. The fine structure of muscle spindles in PL of adult rat; details of the fusimotor innervation.

38. Transverse section of two trail motor terminals on a typical bag fibre. Note the common Schwann cell covering and the absence of primary synaptic clefts. x 12,600
39. Transverse section of two trail motor terminals on a nuclear-chain fibre. Scale as in fig. 38. x 12,600
40. Higher power electron micrograph of one of the terminals shown in fig. 38. Note the thinly spread sole-plate and the absence of post-junctional folds. x 48,000
41. Transverse section of a trail motor terminal on a nuclear-chain fibre. Note the occasional shallow post-junctional folds and "flattened" synaptic vesicles (arrows). Scale as in fig. 40. x 48,000
42. Higher power electron micrograph of one of the terminals shown in fig. 39. Scale as in fig. 40. x 48,000



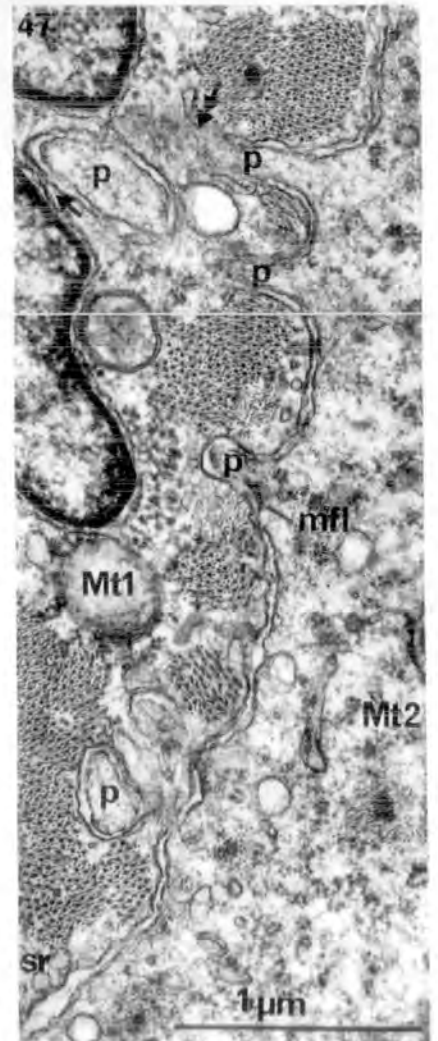
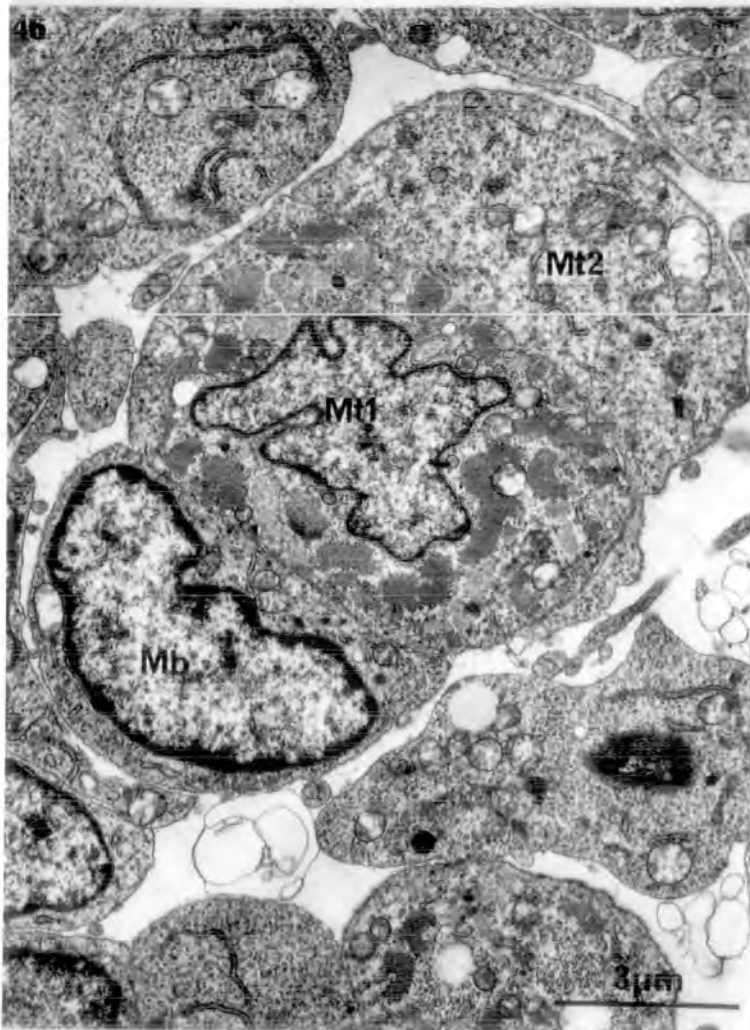
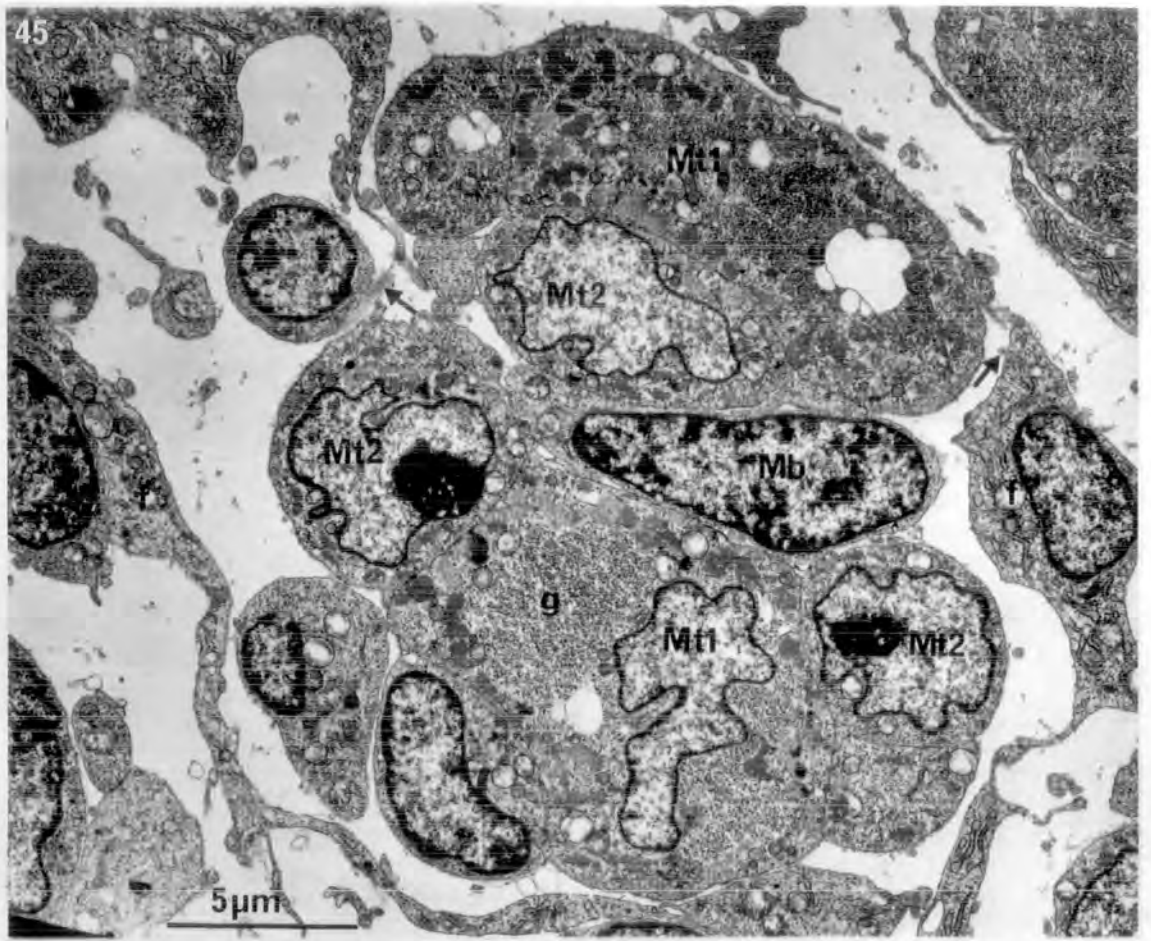
FIGURES 43-44. The fine structure of muscle spindles in PL of adult rat; details of the fusimotor innervation.

43. Transverse section of a polar plate motor terminal on a nuclear-chain fibre. Note the extensive area of myoneural contact and the large sole-plate. x 12,600
44. Higher power electron micrograph of the motor terminal shown in fig. 44. Note the short, unbranched post-junctional folds. x 50,000



FIGURES 45-47. The fine structure of developing muscle cells in 18.5 DF shank muscle of rat.

45. Transverse section of a typical group of muscle cells. Note the large, primary generation myotubes and the smaller, secondary generation myotubes and myoblasts clustered around their walls. The intercellular space is large, with only scanty collagen fibrils (arrows). x 5,000
46. Transverse section of a primary generation myotube and apposing nascent myotube and myoblast. x 8,000
47. Higher power electron micrograph of the apposed surfaces of the parent and nascent myotube shown in fig. 46. Note the paucity of myofibrils in Mt2 compared to Mtl, and the pseudopodial extensions. Single arrow points to the close association of a pseudopodial extension of Mt2 with the nuclear envelope of Mtl. Double arrow points to an area of indistinct membrane separation. x 32,000



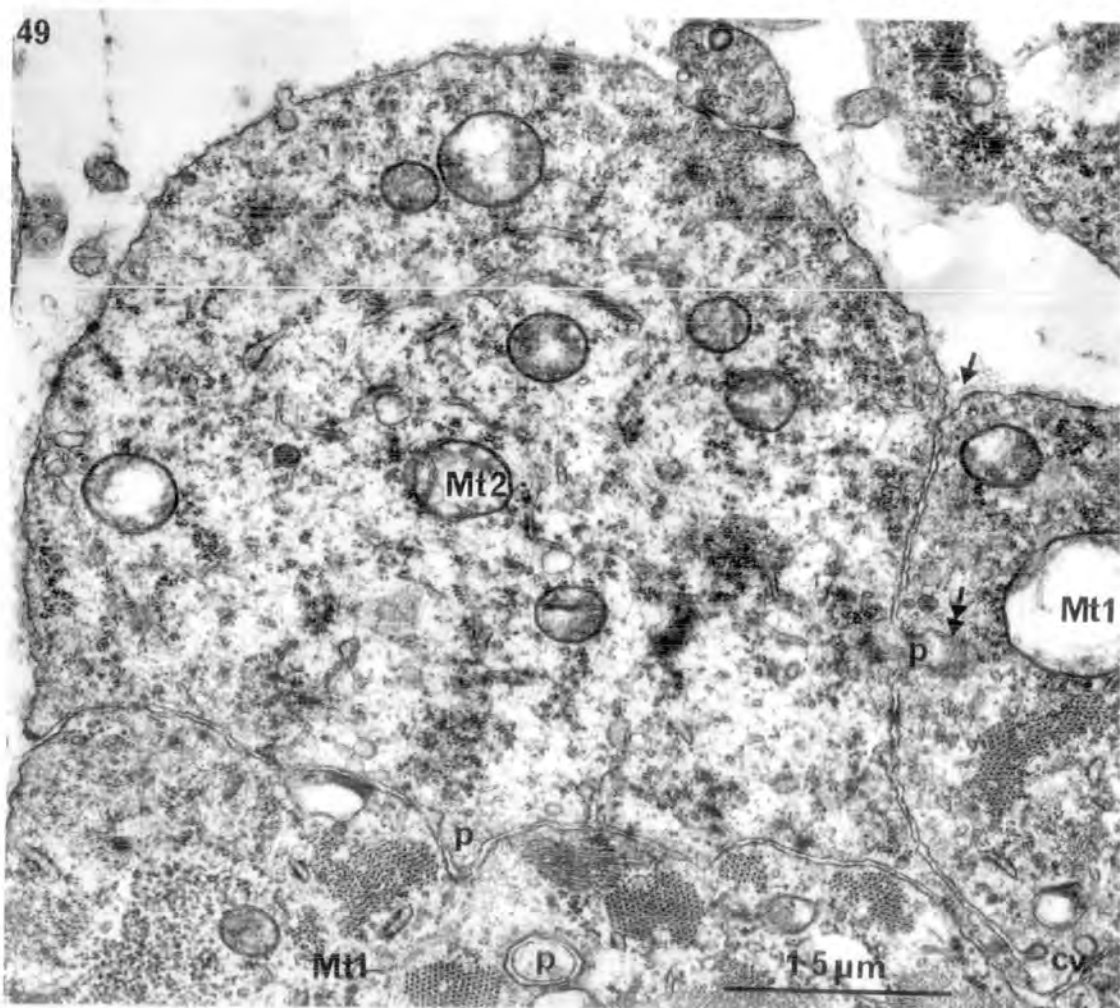
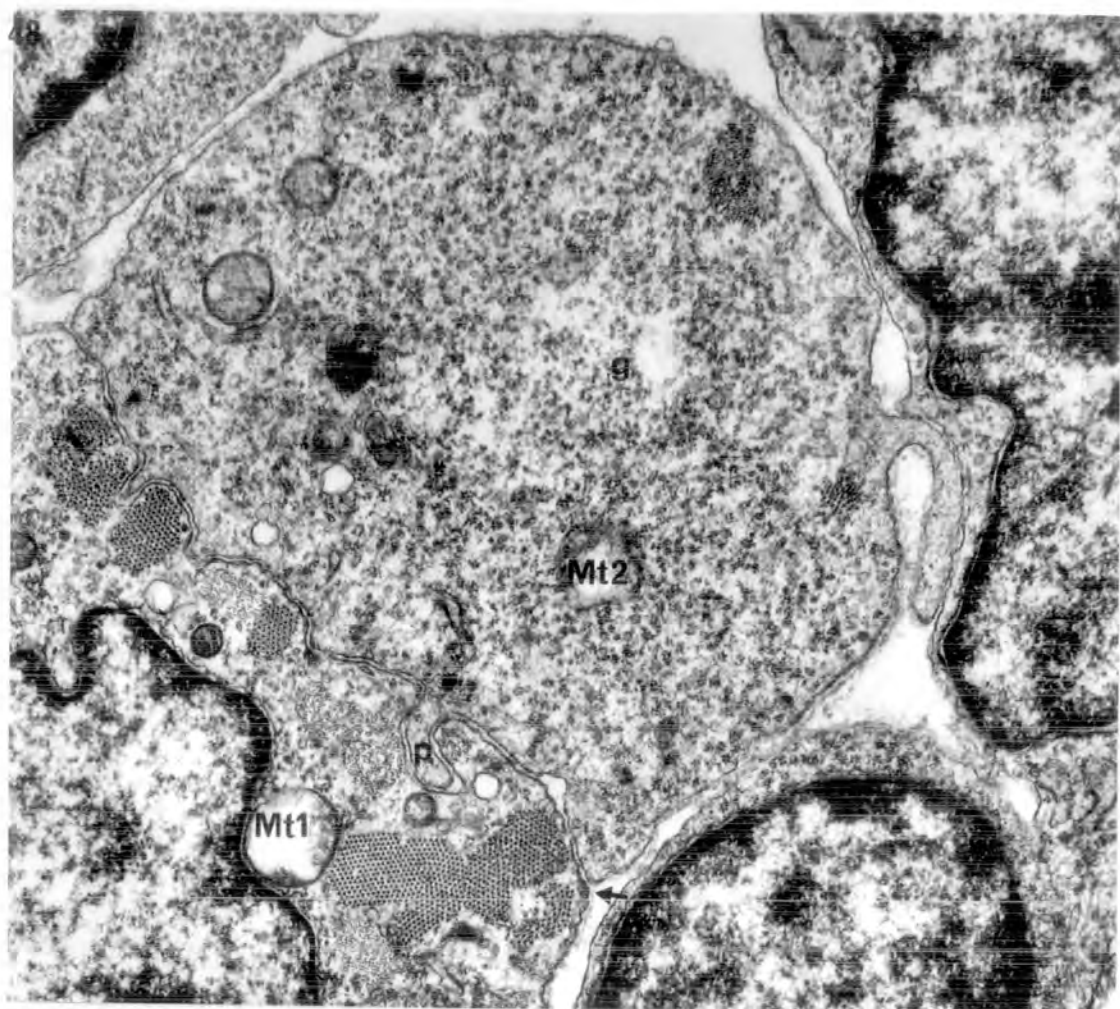
FIGURES 48-49. The fine structure of immature myotubes in 18.5 DF shank muscle of rat.

48. Transverse section of a secondary generation immature myotube. Note the paucity of myofibrils and the pseudopodial extensions. Arrow points to the common basement membrane. Scale as in fig. 49.

x 20,000

49. Transverse section of a secondary generation immature myotube. Note the pseudopodial extensions penetrating two parent myotubes. Double arrow points to an area of indistinct membrane separation, single arrow to basement membrane.

x 20,000



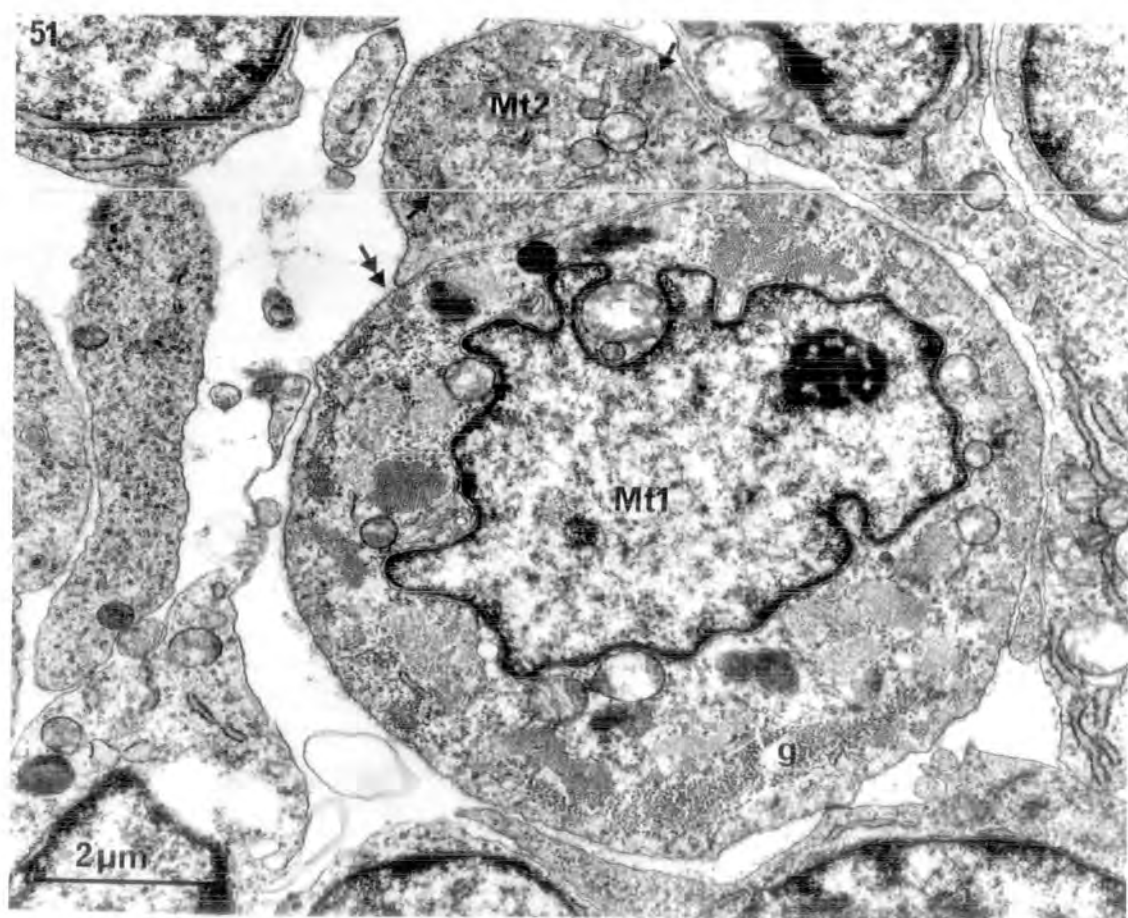
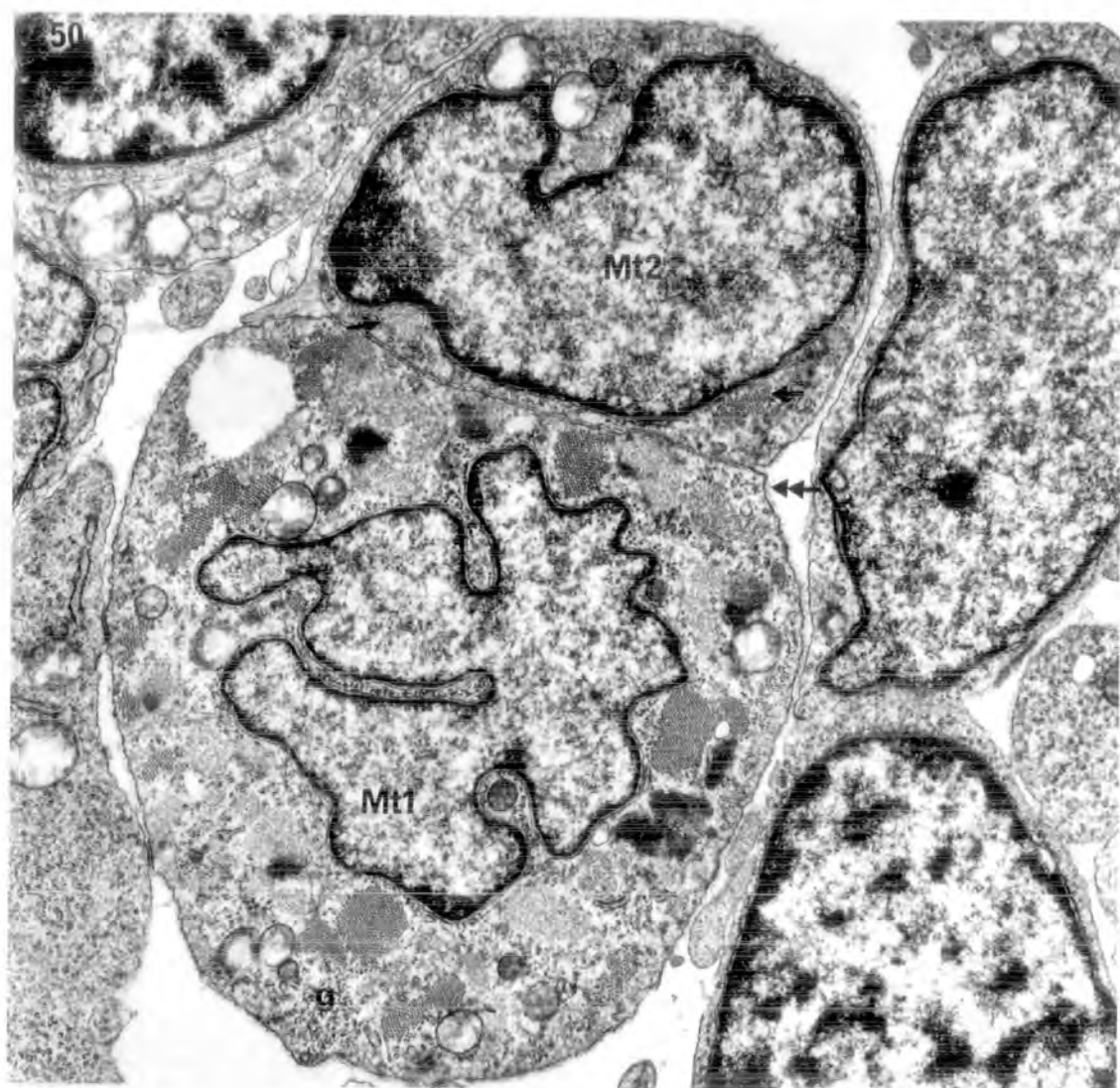
FIGURES 50-51. The fine structure of immature myotubes in 18.5 DF shank muscle of rat.

50. Transverse section of a primary and secondary generation myotube. Note the peripheral myofibrils in Mt2 (single arrows), the absence of pseudopodial extensions and the common basement membrane (double arrow). Scale as in fig. 51.

x 12,600

51. Transverse section of a primary and secondary generation myotube. Note the peripheral myofibrils (arrows) and central core sarcoplasm in Mt2, the absence of pseudopodial extensions and the common basement membrane (double arrow).

x 12,600



FIGURES 52-53. The fine structure of immature muscle cells in 18.5 DF shank muscle of rat.

52. Transverse section of a myoblast.

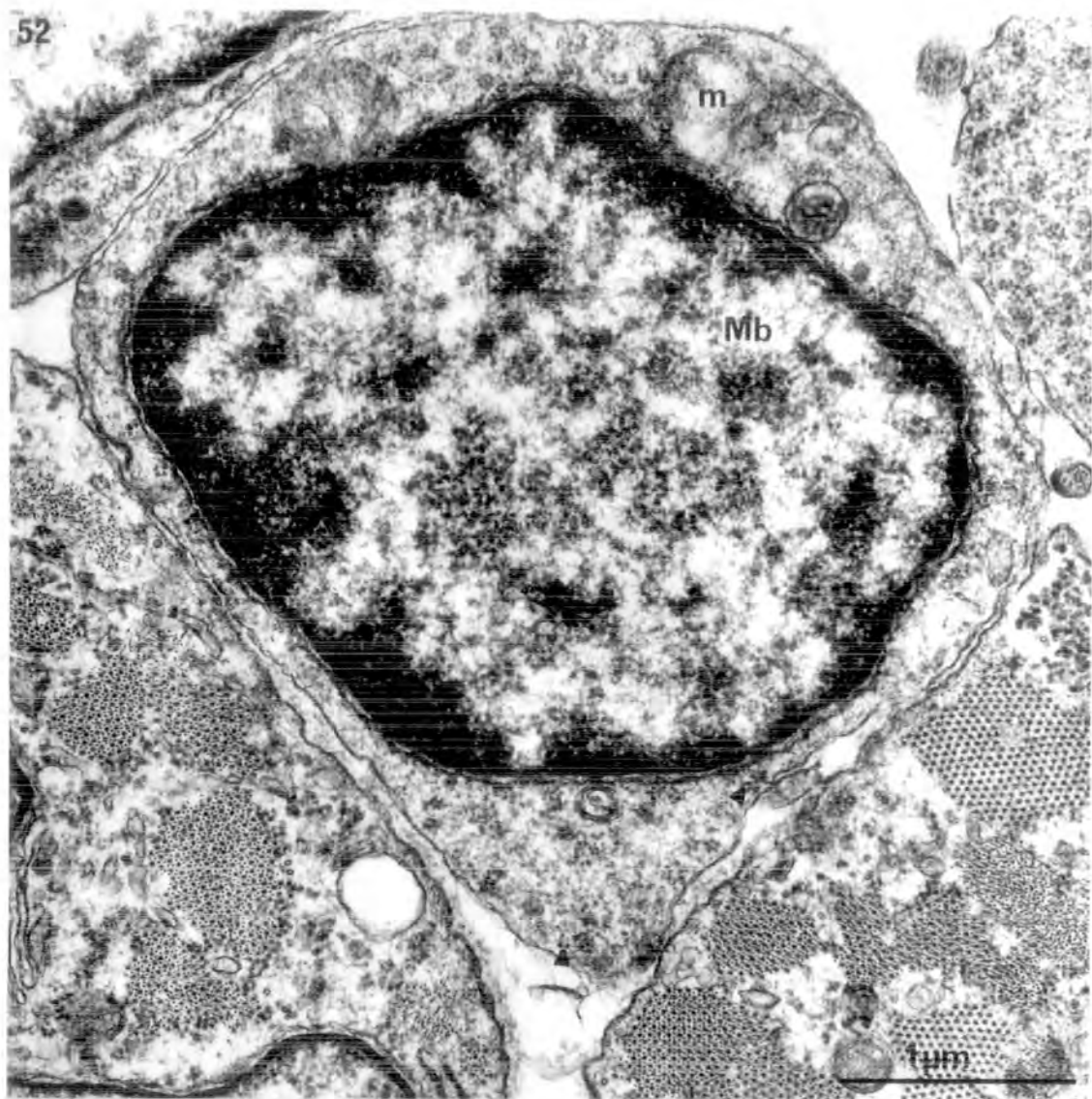
Note the thin perinuclear cytoplasm containing numerous ribosomes (arrow heads) and the absence of pseudopodial extensions.

x 32,000

53. Transverse section of an immature secondary generation myotube, containing few myofibrils (single arrow).

Note the absence of pseudopodial extensions. Double arrows point to close junctions. x 20,000

52



53

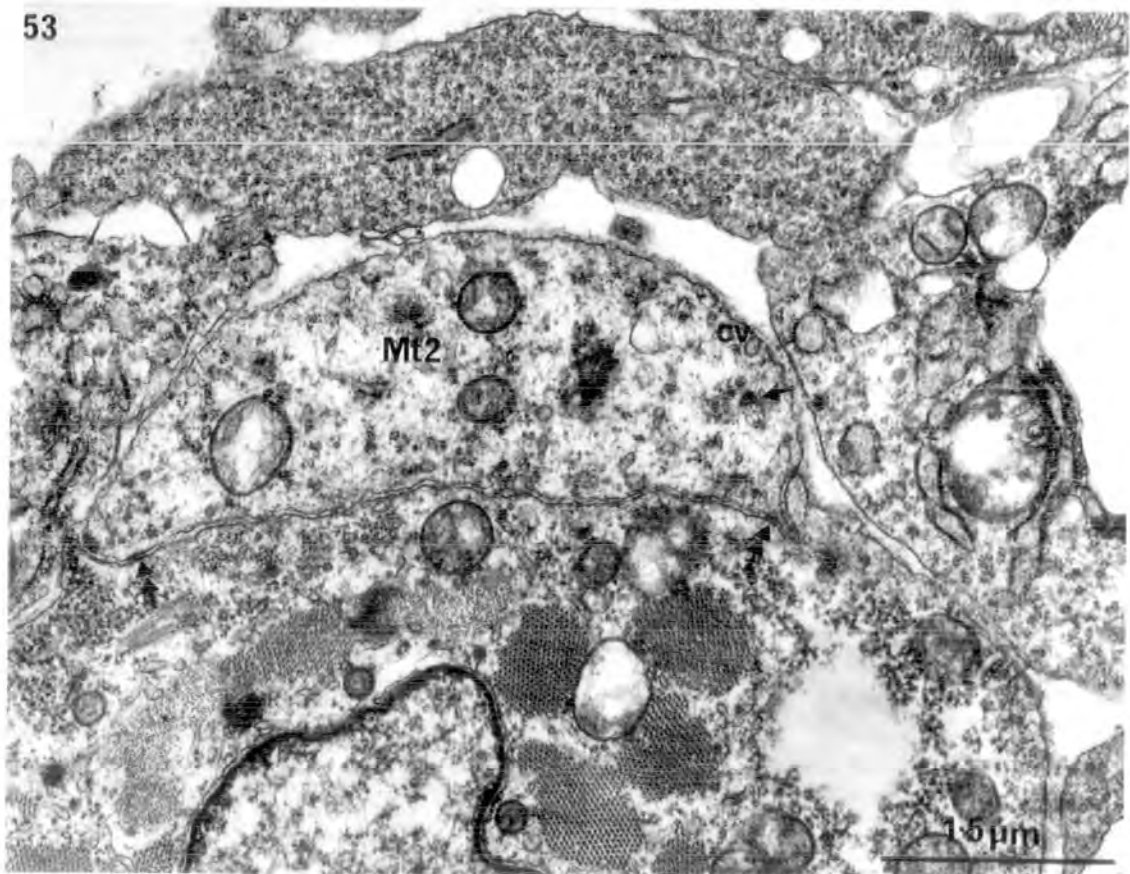
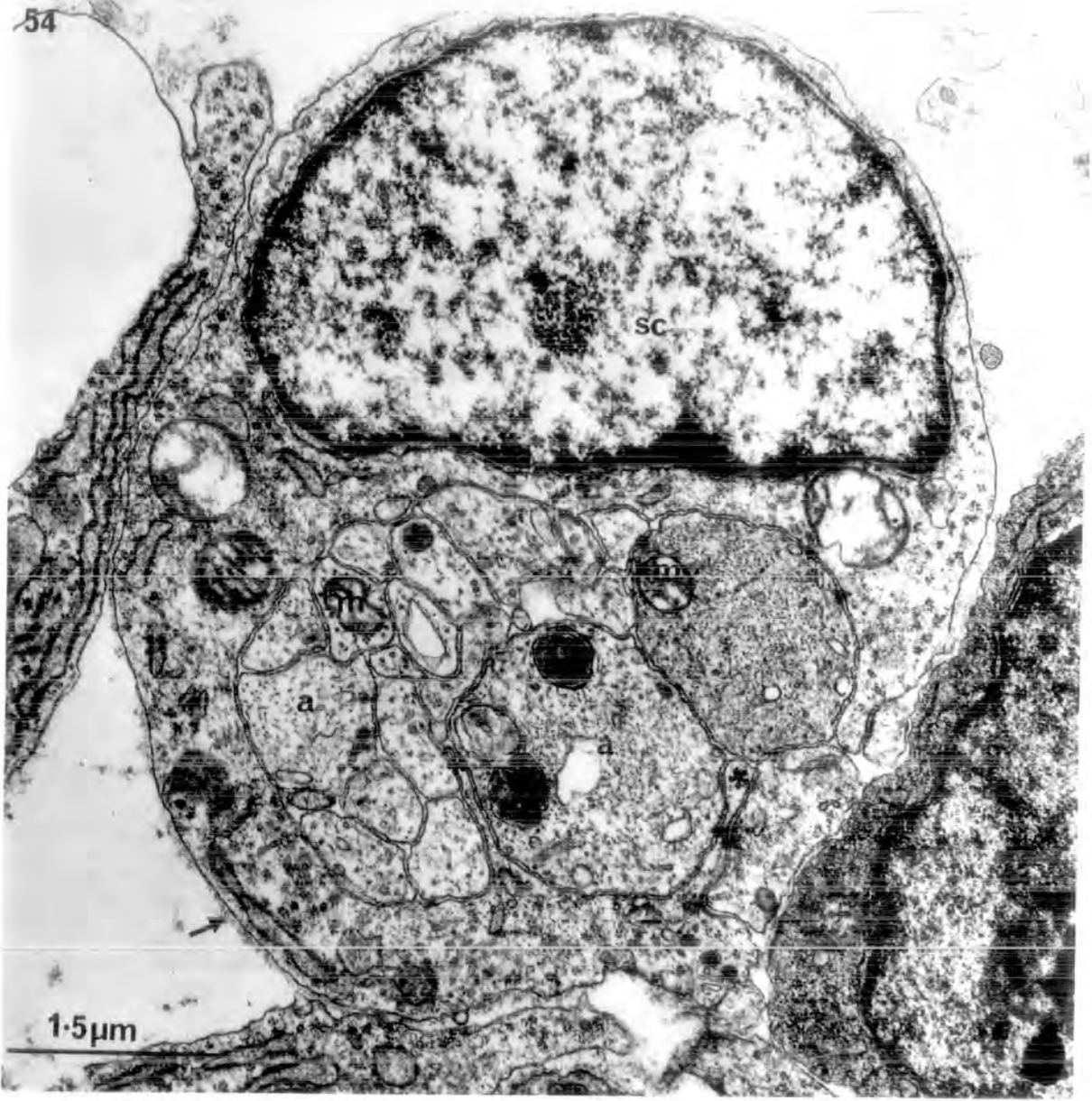


FIGURE 54. Transverse section of an intramuscular nerve trunk in 18.5 DF shank muscle of rat.

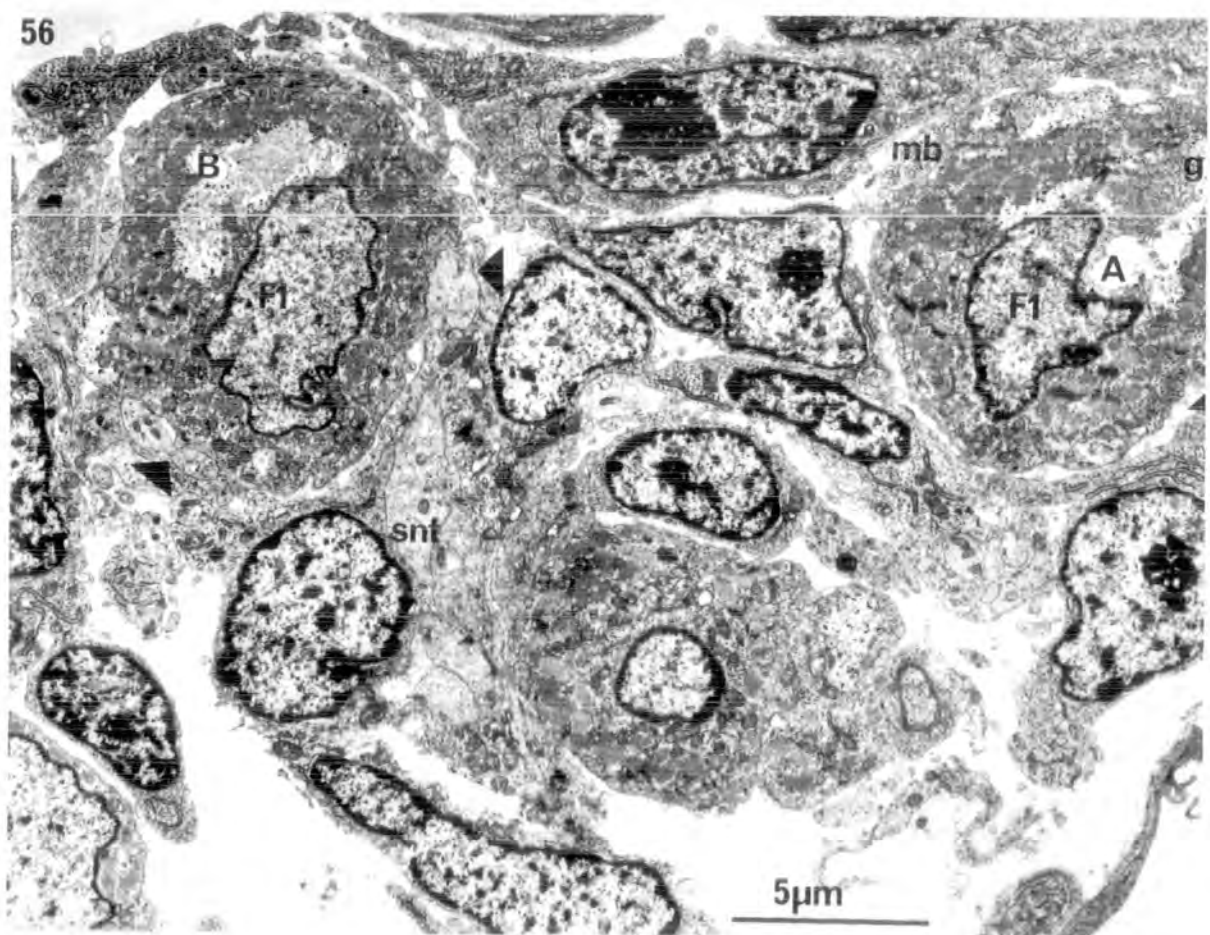
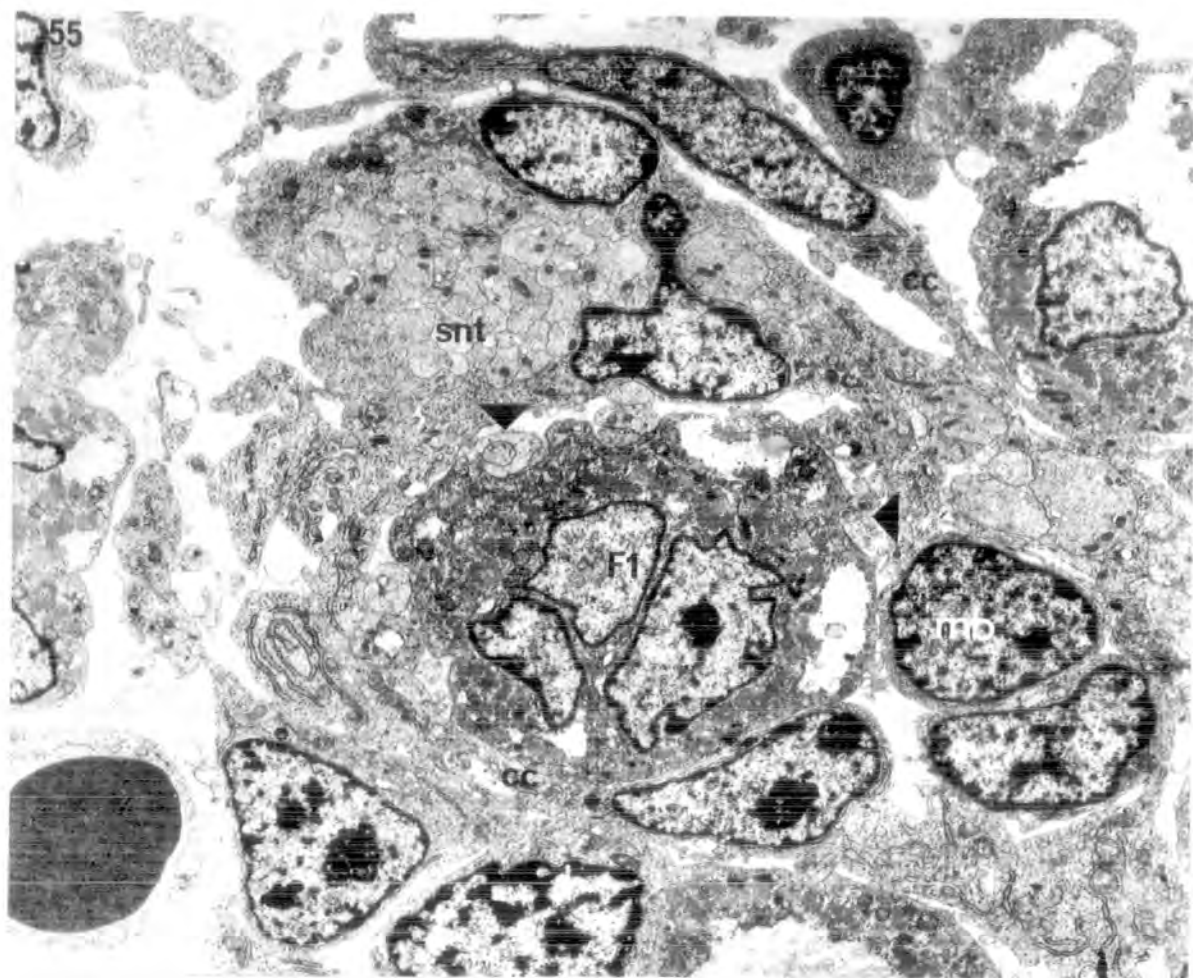
All axons are unmyelinated and enclosed by a single Schwann cell that possesses basement membrane (arrow). Note the septa of Schwann-cell cytoplasm (asterisks) that separate the axons into large groups; the abundance of neurotubules and neurofilaments in all axons; the presence of mitochondria in the large axons only and the fibroblast-like cells that form the first layer of the perineurium.

x 20,000



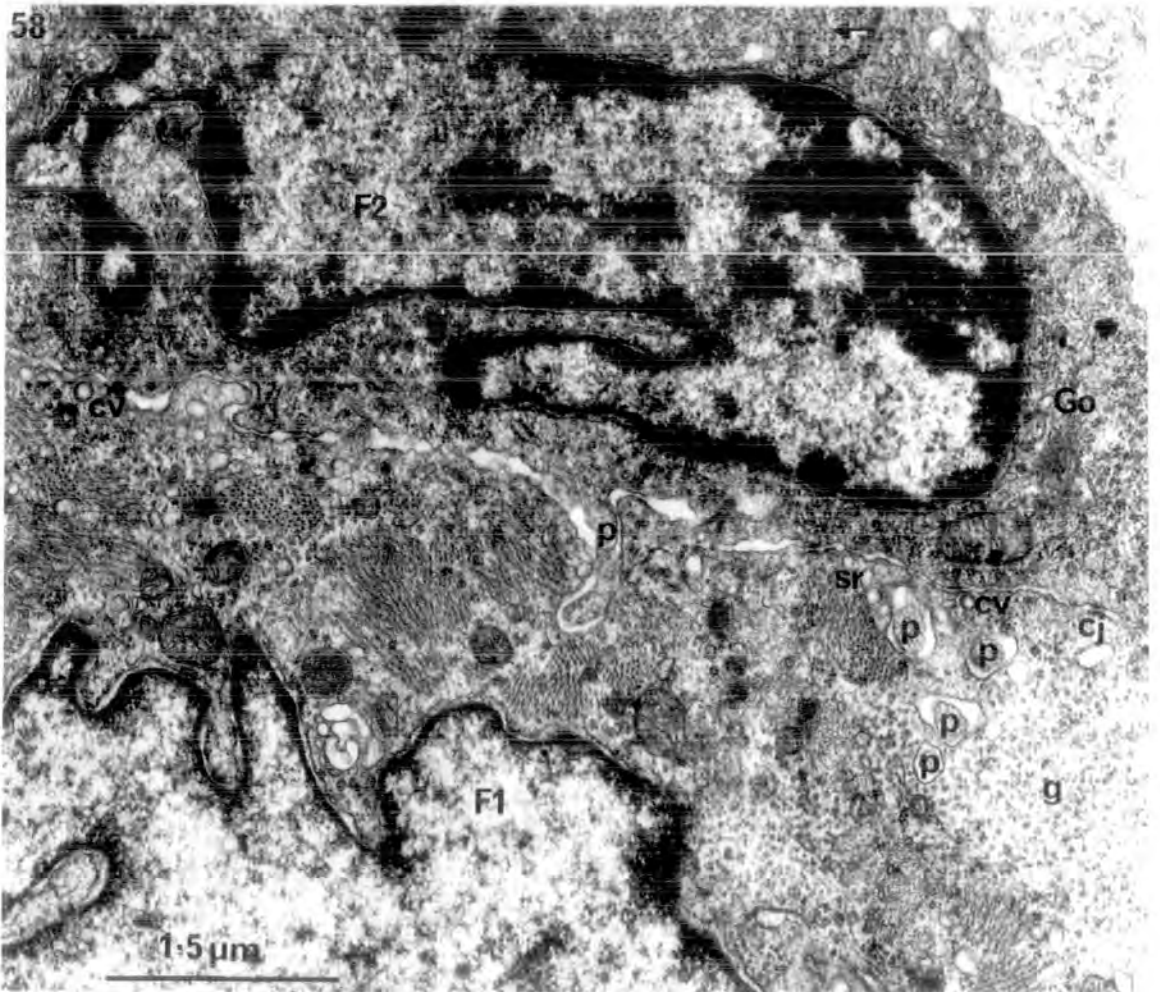
FIGURES 55-56. The fine structure of muscle spindles in
19.5 DF shank muscle of rat.

55. Transverse section through the equatorial region of spindle A. Note the single nuclear-bag fibre (F1) bearing primary sensory nerve terminals (arrow heads). The capsule consists of a single layer of cells that also surrounds the spindle nerve trunk. Myoblasts are contained within the capsule. Scale as in fig. 56. x 5,000
56. Transverse section of two spindles, A and B. Spindle A is sectioned through the juxta-equatorial region, and spindle B through the region of densest sensory innervation. Each spindle contains a single intrafusal fibre (F1). Note the absence of aggregated nuclei in spindle B. Arrow heads point to sensory nerve terminals. x 5,000



FIGURES 57-58. The fine structure of muscle spindles in
20 DF shank muscle of rat.

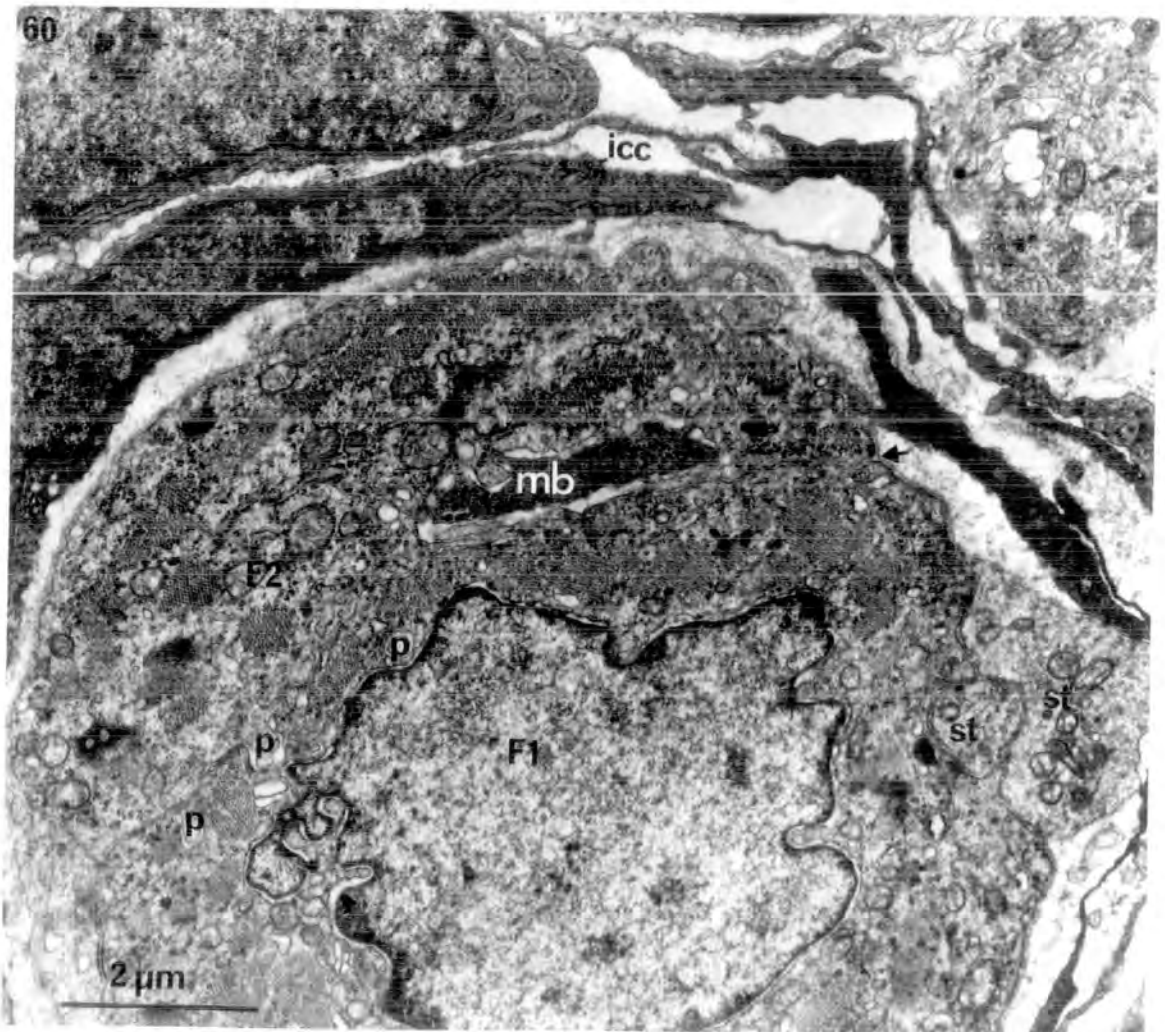
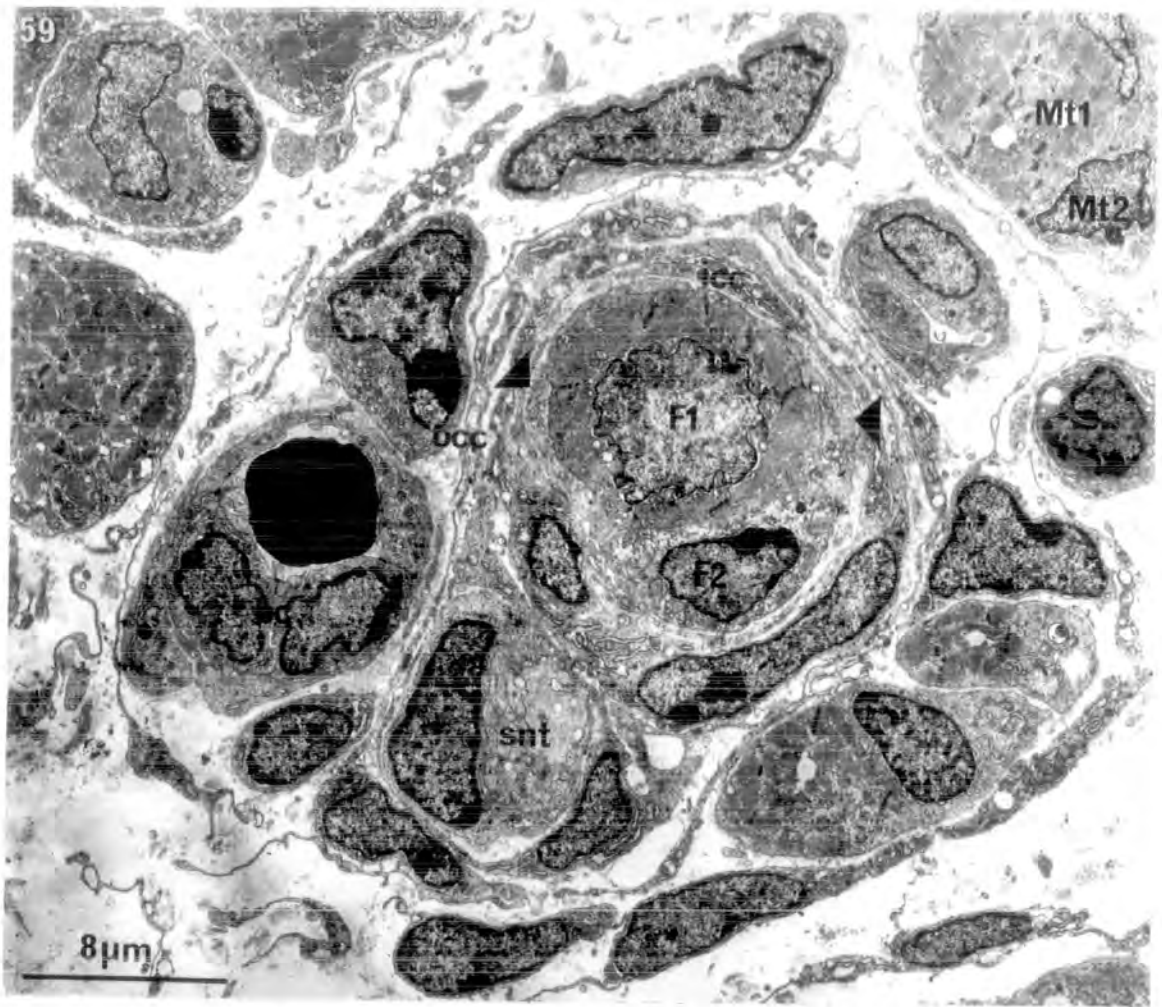
57. Transverse section through the juxta-equatorial region of a spindle. Note the appearance of a second intrafusal myotube (F2), closely associated with F1. Arrowheads point to sensory nerve terminals. x 5,000
58. Higher power electron micrograph of the apposed surfaces of F1 and F2 of the spindle shown in fig. 57. Note the paucity of myofibrils (arrow) in F2, compared to F1. Coated vesicles, close junctions and pseudopodial extensions are all common features of the apposed surfaces. x 20,000



FIGURES 59-60. The fine structure of muscle spindles in
20.5 DF shank muscle of rat.

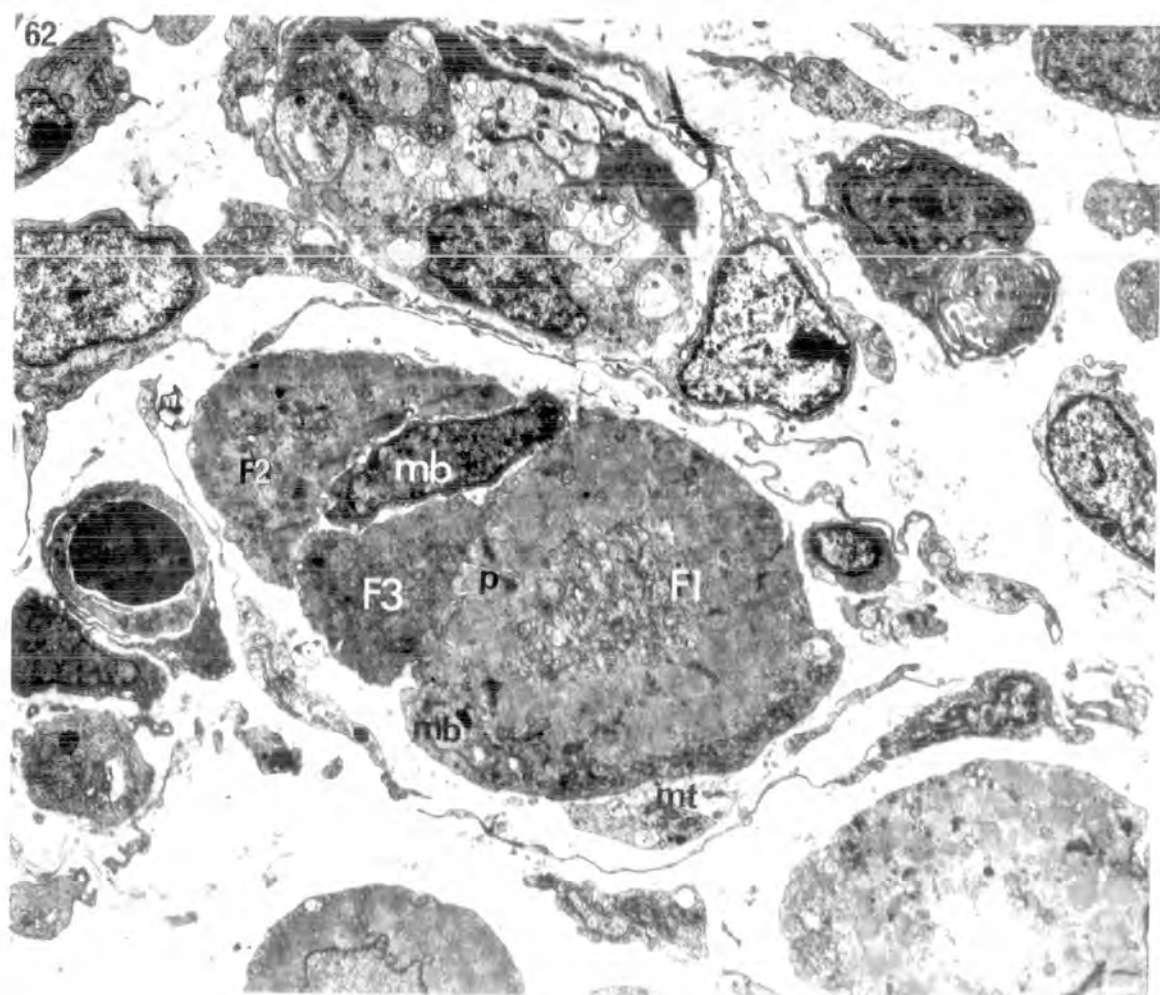
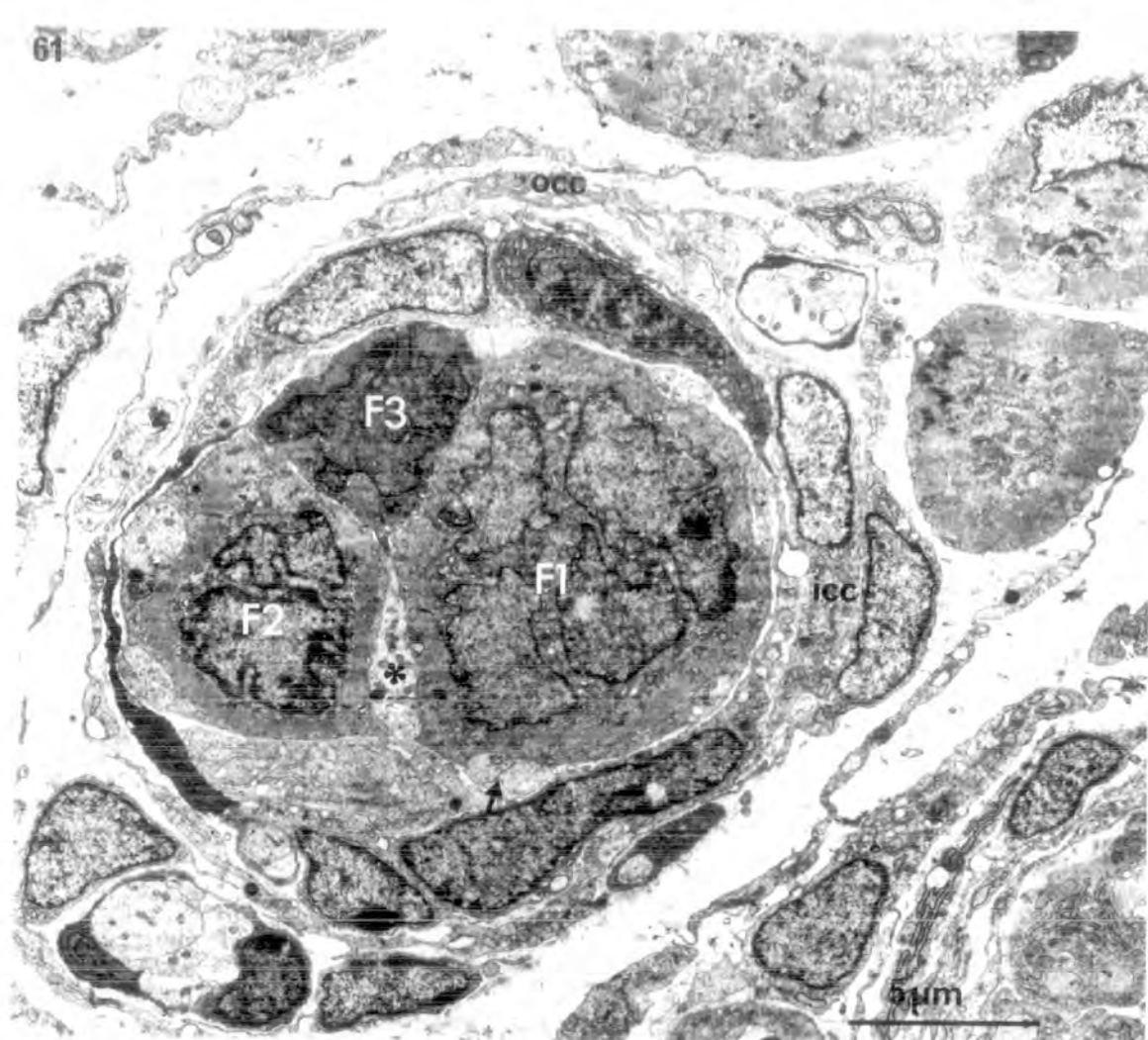
59. Transverse section through the juxta-equatorial region of a spindle. The axial bundle is at a similar stage of development as extrafusal myotubes (Mt1, Mt2). Note the immaturity and smaller diameter of F2 compared to F1. Arrowheads point to sensory nerve terminals. x 3,200

60. Transverse section through the juxta-equatorial region of the axial bundle of a spindle. Note the increased myofibril content of F2 compared to the same fibre in fig. 59. Pseudopodial extensions are still present, except in the area occupied by a myoblast. A common basement membrane (arrow) envelopes the outer surface of the axial bundle. Overlapping sensory nerve terminals (st) are still present. x 12,600



FIGURES 61-62. The fine structure of muscle spindles in newborn shank muscle of rat.

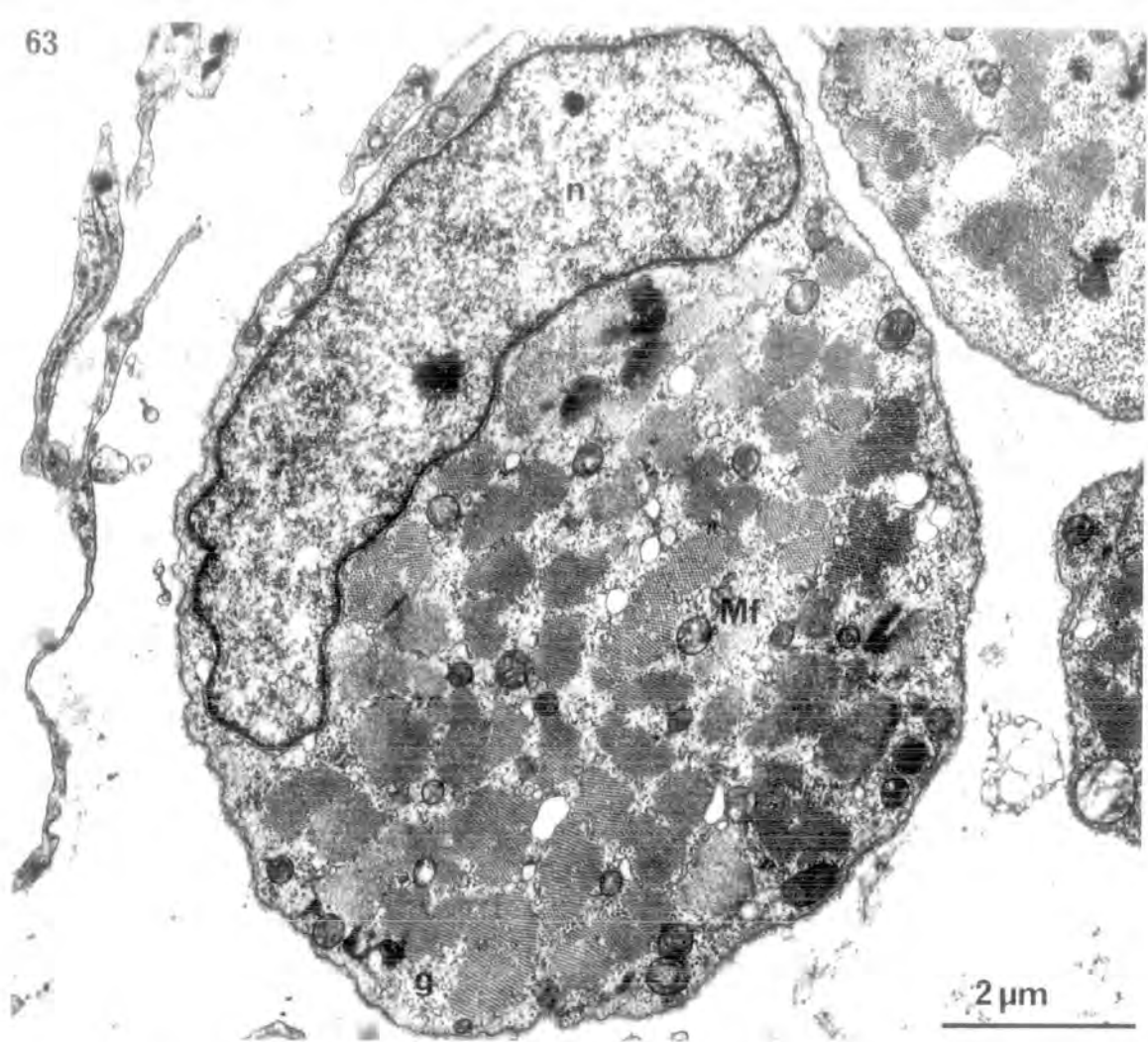
61. Transverse section through the equatorial region of a spindle. Note the large and small nuclear-bag fibres (F1 & F2), the electron-dense sarcoplasm of the immature nuclear-chain (F3) and the absence of pseudopodial extensions. Overlapping sensory terminals (arrow) are still present. A sensory terminal is shared between the two bag fibres (asterisk). x 5,000
62. Transverse section through the polar region of a spindle. Note the diameter differences between the intrafusal myotubes; the pseudopodial extensions from F3 into F1 and the myoblasts enclosed within the outer basement membrane. A thin sole-plate underlies the motor terminal on F1. Scale as in fig. 61. x 5,000



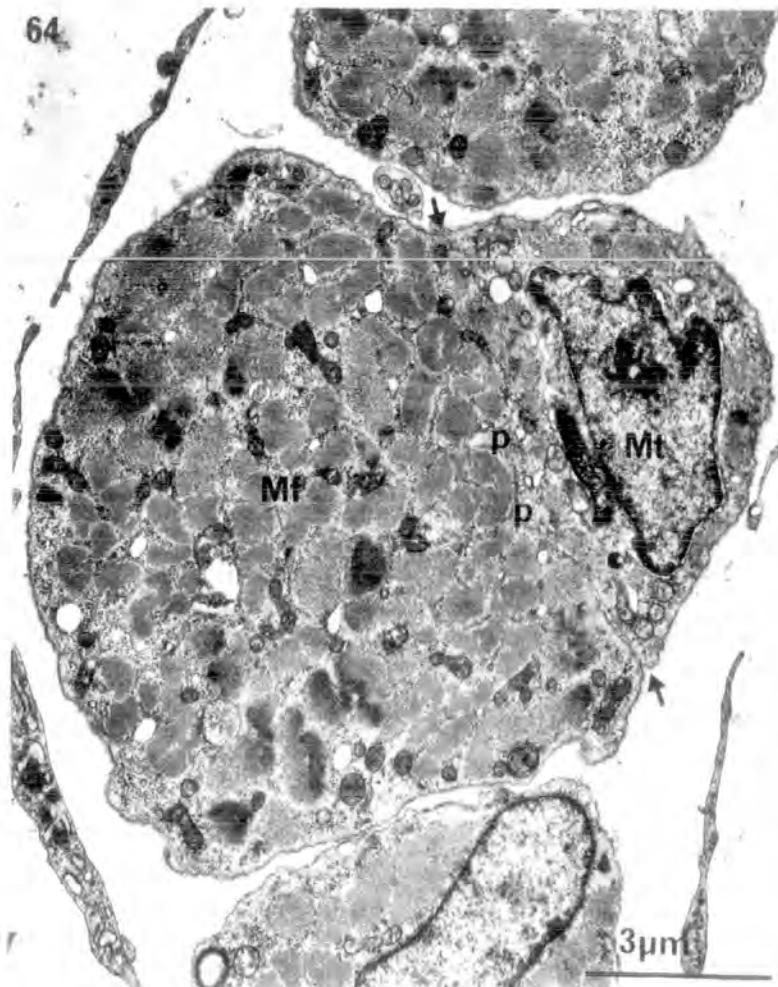
FIGURES 63-65. The fine structure of muscle cells in newborn shank muscle of rat.

63. Transverse section of a muscle fibre. Note the myofibrils occupying the whole section of the fibre and the peripheral nucleus.
x 12,600
64. Transverse section of a muscle fibre and apposed myotube. Note the paucity of myofibrils in the immature myotube compared to the muscle fibre; the central nucleus of the myotube, and pseudopodial extensions. A common basement membrane encloses both muscle cells (arrows).
x 8,000
65. Higher power electron micrograph of the apposed surfaces of the cells shown in fig. 64. The pseudopodial extensions penetrate the interfibrillar sarcoplasm of the muscle fibre. The aggregated vesicles in the myotube probably represent developing T tubules. x 32,000

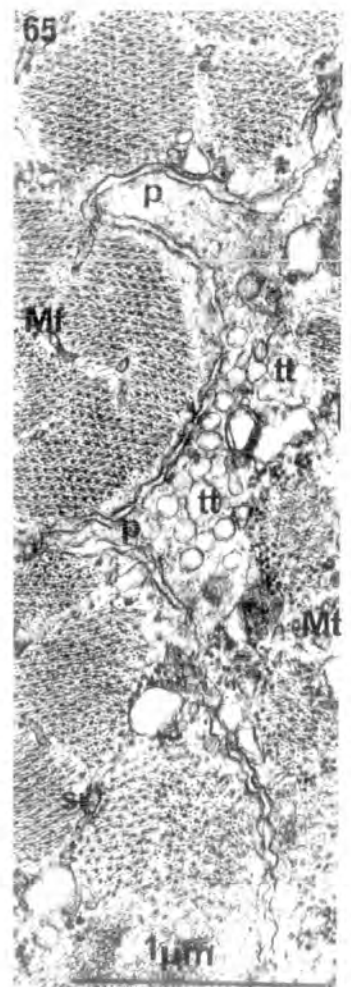
63



64



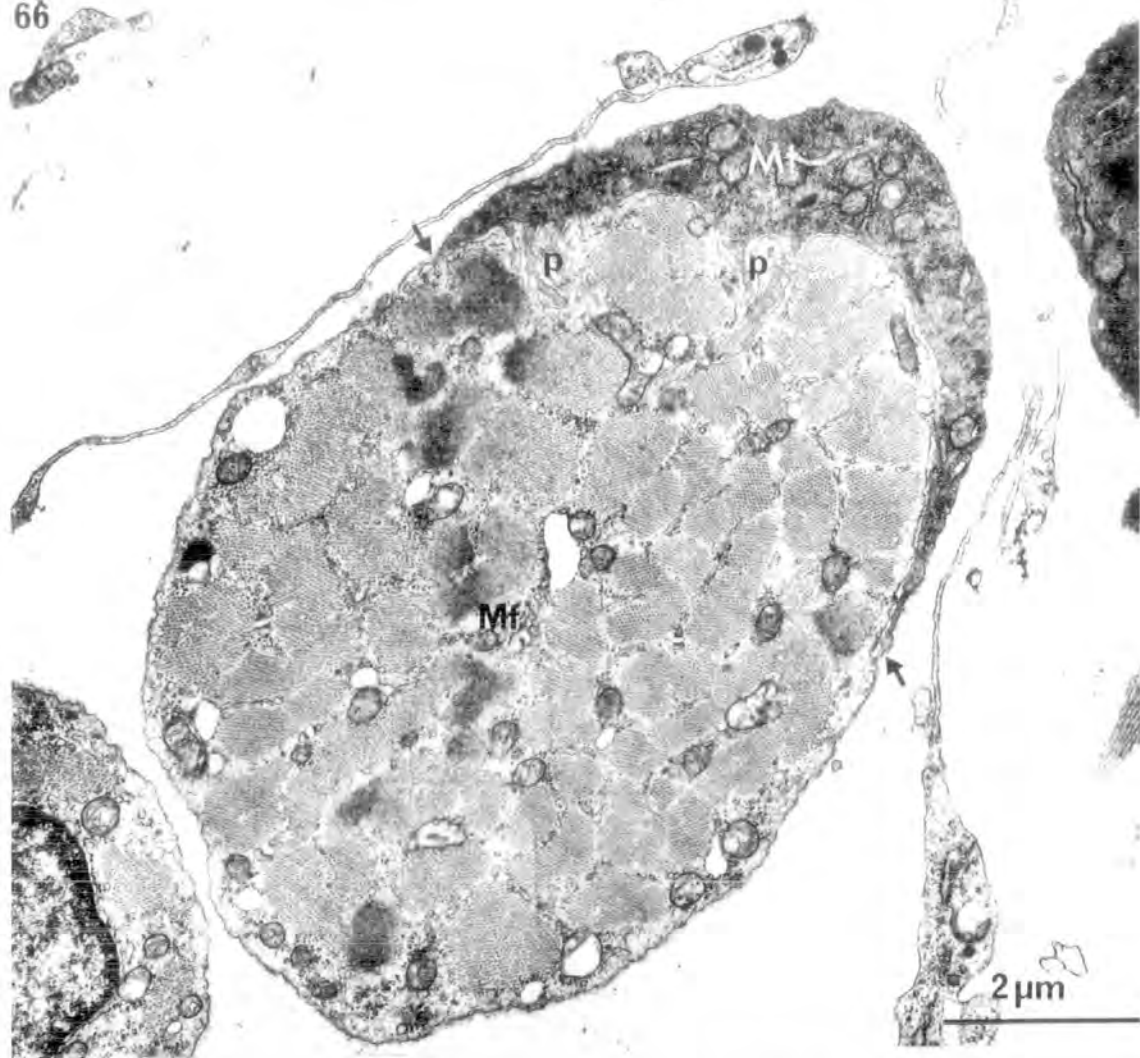
65



FIGURES 66-67. The fine structure of muscle cells in newborn shank muscle of rat.

66. Transverse section of a muscle fibre and apposed myotube. Note the electron density of the sarcoplasm of the myotube; the pseudopodial invaginations, and the common basement membrane (arrows). x 12,600
67. Higher power electron micrograph of the apposed surfaces of the muscle cells shown in fig. 66. Note the absence of assembled myofibrils in the myotube. x 40,000

66



67



FIGURE 68. The fine structure of muscle spindles in
1 DPN shank muscle of rat; transverse
section through the equatorial region of
a spindle.

Note the difference in the size of the nuclear bag of F1 and F2 and the absence of pseudopodial extensions. Myoblasts occupy the central regions of the axial bundle. The outer capsule cells contain many dilated cisternae of granular ER.

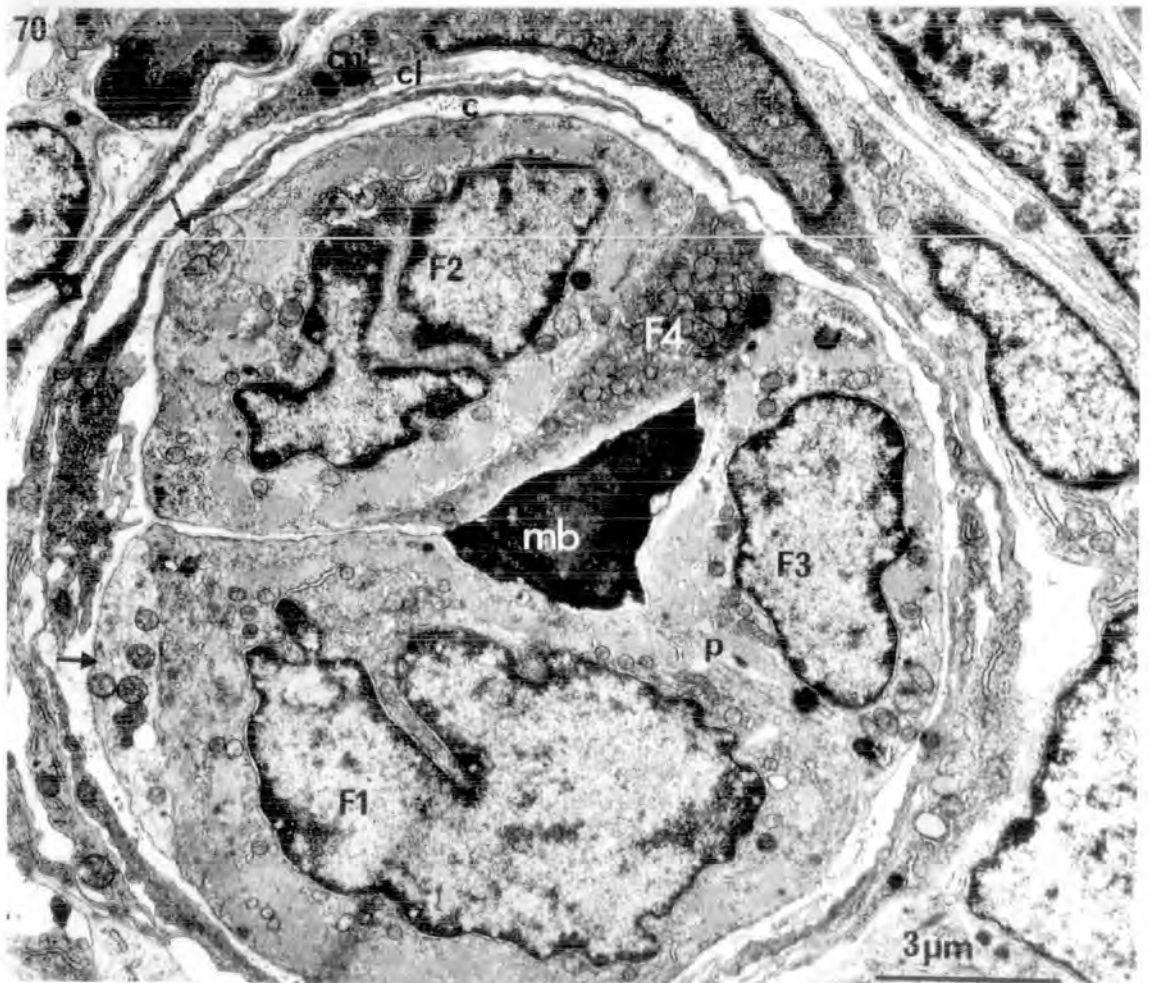
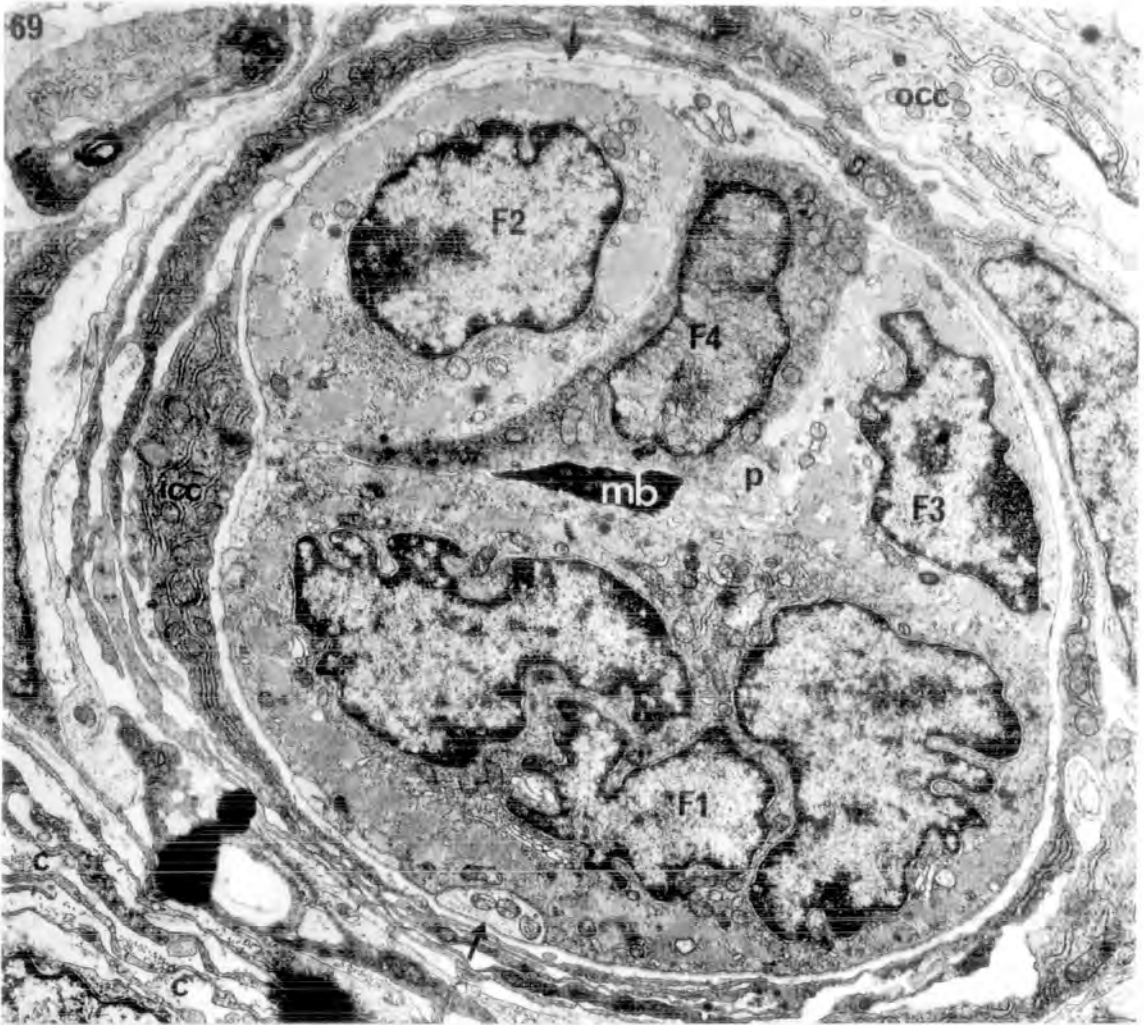
x 5,000



FIGURES 69-70. The fine structure of muscle spindles in
2 DPN shank muscle of rat.

69. Transverse section through the equatorial region of a spindle. A fourth intrafusal myotube (F4) is now present and lies in apposition to F3. Note the aggregated myonuclei of F1 and the single central nucleus of F2. The axial bundle is surrounded by a single layer of basement membrane. Sensory terminals (arrows) are confined to the outer surface. Scale as in fig. 70. x 8,000

70. Transverse section through the more distal equatorial region of the same spindle as in fig. 69. F2 now exhibits a small nuclear bag and F1 a single central nucleus. F3, although more mature than at birth, still lies in apposition to F1. Note the electron density of F4, the abundance of collagen between the capsule layers and the atypical cilium associated with the centriole of an inner capsule cell. Arrows point to sensory terminals. x 8,000



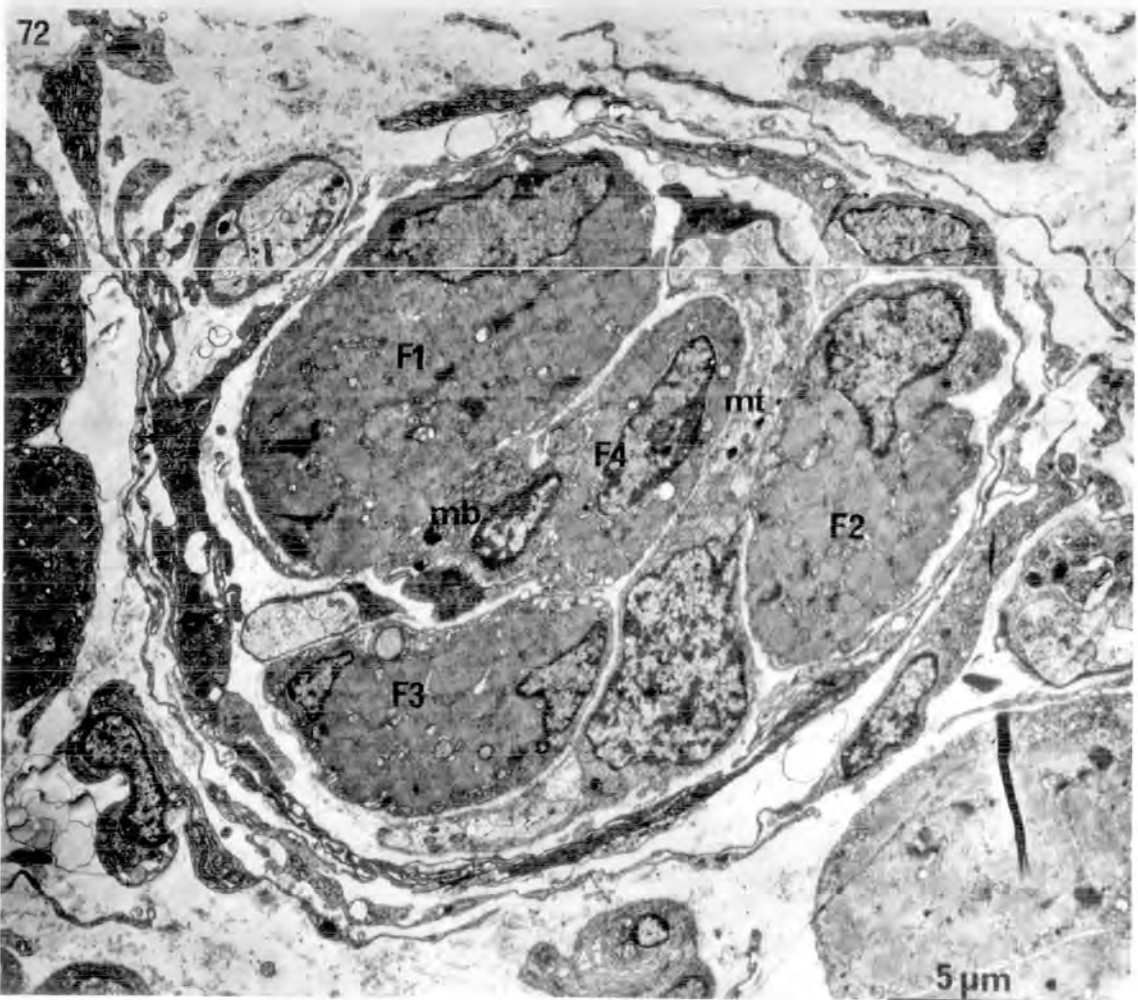
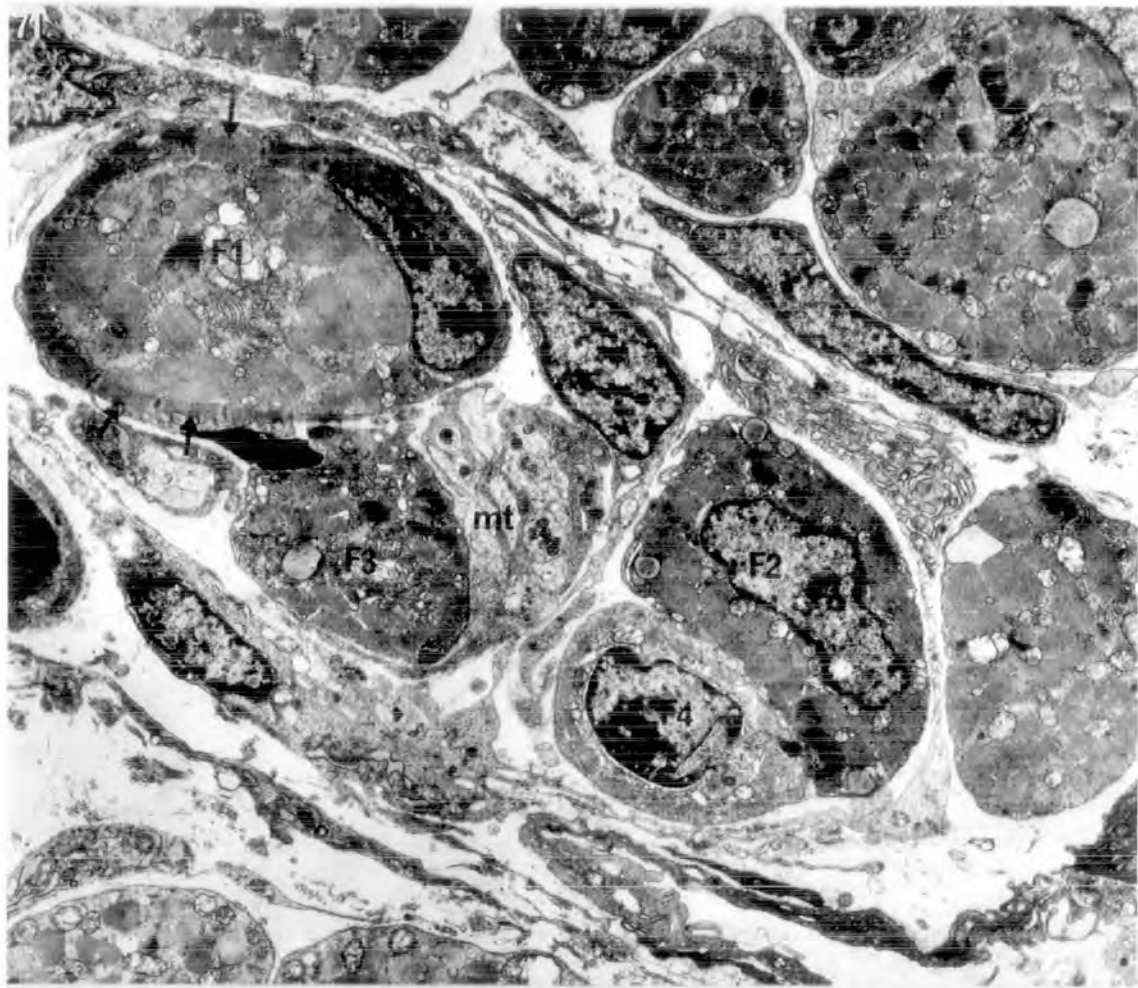
FIGURES 71-72. The fine structure of muscle spindles in
4 DPN shank muscle of rat.

71. Transverse section through the mid-polar region of a spindle. The full adult complement of four intrafusal muscle fibres is attained. F4 is not fully mature and lies in apposition to F2. Note the motor terminal on F3. The nuclei in F1 are peripheral in position. In the same fibre, the peripheral myofibril adopts a circular orientation; arrows point to the M line in this myofibril. Scale as in fig. 72.

x 5,000

72. Transverse section through the polar region of a spindle. Note the peripheral nuclei in fibres 1, 2 and 3; the presence of myoblasts, and the absence of pseudopodial extensions. Many small mitochondria occupy the interfibrillar sarcoplasm of each fibre.

x 5,000



FIGURES 73-74. The fine structure of muscle spindles in 12-16 DPN shank muscle of rat.

73. Transverse section through the equatorial region of a spindle in 12 DPN rat. Note the difference in the size of the nuclear bags of F1 and F2; sensory nerve terminals (arrows) that are located on all surfaces of the muscle fibres; endomysial cells forming the axial sheath and endomysial enclosures, and the formation of the periaxial space. One of the inner capsule cells (asterisk) extends across the periaxial space to form an endomysial enclosure.

x 3,200

74. Transverse section through the juxta-equatorial region of a spindle in 16 DPN rat. Note the differences in the diameters of the intrafusal fibres, the absence of close apposition between the fibres of the axial bundle and the development of the periaxial space. Arrow points to a possible secondary sensory terminal on F3.

Scale as in fig. 73. x 3,200

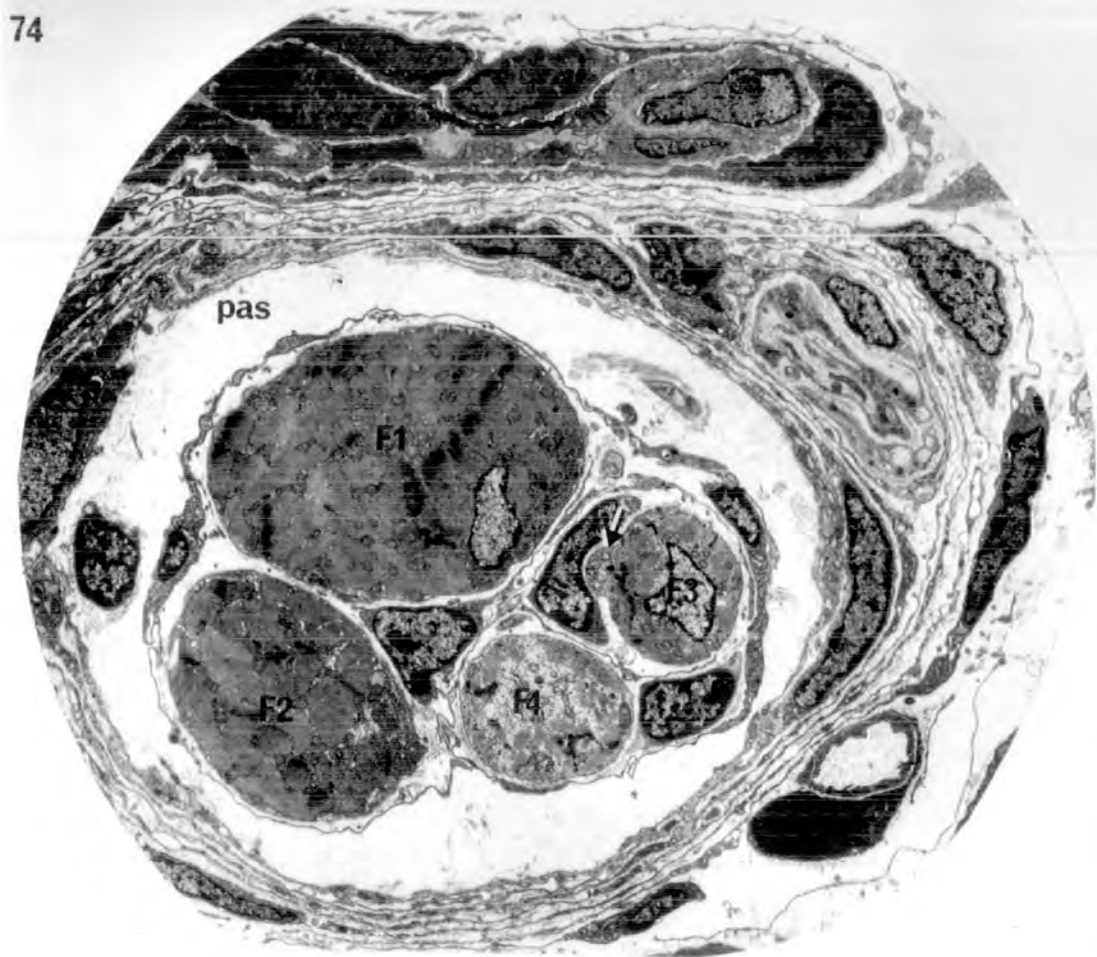
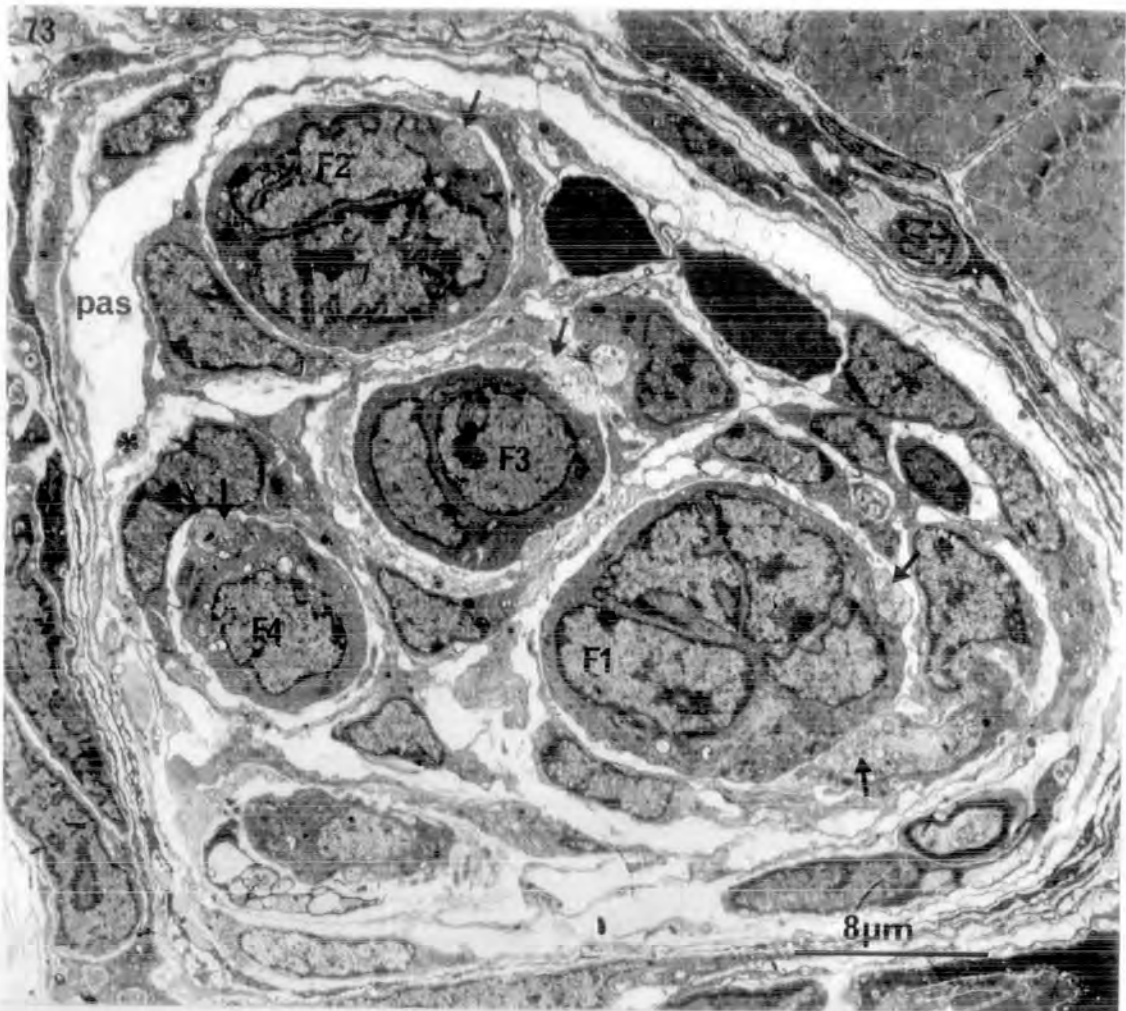


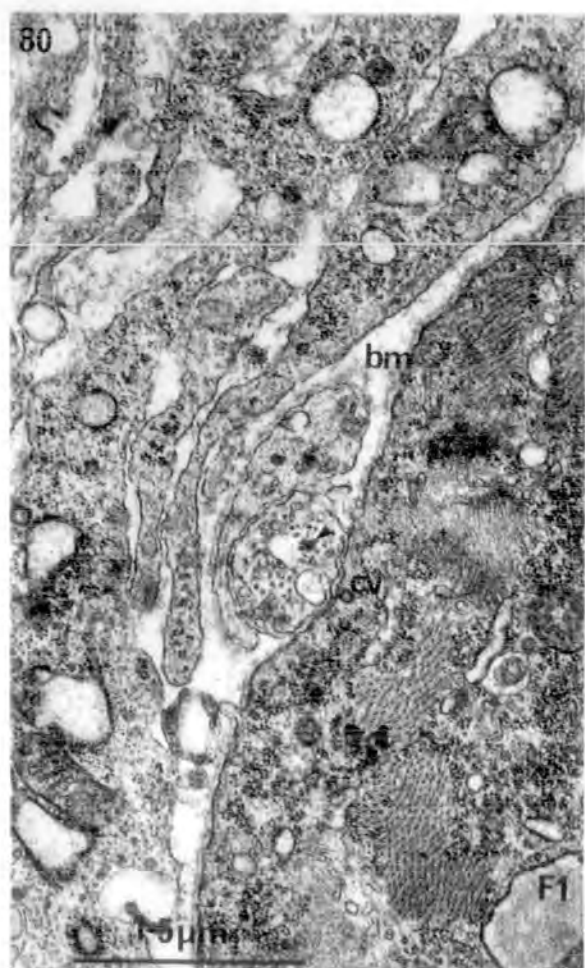
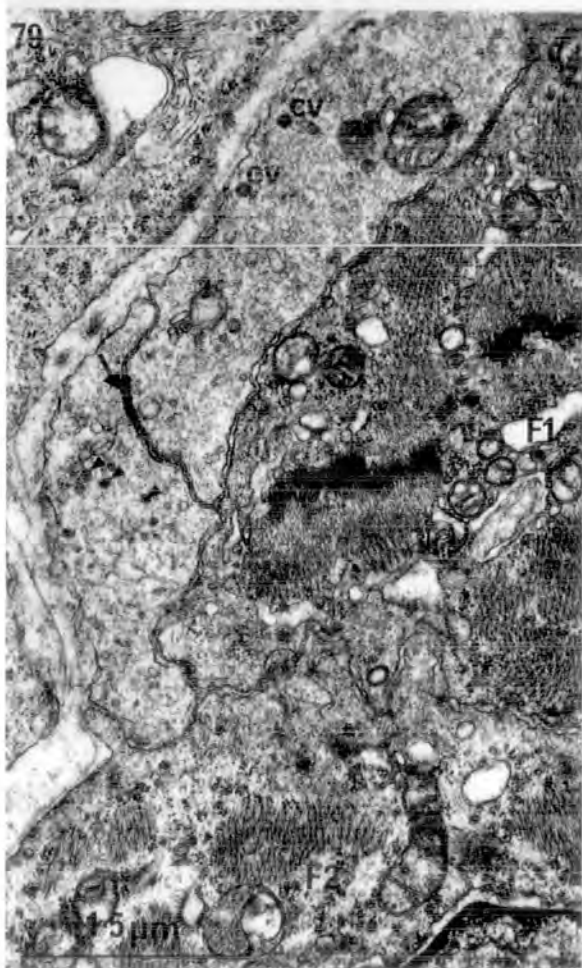
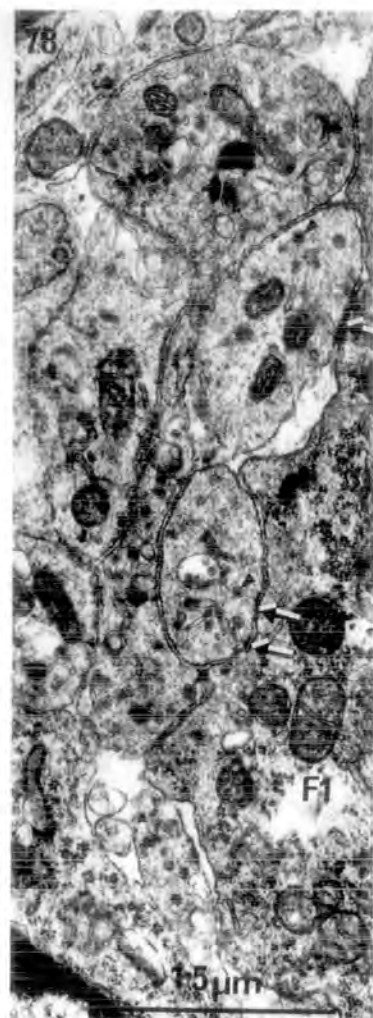
FIGURE 75. The fine structure of muscle spindles in PL of 16 DPN rat; transverse section through the juxta-equatorial region of a spindle.

Note the pairing of the two nuclear-bag fibres (F1 and F2), which share a common basement membrane, endomysial enclosure and satellite cell (double arrow). The large periaxial space houses two vacuolated cells. Single arrows point to primary sensory nerve terminals. Circle encloses an atypical cilium that stems from a centriole in one of the capsular sheet cells. x 3,200



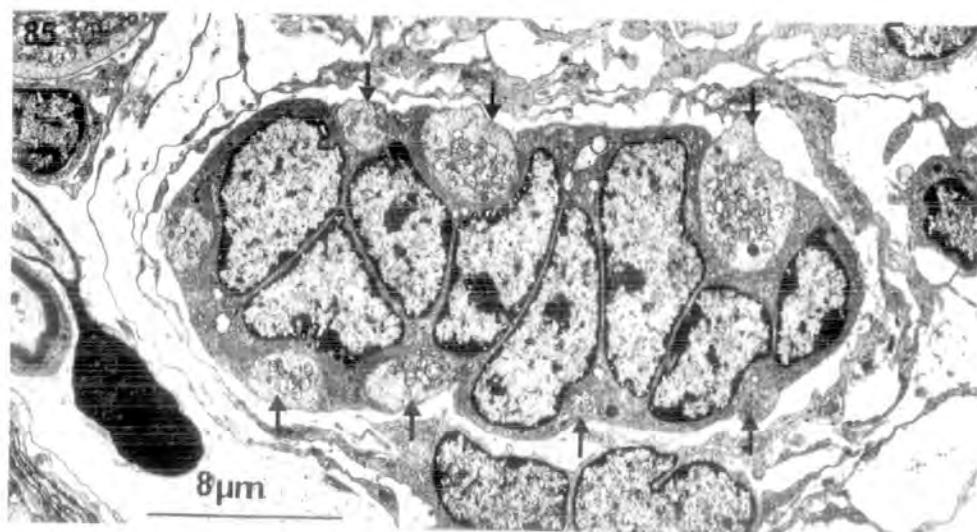
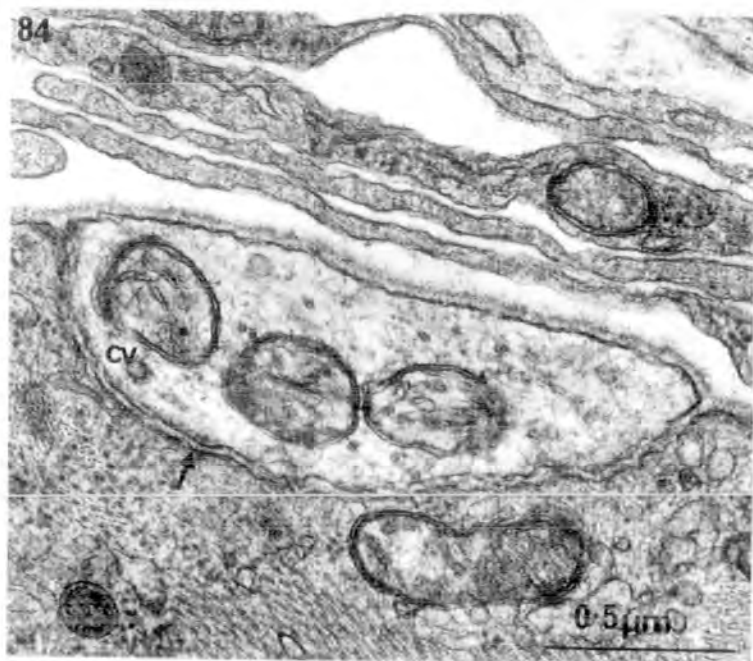
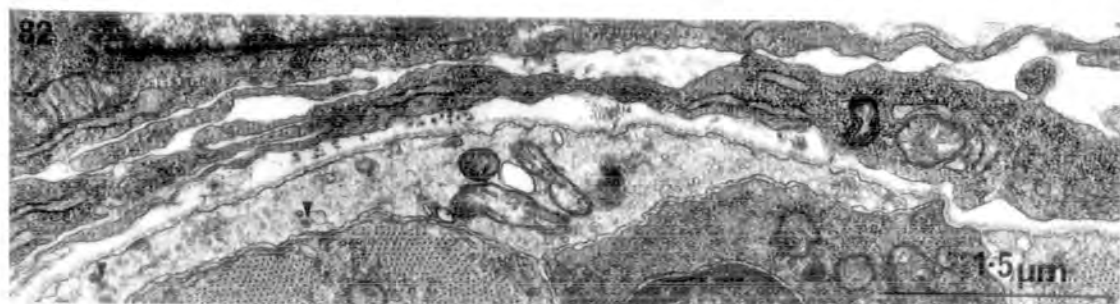
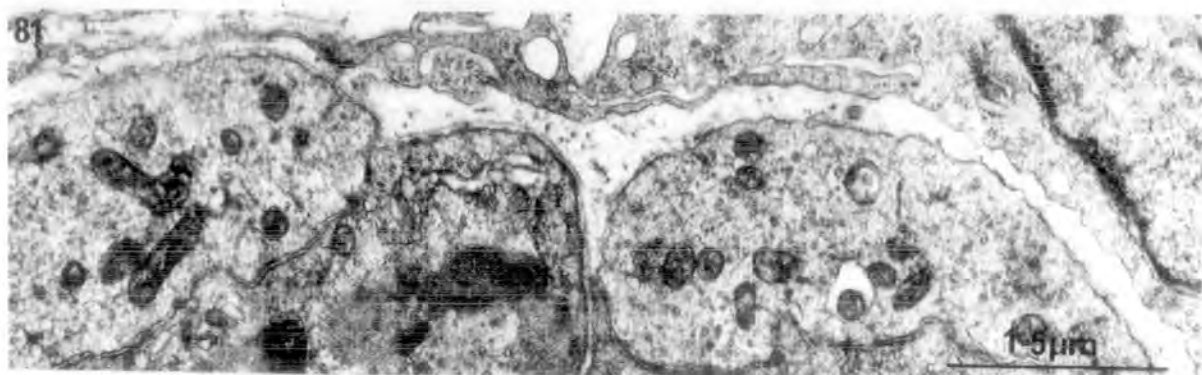
FIGURES 76-80. The fine structure of sensory nerve terminals in developing muscle spindles of rat.

76. 19.5 DF. Transverse section of two adjacent sensory terminals. Note the small mitochondria at the core of the terminals; the aggregation of smooth clear vesicles in the upper terminal; the presence of dense-cored vesicles (arrowheads) and the "desmosome-like" thickenings of the synaptic membranes (arrows). x 20,000
77. 19.5 DF. Transverse section of two overlapping sensory terminals. Note the abundance of neurofilaments and neurotubules in the inner non-synaptic terminal; the presence of smooth and dense-cored (arrowheads) vesicles in both terminals and the absence of mitochondria. x 32,000
78. 19.5 DF. Transverse section of adjacent sensory terminals. Arrowheads point to dense-cored vesicles, arrows to "desmosome-like" thickenings of the synaptic membranes. x 20,000
79. 20.5 DF. Transverse section of adjacent sensory terminals. Note the thickening of adjacent axolemmae (arrow) and the coated vesicles in the upper terminal. Arrowheads point to dense-cored vesicles. x 18,900
80. Newborn, FHL. Transverse section of a "bundled" type of sensory terminal. Note the absence of mitochondria and the presence of neurotubules, neurofilaments, smooth and dense-cored (arrowhead) vesicles in the terminal. x 20,000



FIGURES 81-85. The fine structure of sensory nerve terminals in developing muscle spindles of rat.

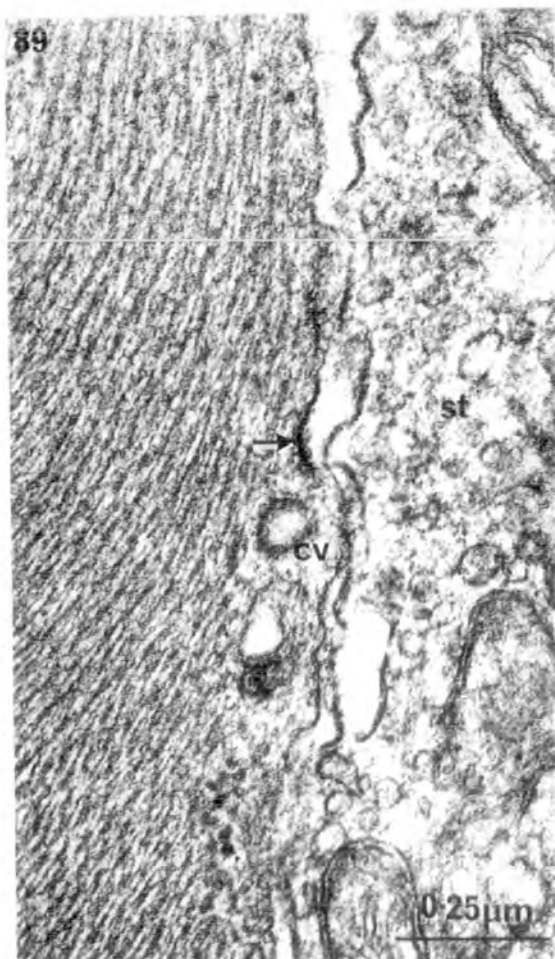
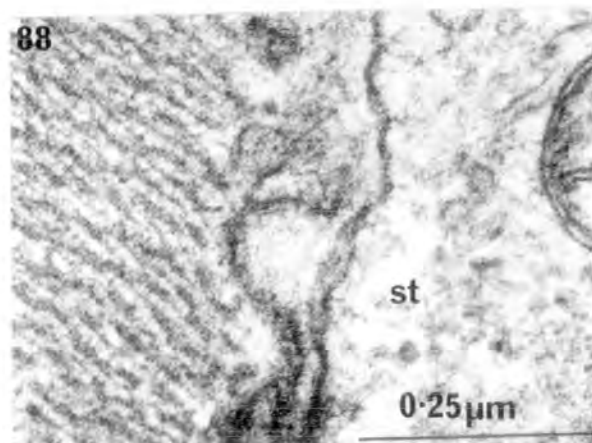
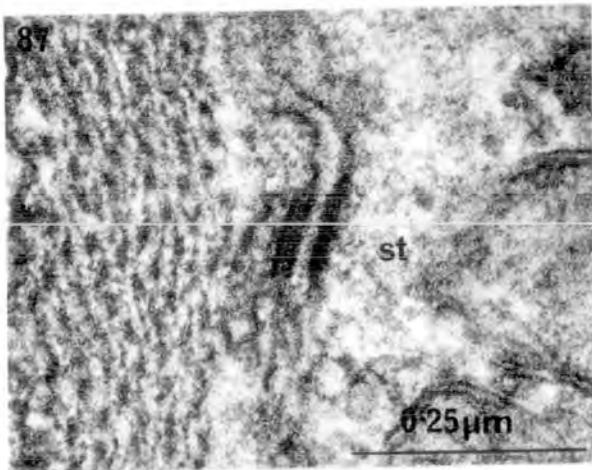
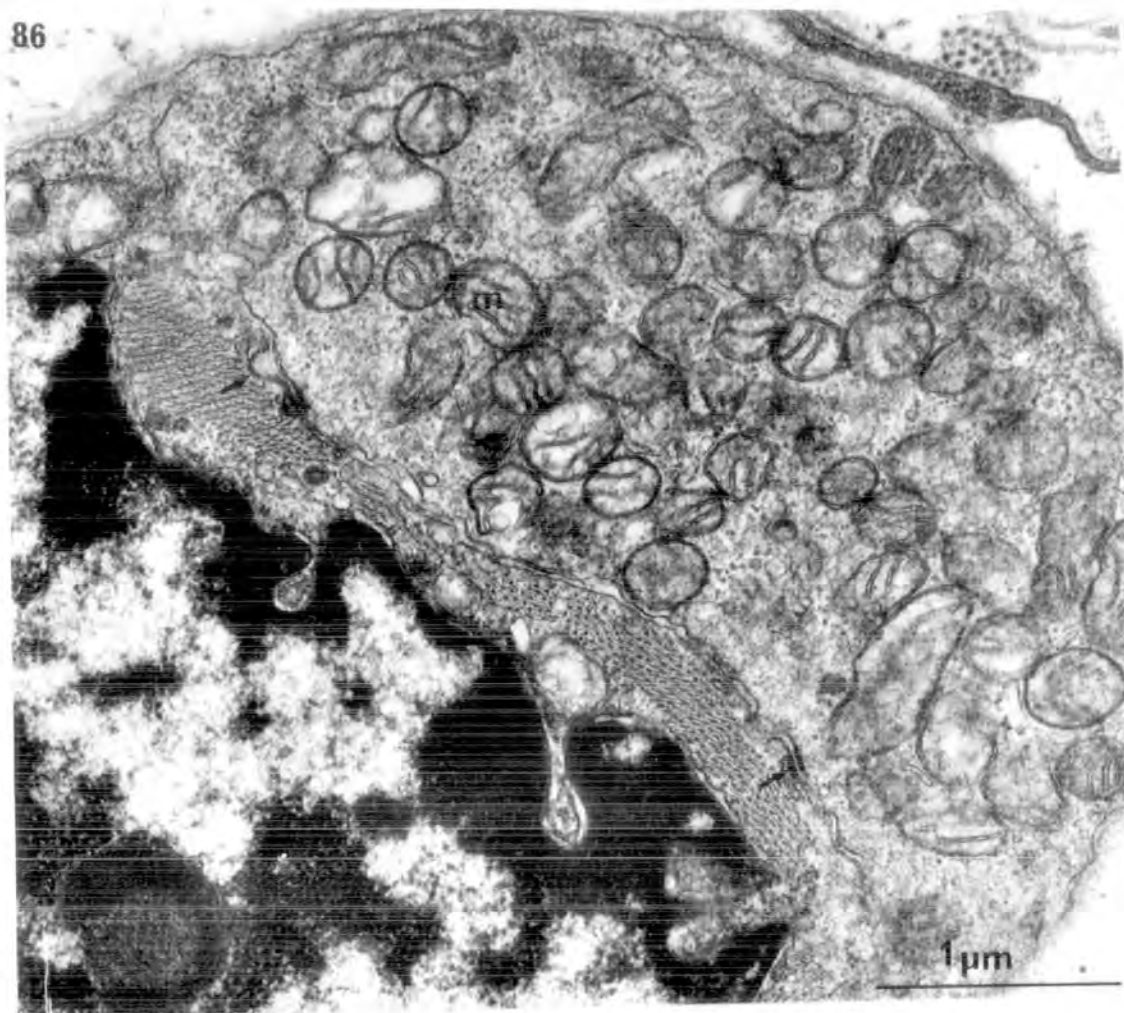
81. 1 DPN. Transverse section of spiral sensory terminals on the outer surface of the axial bundle. Note the numerous "desmosome-like" thickenings of the synaptic membranes. x 19,000
82. 2 DPN. Transverse section of a single spiral sensory terminal, contacting two intrafusal muscle fibres. Arrowheads point to dense-cored vesicles. x 20,000
83. 4 DPN. Transverse section of a sensory terminal. Note the paucity of dense-cored vesicles (arrowhead). x 20,000
84. 2 DPN. Transverse section of a sensory terminal. Note the coated vesicle in the axoplasm and the specialization of the synaptic membranes (arrow). x 50,000
85. 12 DPN. Oblique longitudinal section of a nuclear-bag fibre. Note the spiral course adopted by the primary sensory terminals (arrows). x 3,200



FIGURES 86-89. The fine structure of sensory nerve terminals in muscle spindles of 16 DPN rat.

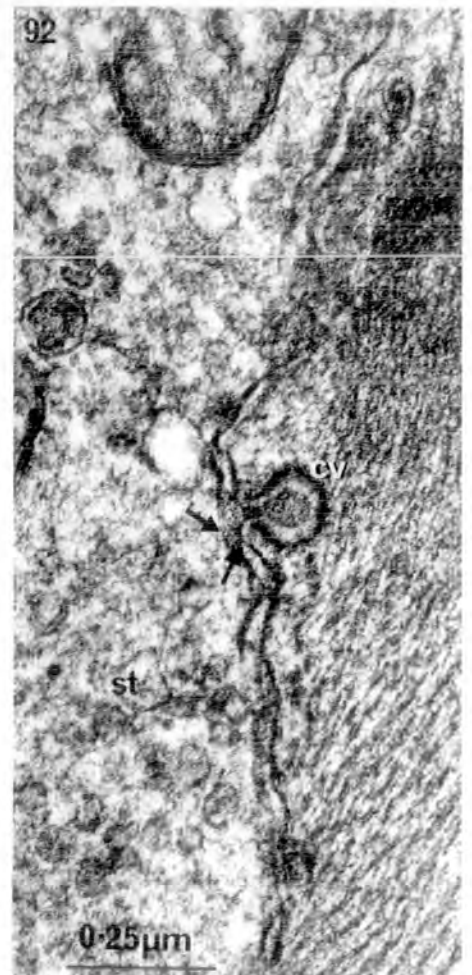
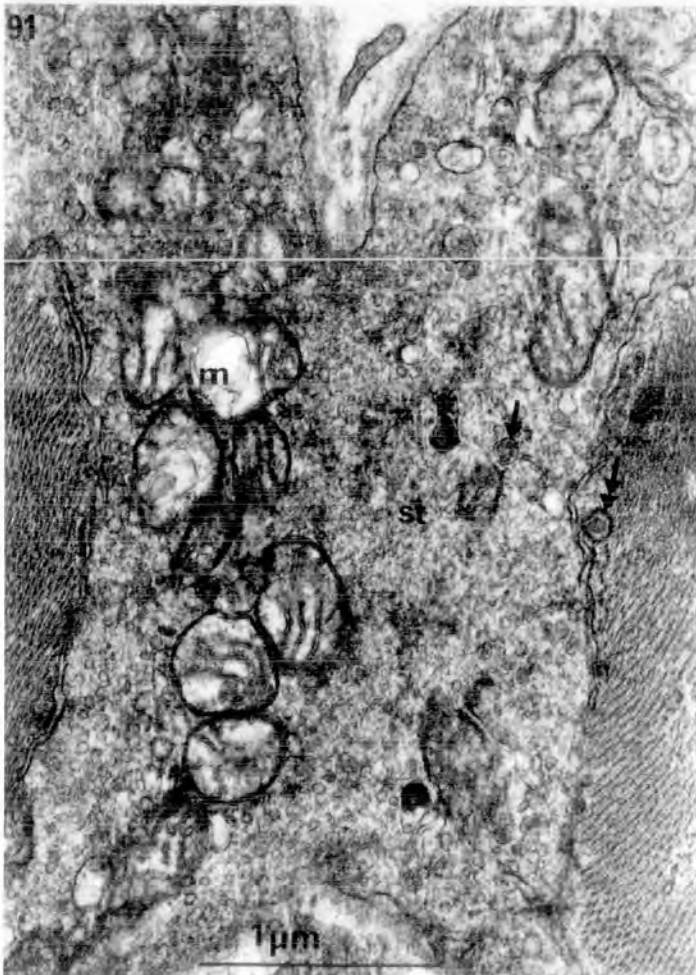
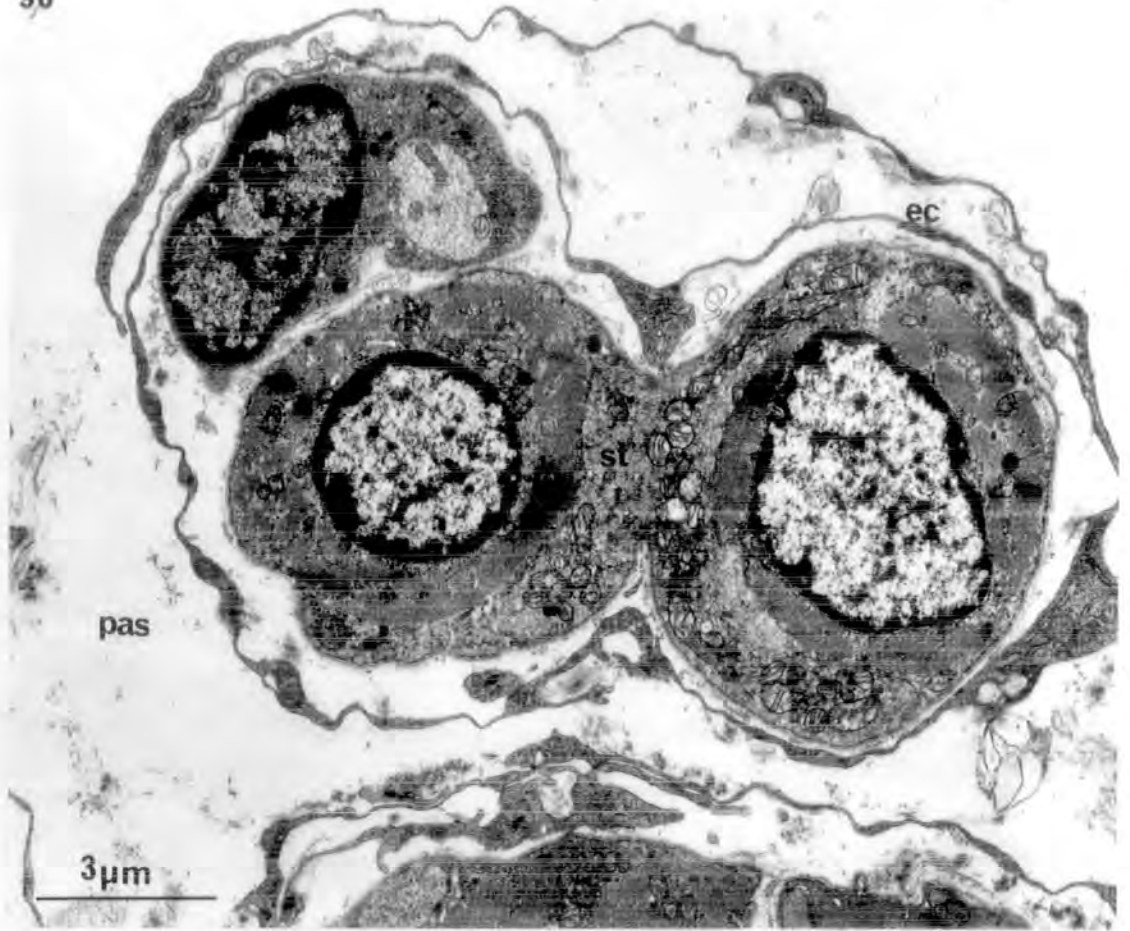
86. Transverse section of a primary sensory terminal on a nuclear-chain fibre. Note the numerous mitochondria, and smooth, clear vesicles, and the absence of dense-cored vesicles. Arrows point to specializations of the synaptic membranes. x 32,000
87. Higher power electron micrograph of a "desmosome-like" thickening of the synaptic membranes, shown in fig. 86. x 126,000
88. Higher power electron micrograph of an incompletely-formed coated vesicle at the synaptic sarcolemma, shown in fig. 86. x 126,000
89. Transverse section of a sensory terminal, showing two stages in the formation of coated vesicles in the underlying sarcoplasm. Arrow points to a thickened region of the sarcolemma that is beginning to invaginate. A fully-formed coated vesicle lies to one side of it. Note the numerous smooth vesicles in the sensory terminal. x 80,000

86



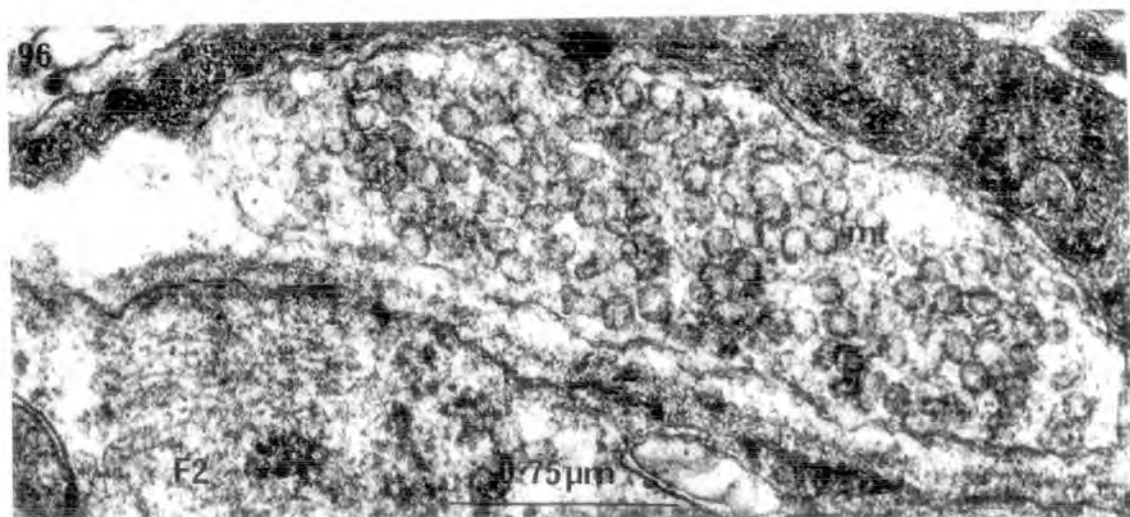
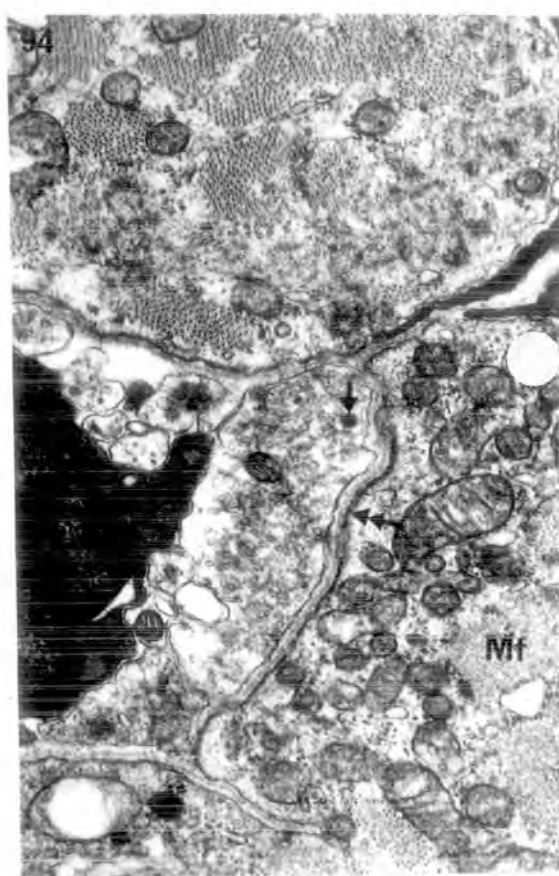
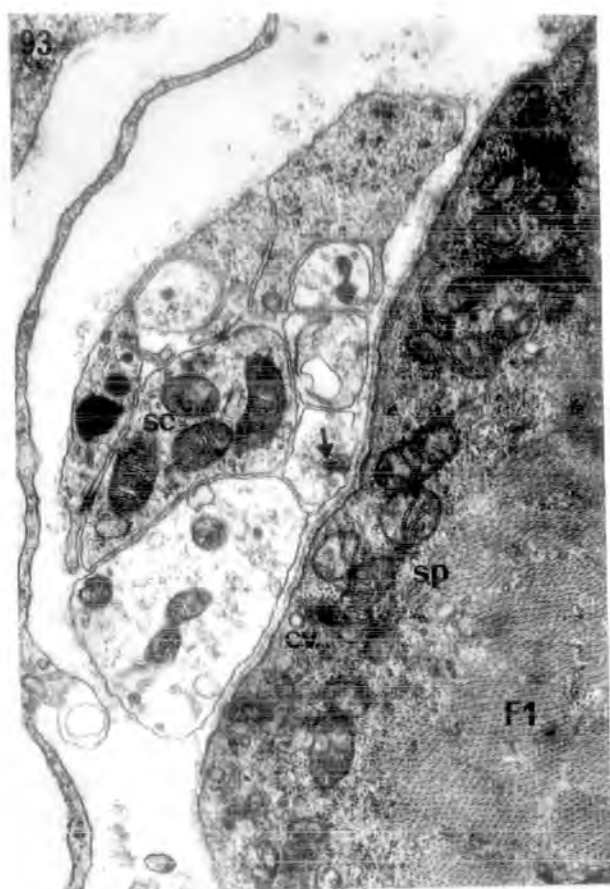
FIGURES 90-92. The fine structure of sensory nerve terminals in muscle spindles of 16 DPN rat.

90. Transverse section of a sensory cross-terminal on two nuclear-chain fibres. Note the common basement membrane and endomysial enclosure. x 8,000
91. Higher power electron micrograph of the terminal shown in fig. 90. Note the central core of mitochondria, the smooth, clear vesicles and the large dense-cored vesicle (arrow) in the terminal. Double arrow points to an invaginating coated vesicle of the sarcolemma, that contains a core of material. x 32,000
92. Higher power electron micrograph of the synaptic surfaces of the terminal shown in figs. 90 and 91. The invaginating coated vesicle contains a core of electron-dense material that appears to be continuous with the axolemma and axoplasm of the terminal. Arrows point to a double layer of plasma membrane in the supposed area of exocytosis. x 80,000



FIGURES 93-96. The fine structure of motor nerve terminals in shank muscle of newborn rat.

93. Transverse section of a polar motor terminal, on F1 of a spindle. Note the absence of primary and secondary synaptic clefts; the thinly spread sole-plate containing a coated vesicle; occasional synaptic and dense-cored (arrow) vesicles in the terminal, and the basement membrane in the synaptic gap. Scale as in fig. 95. x 20,000
94. Transverse section of a motor nerve terminal on extrafusal muscle fibres. Note the sole-plate, primary synaptic cleft, the thickening of the post-synaptic sarcolemma (double arrow), the abundance of synaptic vesicles and single dense-cored vesicle (single arrow) in the large terminal. Scale as in fig. 95. x 20,000
95. Transverse section of a juxta-equatorial motor terminal, innervating F1 of a spindle. Note the abundance of synaptic vesicles, the single dense-cored (single arrow) vesicle, and the absence of mitochondria from the terminal. Schwann cell coverings, post-junctional folds and sole-plate are absent. Basement membrane occupies the synaptic cleft. Note the adjacent overlapping sensory terminals containing numerous dense-cored vesicles (single arrows). x 20,000
96. Transverse section of a mid-polar nerve terminal innervating F2 of a spindle. Note the absence of mitochondria, dense-cored vesicles and post-junctional folds. x 40,000



FIGURES 97-99. The fine structure of fusimotor terminals
in developing muscle spindles of rat.

97. Transverse section of a mid-polar motor terminal on F1 and F3 of 4 DPN spindle. Note the absence of primary and secondary synaptic clefts and sole-plate from the sub-terminal sarcoplasm.

Arrows point to dense-cored vesicles.

x 20,000

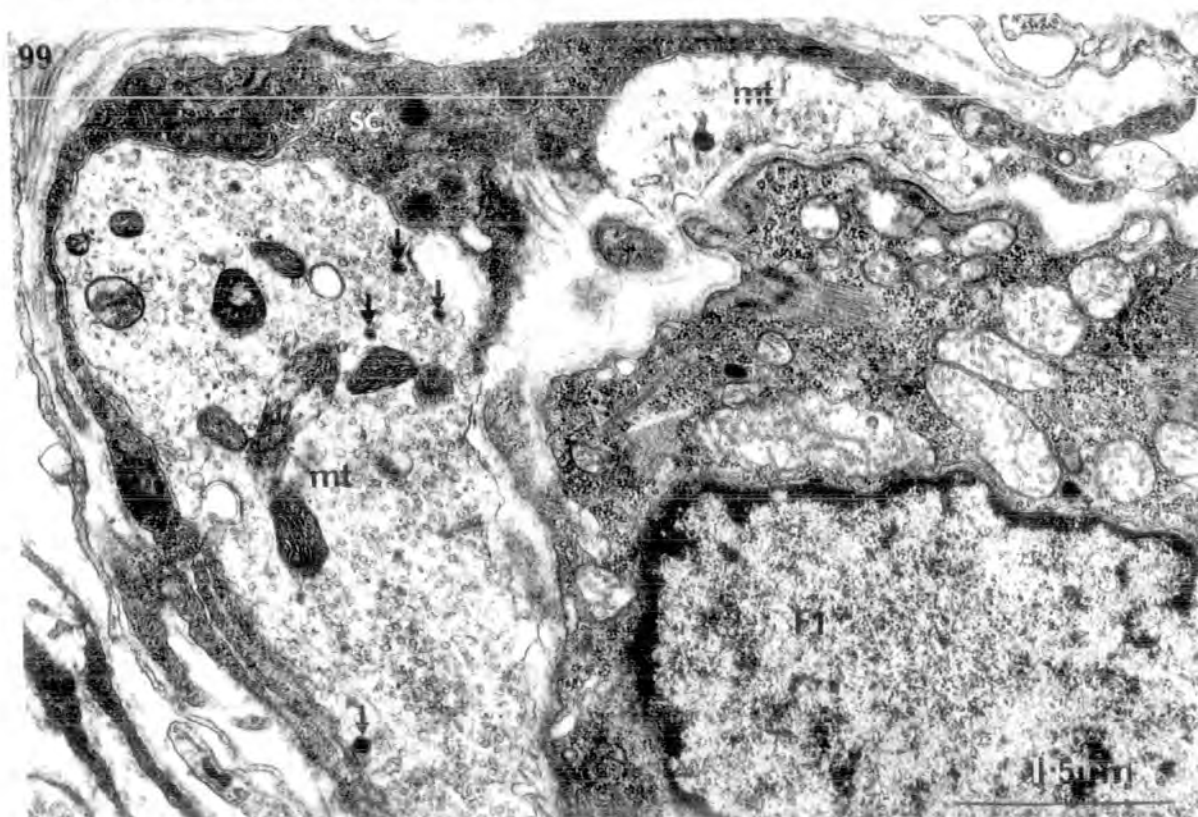
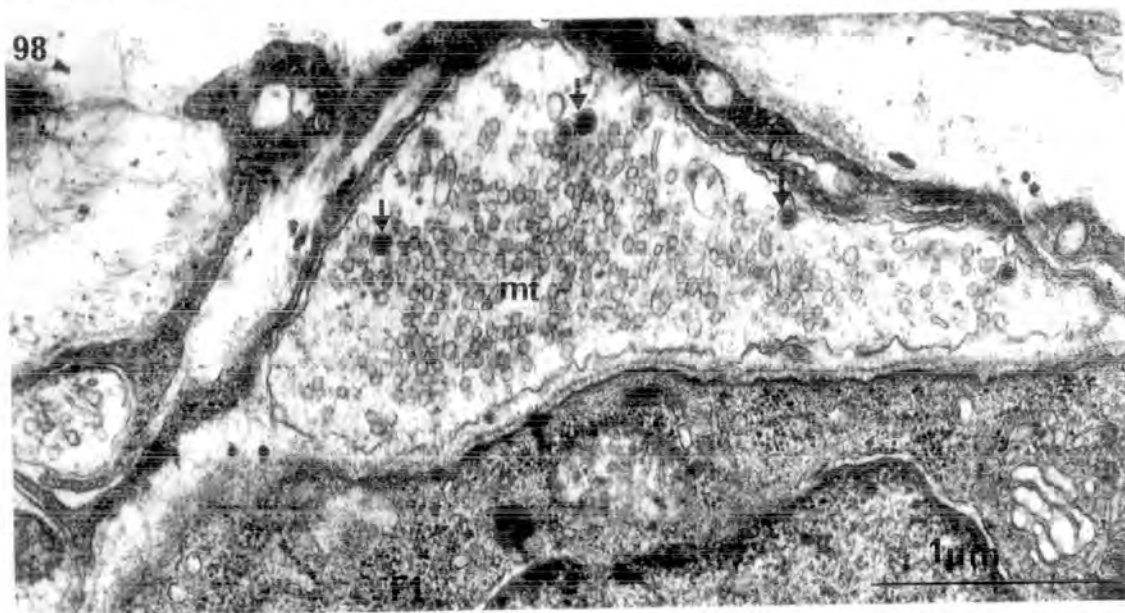
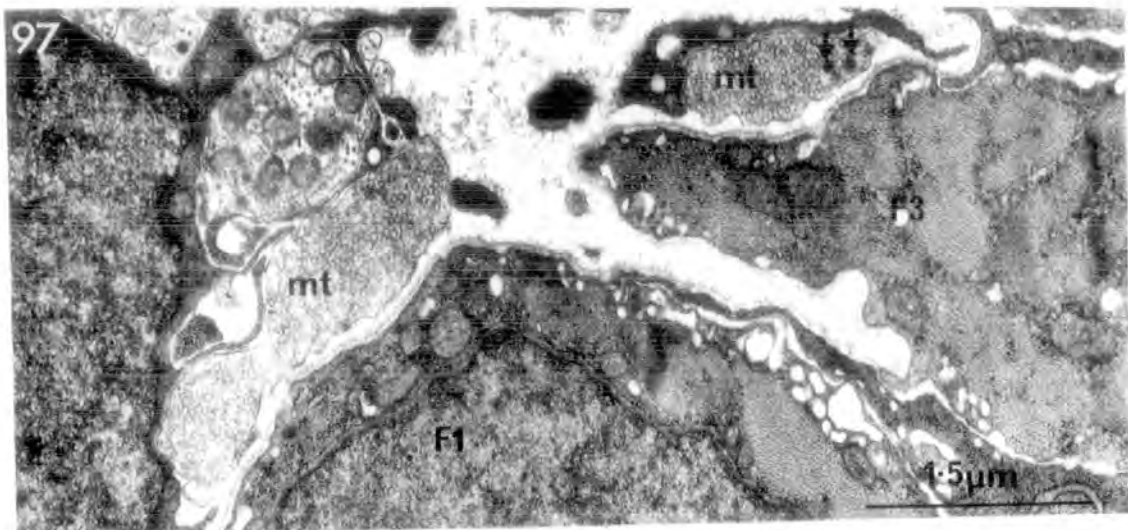
98. Transverse section of a mid-polar motor terminal on F1 of a 12 DPN spindle. Note the absence of post-junctional folds and sole-plate sarcoplasm. The terminal axolemma has a crenate appearance. Arrows point to dense-cored vesicles.

x 32,000

99. Transverse section of a polar plate motor terminal on a nuclear-bag fibre of a 12 DPN spindle. Note the thinly spread sole-plate and the wide and shallow post-junctional folds.

Arrows point to dense-cored vesicles.

x 19,000



FIGURES 100-103. The fine structure of capsule cells in developing muscle spindles of rat.

100. 19.5 DF. Transverse section of an extrafusal fibroblast and myoblast. Note the elongate shape of the fibroblast and the numerous profiles of granular ER cisternae in its cytoplasm. The nucleus of the myoblast is in mitosis.
x 8,000
101. 19.5 DF. Transverse section of a spindle capsule cell, that also surrounds the spindle nerve trunk. Note the similarity in structure between this cell and the extrafusal fibroblast shown in fig. 100. Basement membrane is absent from the capsule cell but surrounds a nearby Schwann cell. x 7,500
102. 20 DF, Transverse section of spindle capsule cells. Note the electron density of the inner capsule cell and the micropinocytotic vesicles (arrows) in the outer cells. Basement membrane is absent from both types of cell.
x 7,500
103. Newborn. Transverse section of spindle capsule cells. Note the more compact shape and the abundance of granular ER cisternae in the inner cells compared to the outer cells. Basement membrane covers the Schwann cell only.
x 12,600



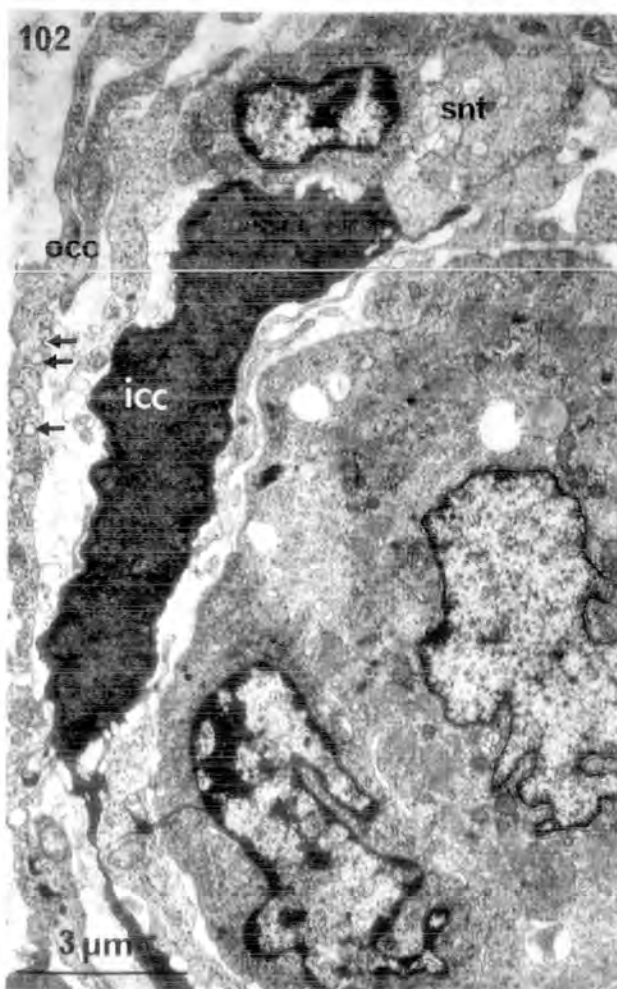
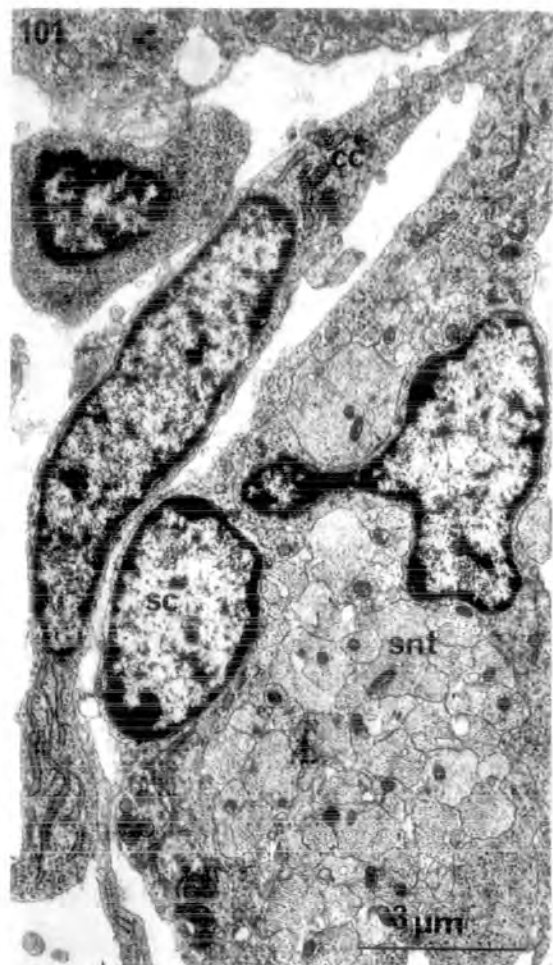
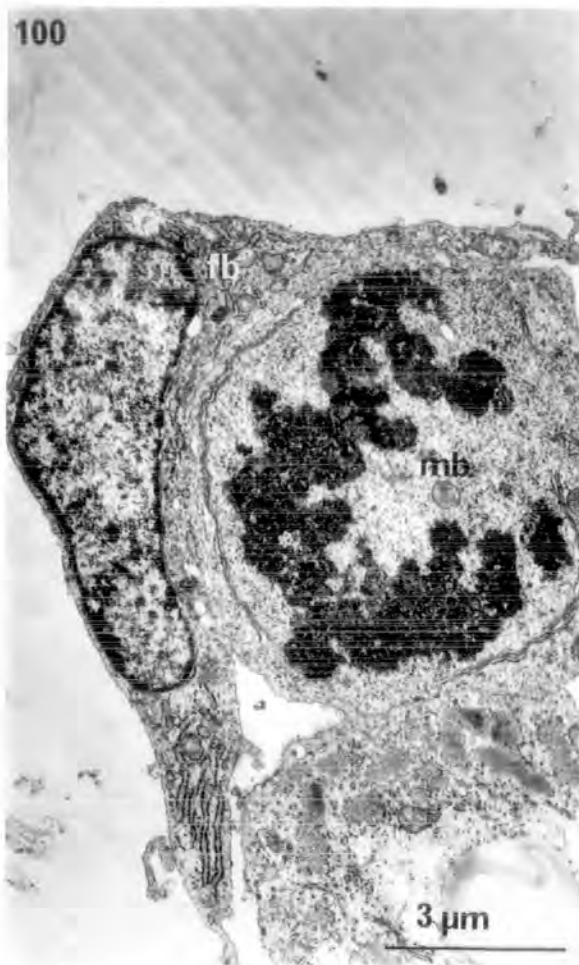


FIGURE 104. The fine structure of the capsule cells of a muscle spindle in 20.5 DF rat; transverse section through the juxta-equatorial region.

Note the numerous profiles of granular ER cisternae and polyribosomes in the inner capsule cells, that lack basement membrane. Single arrows point to close-junctions between capsule cells.

The outer capsule cells differ by their more flattened elongate shape, paucity of granular ER cisternae and the presence of micropinocytotic vesicles. The spindle nerve trunk is enclosed by the outer capsule cells.

x 12,800

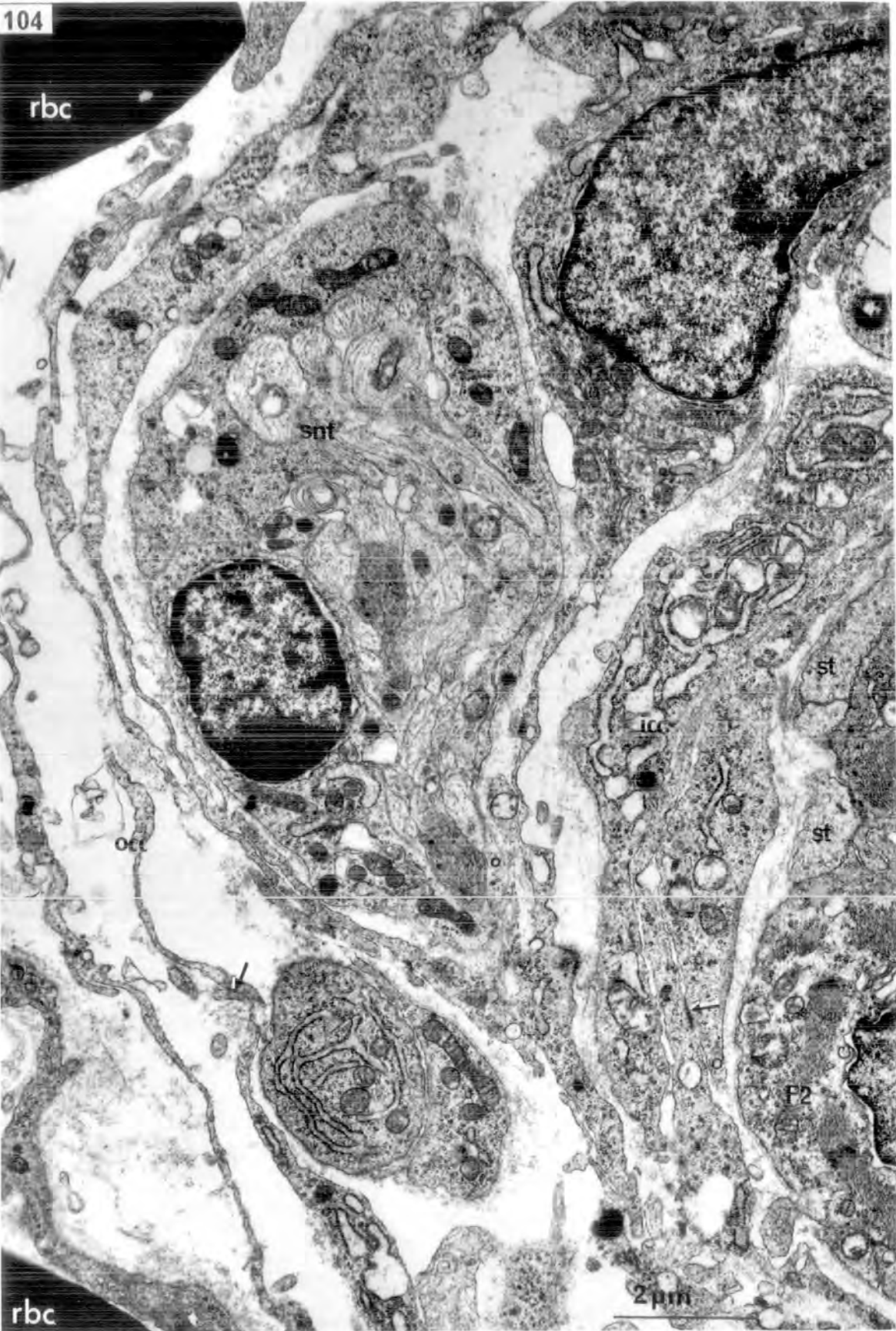
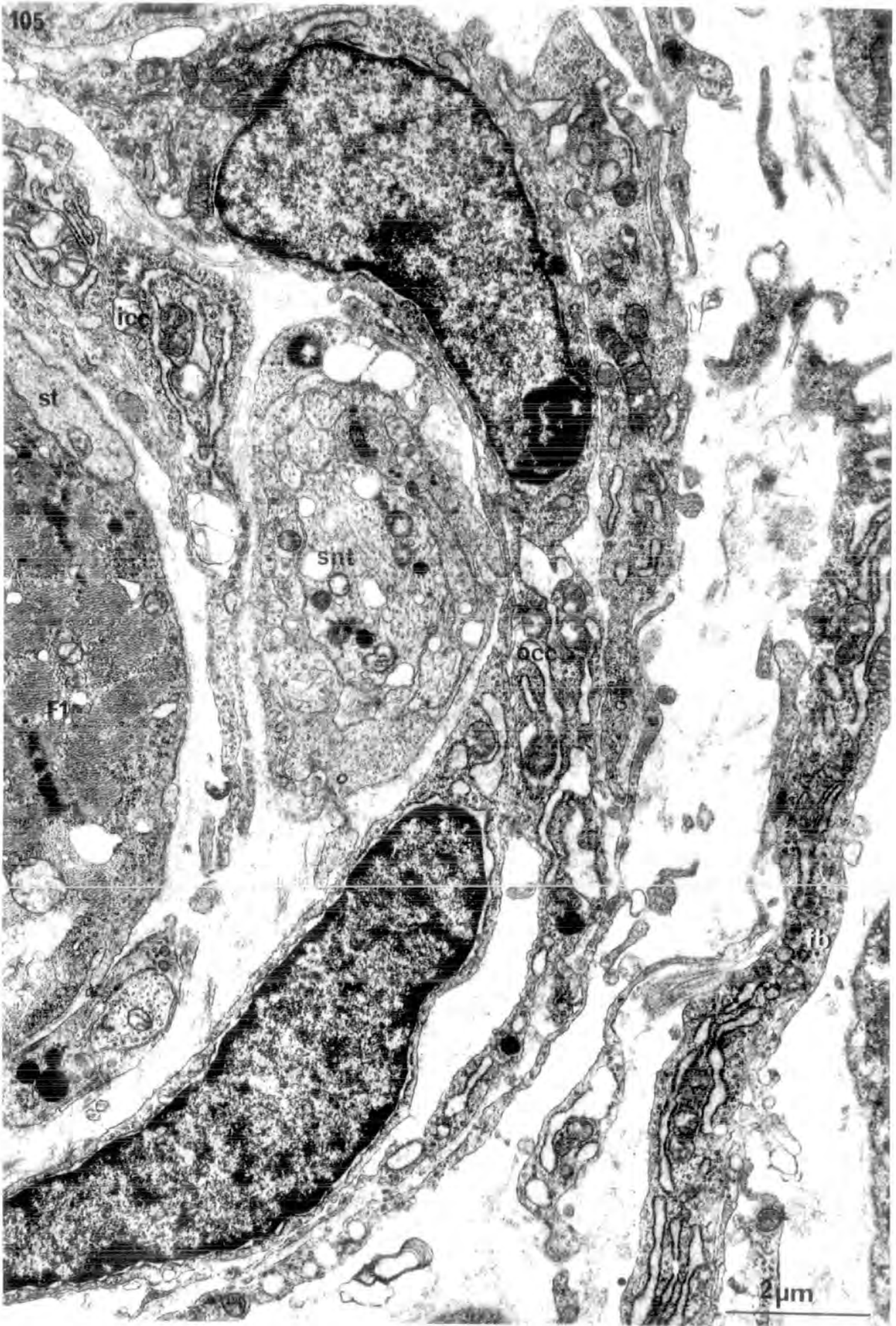


FIGURE 105. The fine structure of the capsule cells of a muscle spindle in 20.5 DF rat; transverse section through the juxta-equatorial region.

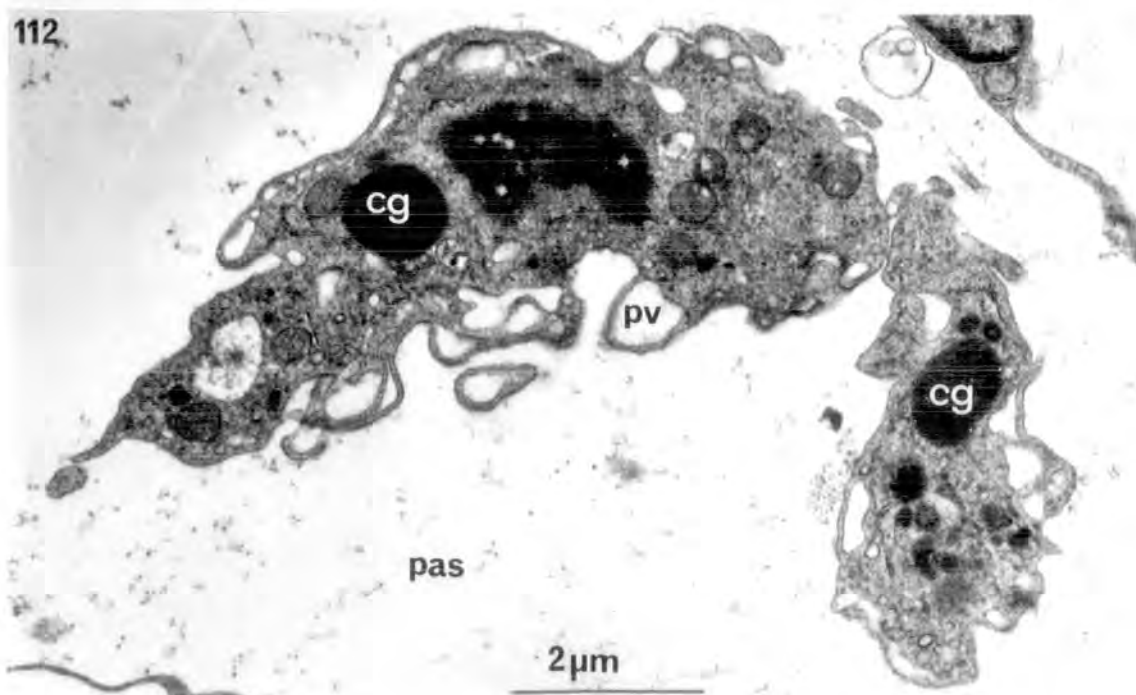
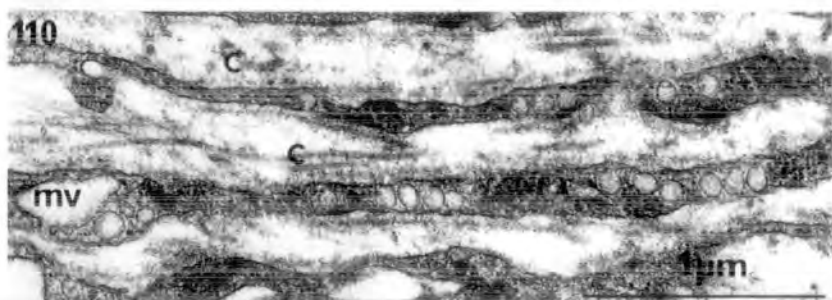
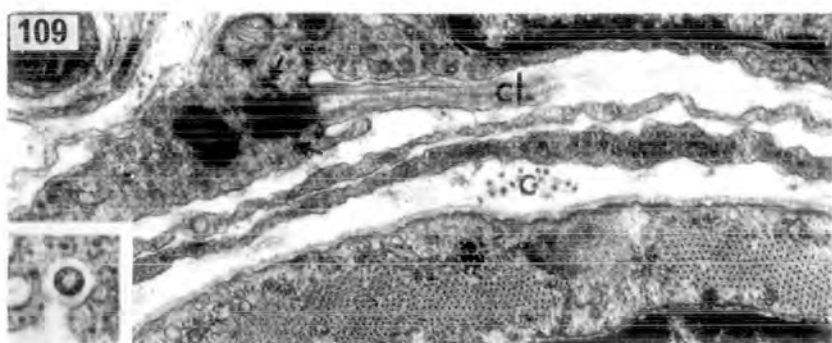
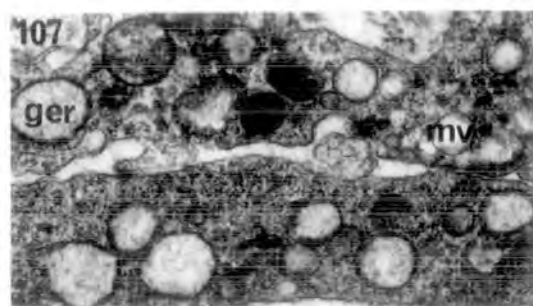
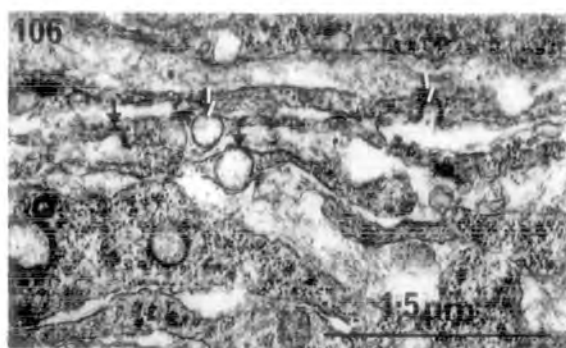
Both outer and inner capsule cells are of a similar structure to the extrafusal fibroblast; all contain numerous profiles of granular ER and lack basement membrane.

x 12,800



FIGURES 106-112. The fine structure of capsule cells in developing muscle spindles of the rat.

106. Newborn. Transverse section of an outer capsule cell. Arrows point to micropinocytotic vesicles.
x 20,000
107. 2 DPN. Transverse section of outer capsule cells. Note the dilated micropinocytotic vesicles and granular ER cisternae. Scale as in fig. 106.
x 20,000
108. 2 DPN. Transverse section of outer capsule cells, showing the distribution of collagen and elastic fibrils between the cell layers. Scale as in fig. 106.
x 20,000
109. 2 DPN. Transverse section of an inner capsule cell of the spindle shown in fig. 70. Note the paired centrioles, one of which gives rise to an atypical cilium that lies in an invagination of the plasma membrane. Arrows point to satellite elements associated with the centriole. Inset: transverse section of a similar cilium. Note the absence of central fibres. Scale as in fig. 106. x 20,000
110. 16 DPN. Transverse section of capsular sheet cells. Note the numerous micropinocytotic vesicles, the thin covering of basement membrane and collagen fibrils.
x 32,000
111. 16 DPN. Transverse section of endomysial cells. Note the electron-dense cytoplasm. Arrows point to close junctions. Basement membrane is absent.
x 12,600
112. 16 DPN. Transverse section of a vacuolated cell in the periaxial space of the spindle shown in fig. 75. Note the peripheral pinocytotic vacuoles and the absence of basement membrane. x 12,800

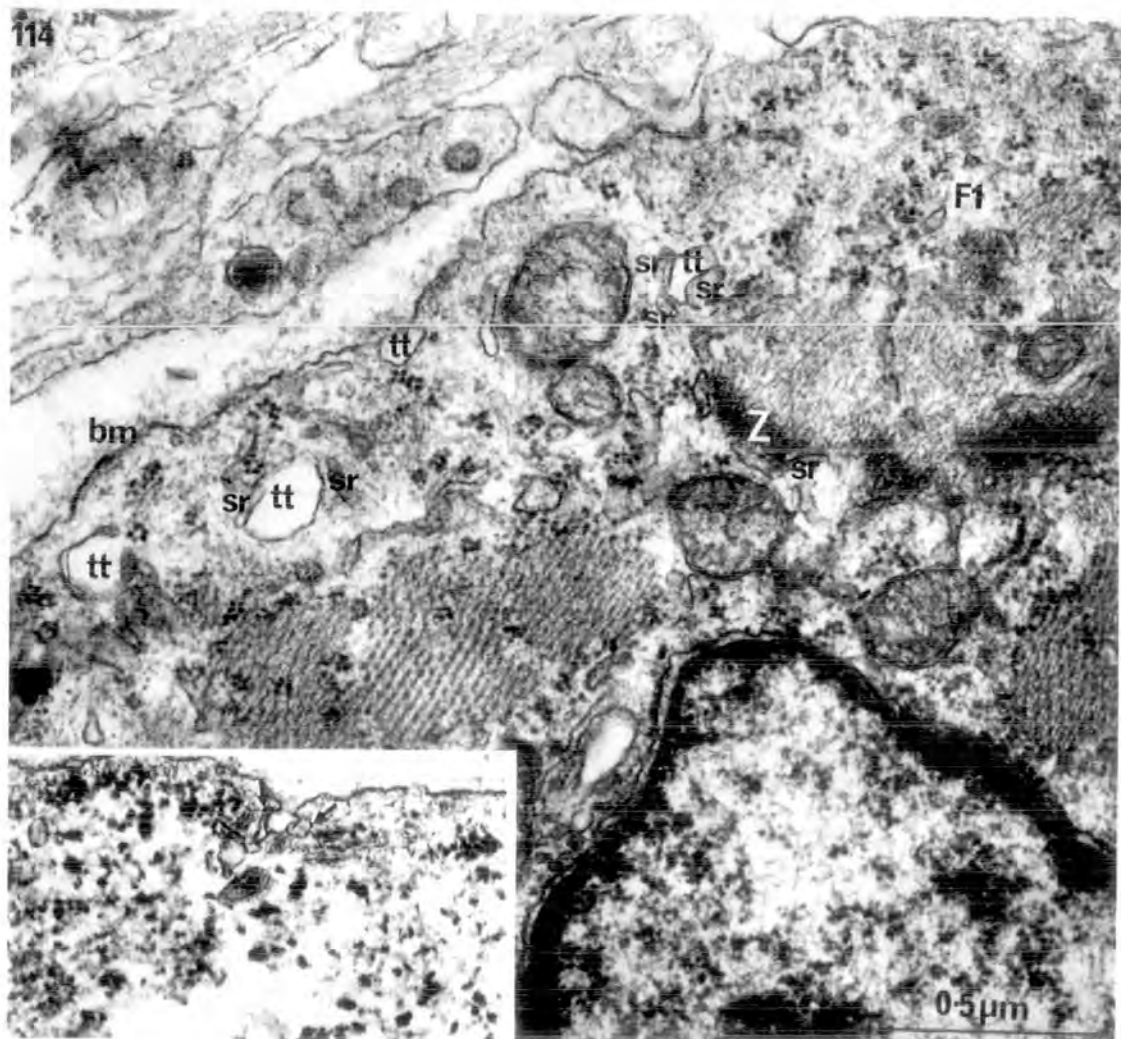
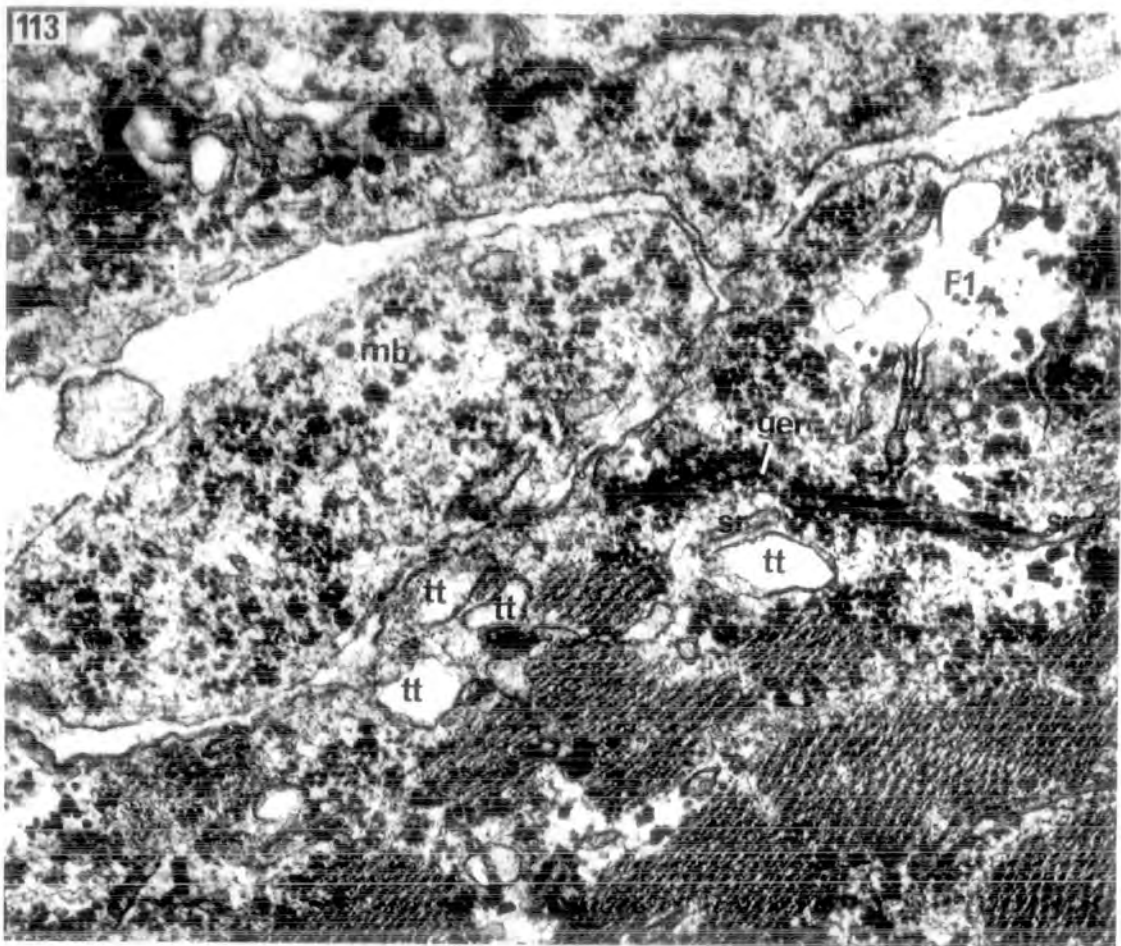


FIGURES 113-114. The fine structure of Fl in muscle spindles of 19.5 DF rat.

113. Transverse section through the juxta-equatorial region of Fl. A myoblast lies within the basement membrane of Fl. Note the flattened SR tubules, some of which stem from granular ER cisternae. T tubules have clear lumens and are longitudinally orientated. Scale as in fig. 114. x 60,000

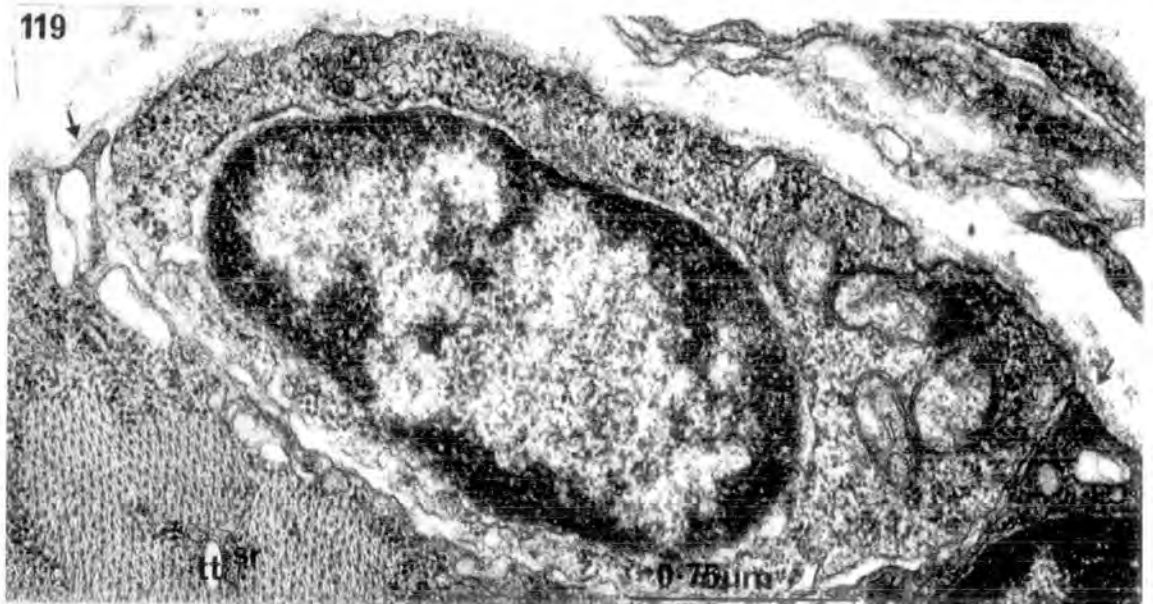
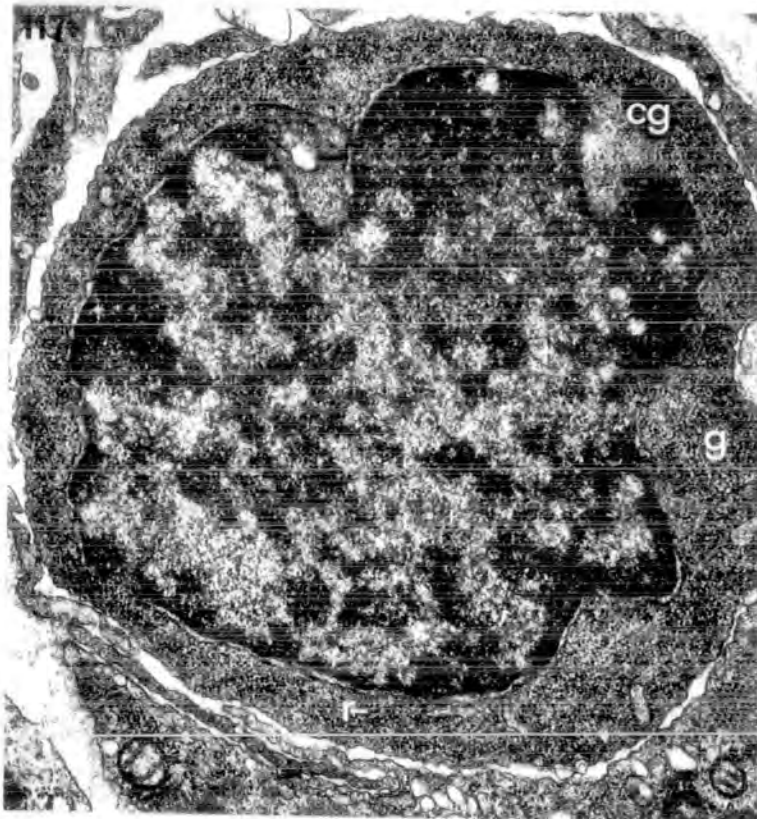
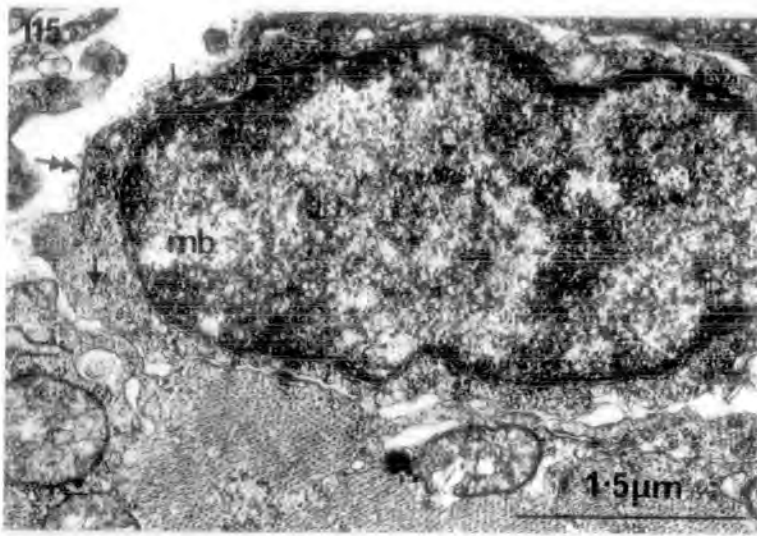
114. Transverse section through the juxta-equatorial region of Fl. Note the numerous junctional complexes of the SR and TT systems; the T tubule budding from the sarcolemma and the association of SR tubules with the Z-band region of the myofibril. x 60,000

Inset shows an invaginating T tubule of the sarcolemma associated with two SR tubules (arrows). Scale as in fig. 114. x 60,000



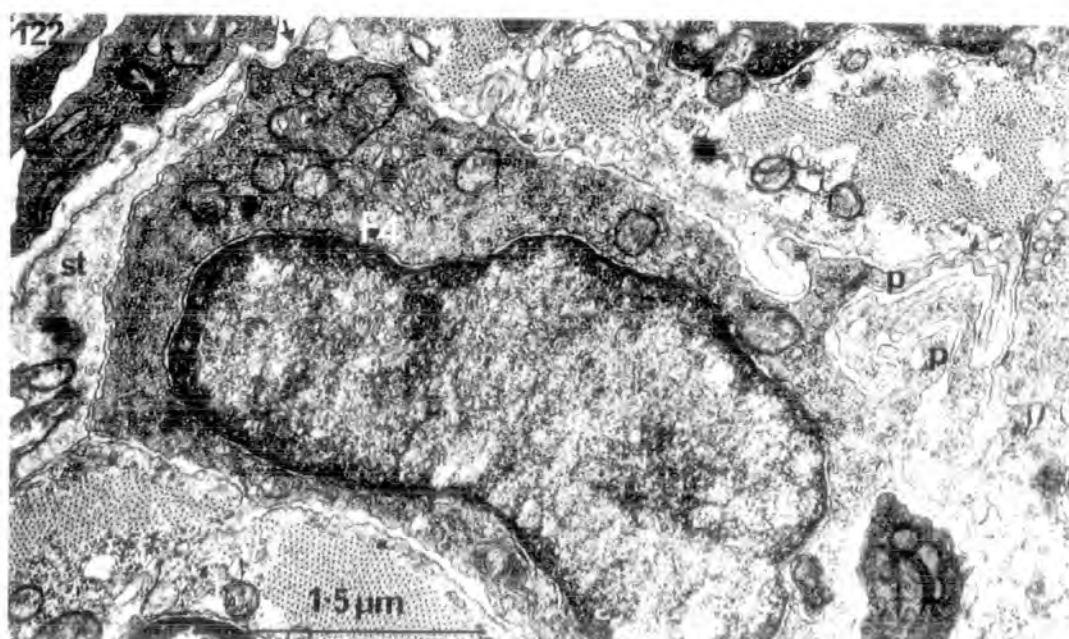
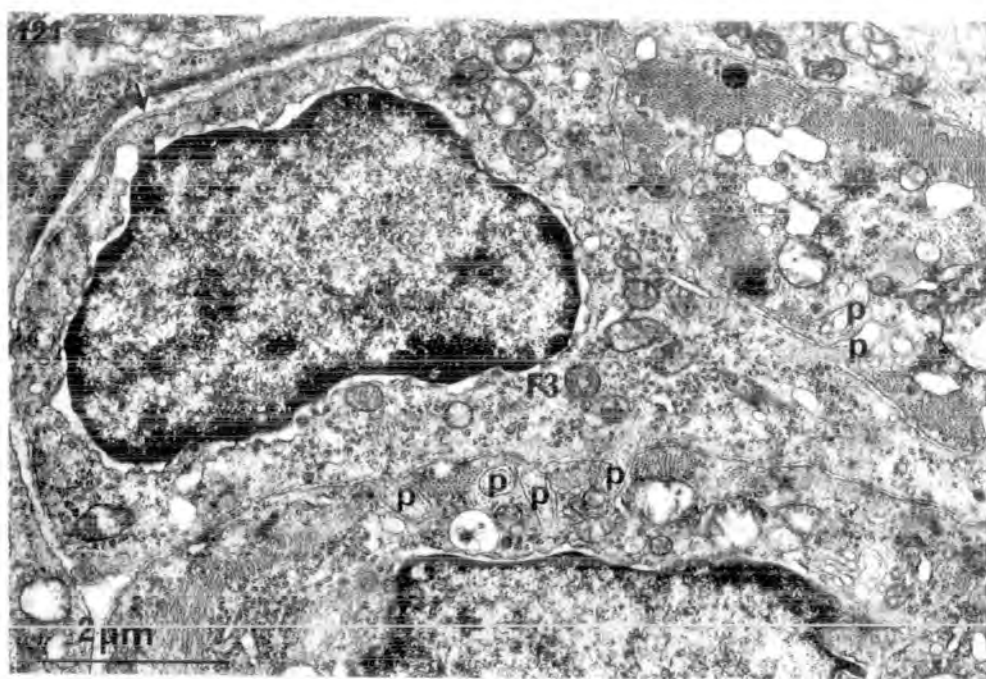
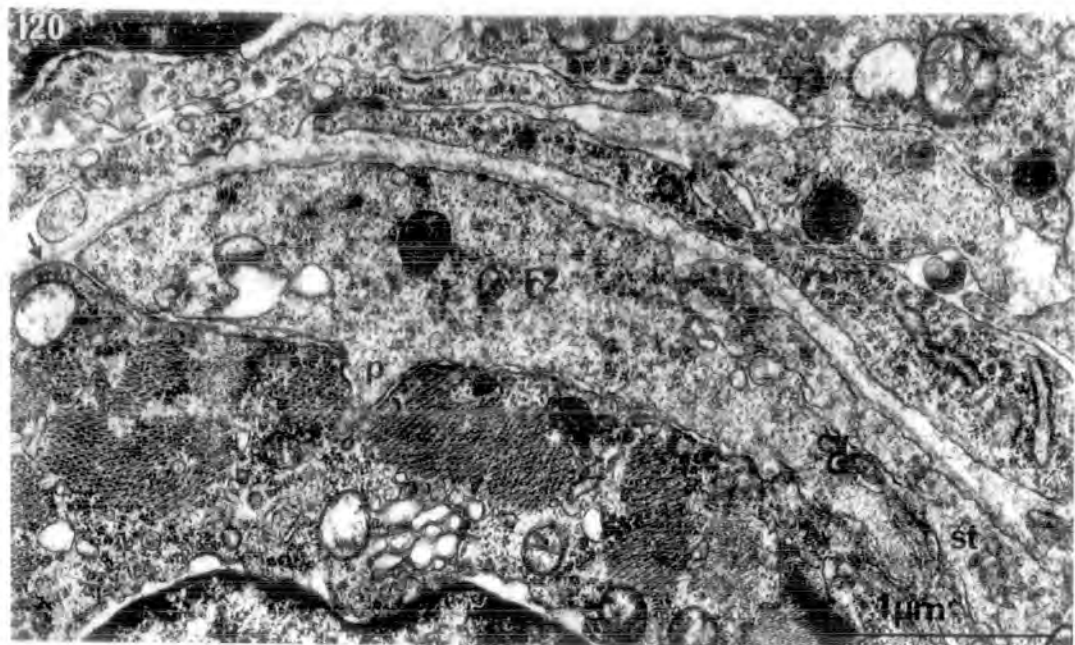
FIGURES 115-119. The fine structure of myoblasts in developing muscle spindles of rat.

115. 20.5 DF. Transverse section of an intrafusal myoblast. Note the large chromatin-packed nucleus that occupies most of the cytoplasm. Single arrows point to free ribosomes. Double arrow points to basement membrane. x 20,000
116. Newborn. Transverse section of the anucleate portion of an intrafusal myoblast. Note the elongate mitochondria, granular ER cisternae (single arrows) and numerous free ribosomes. Double arrow points to basement membrane. x 12,600
117. Newborn. Transverse section of an intrafusal myoblast that is totally enclosed by the myotubes of the axial bundle. Scale as in fig. 115. x 20,000
118. 4 DPN. Transverse section of an enclosed intrafusal myoblast. Note the single juxta-nuclear centriole (double arrow), large mitochondria and dilated cisternae of granular ER. Scale as in fig. 116. x 12,600
119. 12 DPN. Transverse section of a satellite cell enclosed within the basement membrane (arrows) of a nuclear-chain fibre. Note the similarity in structure to the myoblast shown in fig. 115. x 40,000



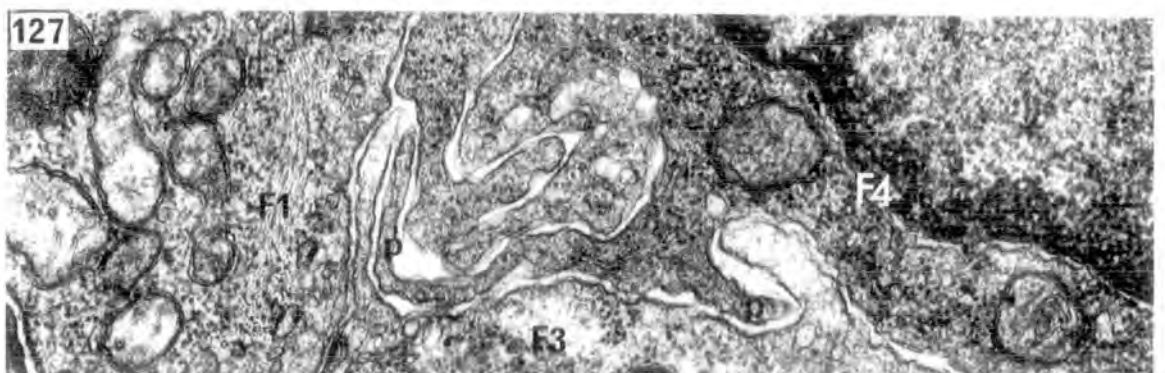
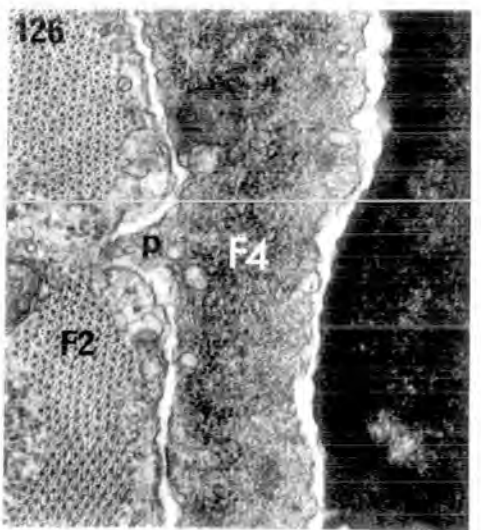
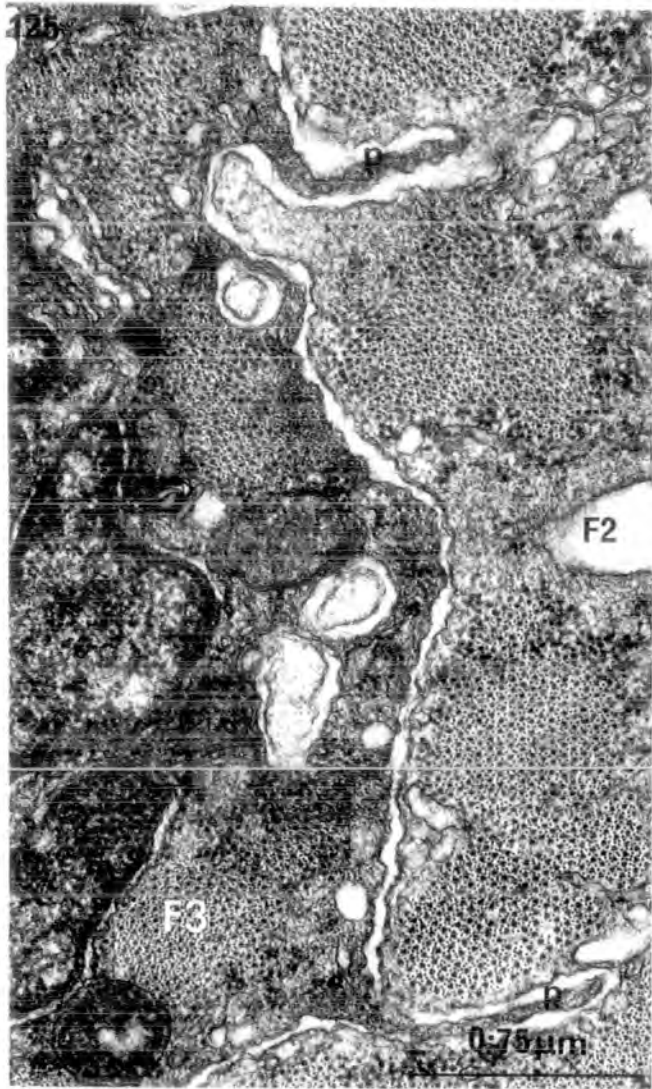
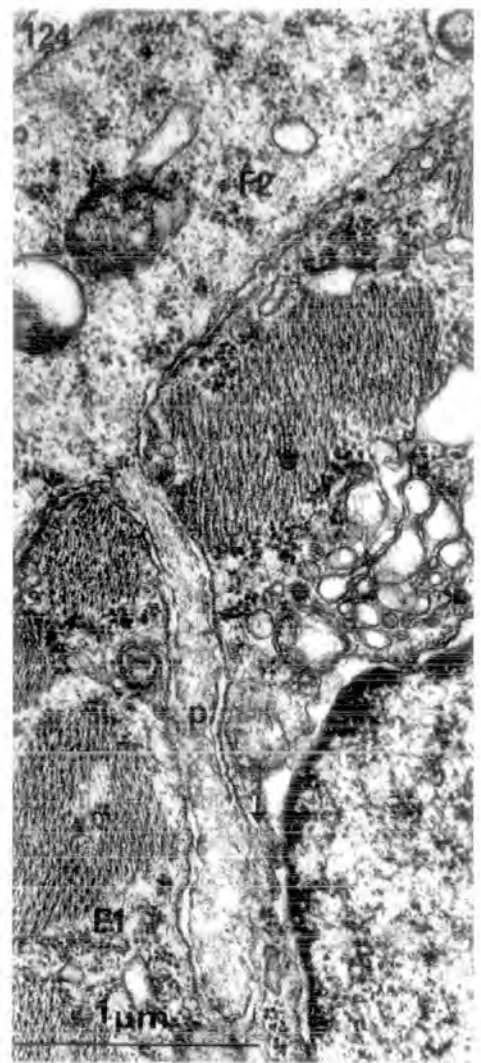
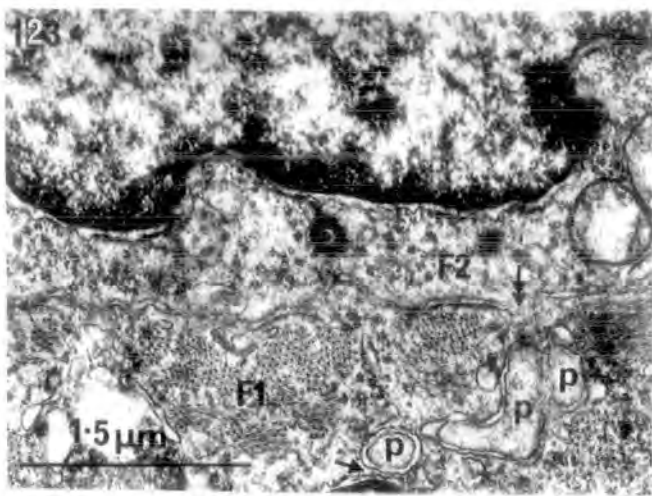
FIGURES 120-122. The fine structure of immature myotubes
in developing muscle spindles of rat.

120. 20 DF. Transverse section of immature F2. Note the short unbranched pseudopodial extension of the sarcoplasm of F2.
x 32,000
121. Newborn, FHL. Transverse section of immature F3. Note the short unbranched pseudopodial extensions, running both transversely and longitudinally in the sarcoplasm of F1 and F2. x 12,600
122. 2 DPN. Transverse section of immature F4. Note the paucity of myofibrils and the electron density of the cytoplasm of F4. Pseudopodial extensions are long and unbranched. x 20,000
Arrows point to basement membrane.



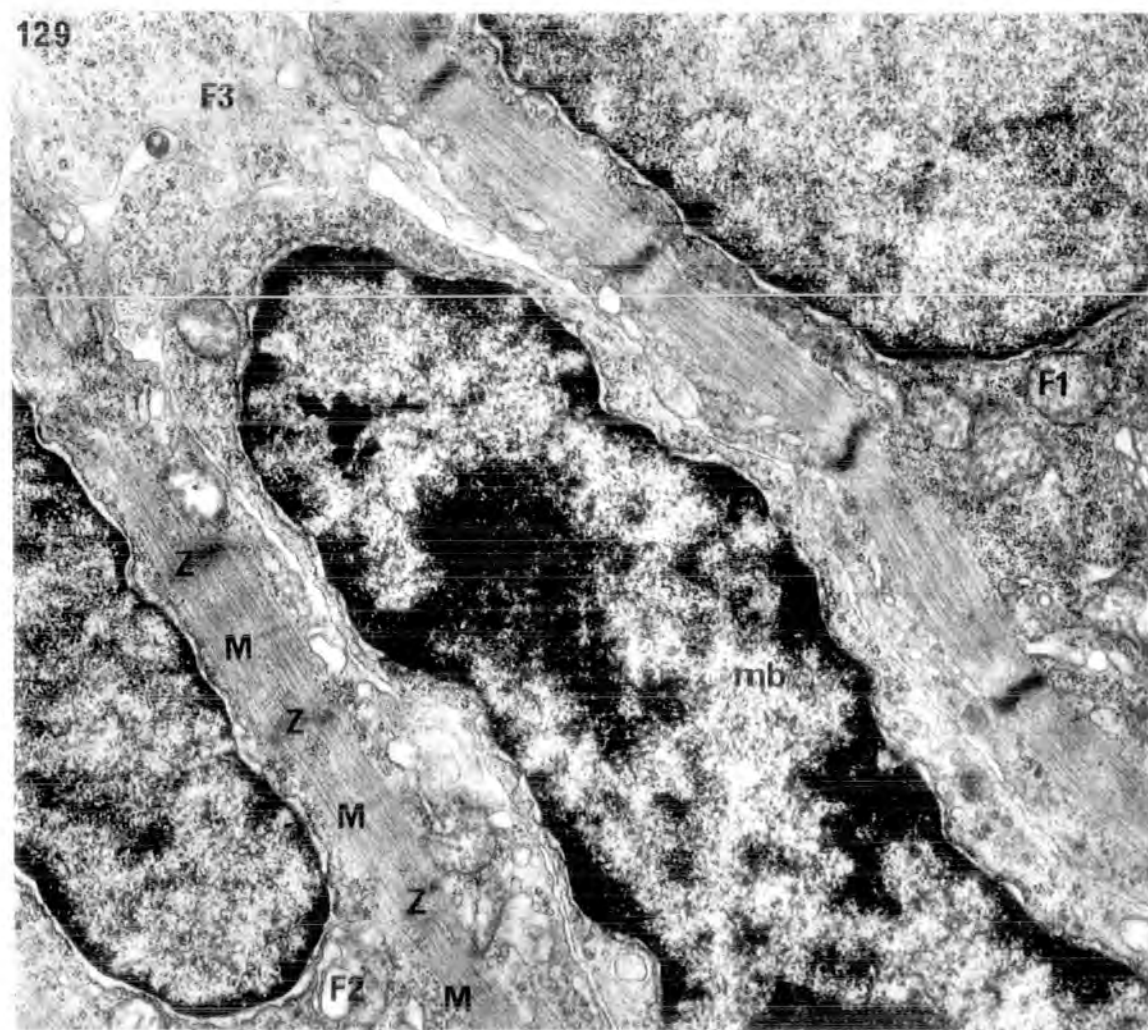
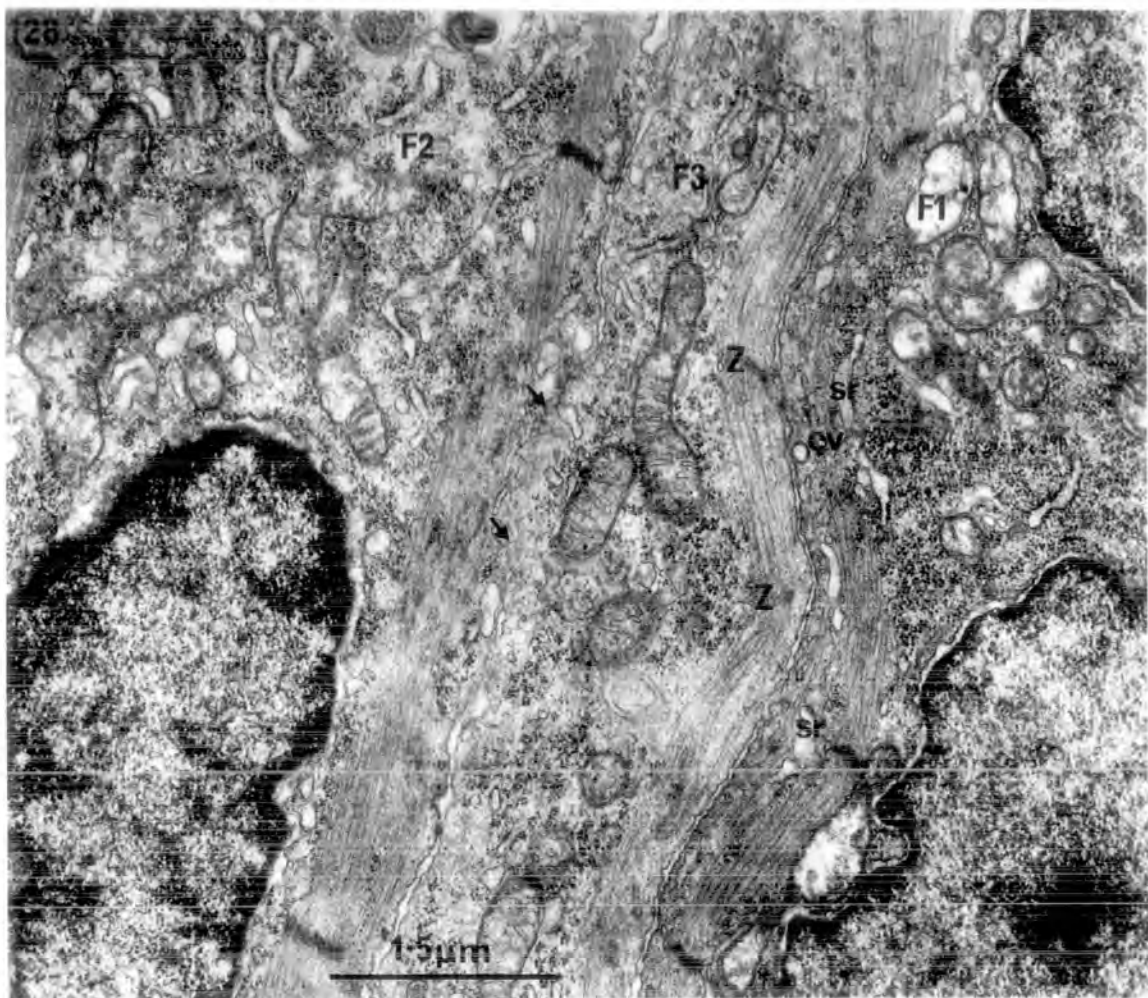
FIGURES 123-127. The fine structure of the pseudopodial extensions of immature myotubes in developing muscle spindles of rat.

123. 20 DF. Transverse section of immature F2. Note the association of a longitudinally orientated pseudopodial extension with the nuclear envelope (single arrow). Double arrow points to an area of indistinct membrane separation. Note also the centriole in F2.
x 20,000
124. 20.5 DF. Transverse section of immature F2. Single arrow points to the close association of the long unbranched pseudopodial extension with the nuclear envelope of F1. Note the immaturity of F2 compared to F1. x 32,000
125. Newborn. Transverse section of immature F3. Note the long, unbranched pseudopodial extensions that are transversely orientated, and the abundance of myofibrils in F3. x 40,000
126. 2 DPN. Transverse section of immature F4. The pseudopodial extension is short and unbranched. Note the paucity of assembled myofibrils in F4. Scale as in fig. 124.
x 32,000
127. 2 DPN. Transverse section of immature F3. The pseudopodial extensions are elaborate branched structures that penetrate the superficial sarcoplasm only of F3. Scale as in fig. 125. x 40,000



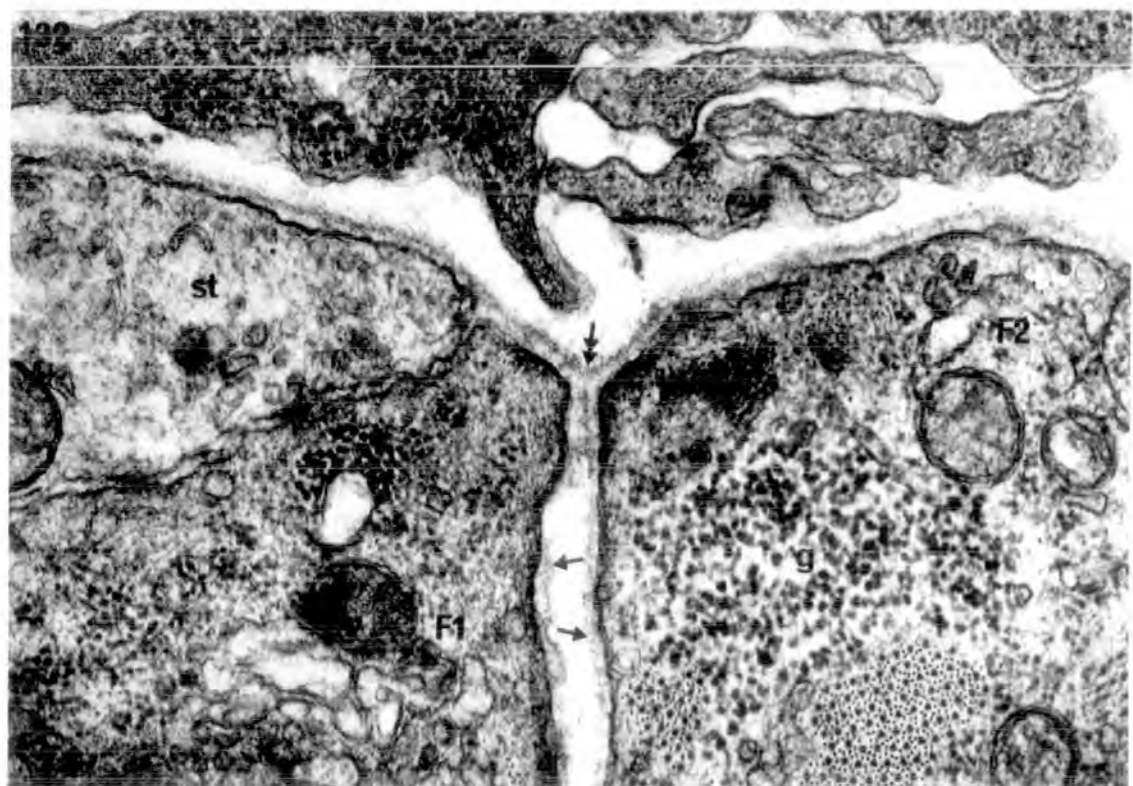
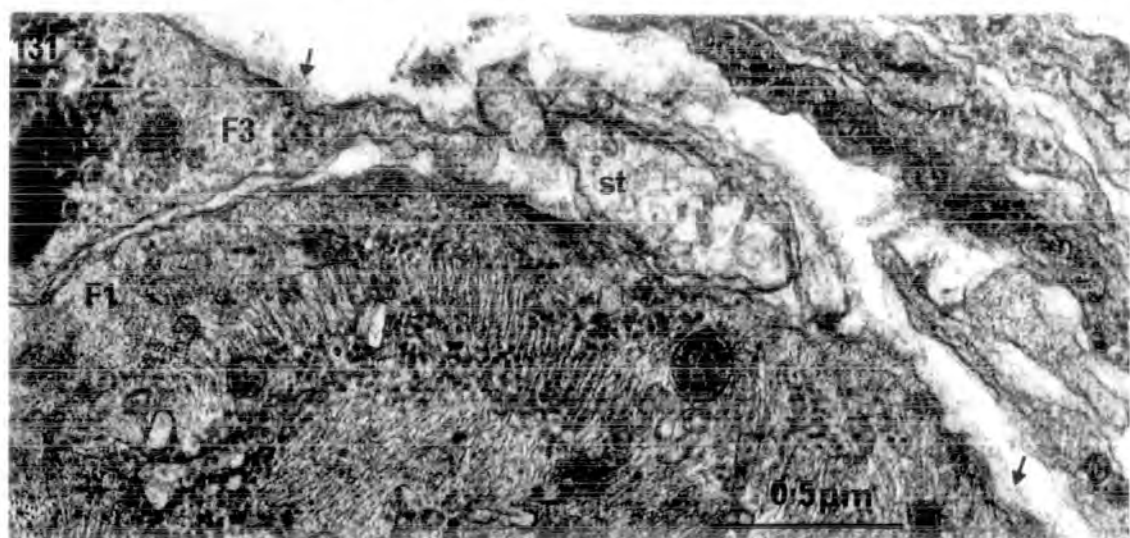
FIGURES 128-129. The fine structure of immature myotubes in muscle spindles of newborn rat FHL.

128. Longitudinal section through the polar region of three intrafusal myotubes that constitute the axial bundle. Note the core of sarcoplasm containing numerous mitochondria, ribosomes and glycogen granules in all three myotubes. F3 is newly formed and contains a single peripheral myofibril in the early stages of assembly. Note the presence of Z bands before any other banding pattern. Arrows point to areas of indistinct membrane separation between F2 and F3.
x 20,000
129. Longitudinal section through the polar region of intrafusal myotubes of the same spindle as shown in fig. 128. F3 is incompletely formed and breaks up into longitudinally orientated myoblasts, occupying a similar position between F1 and F2. Note the M and Z lines in the myofibrils of F2, where no other banding pattern is visible. Scale as in fig. 128. x 20,000



FIGURES 130-132. The fine structure of basement-membrane formation in a muscle spindle of 2 DPN rat.

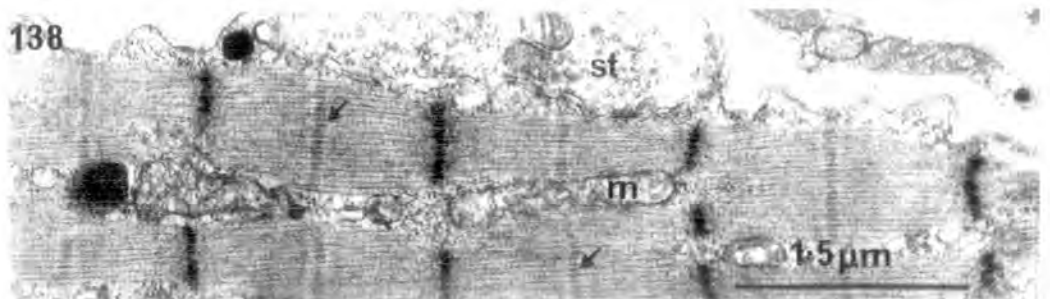
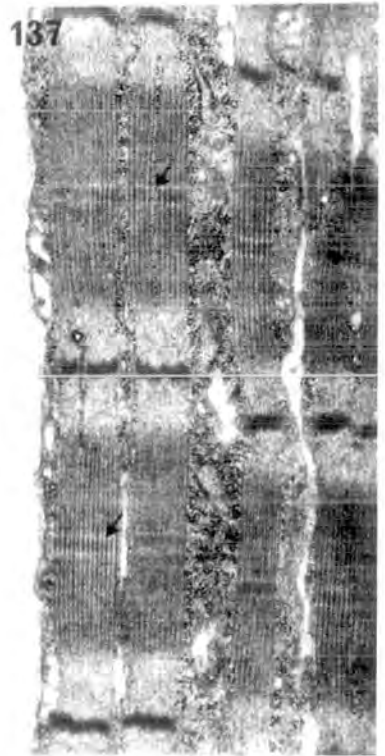
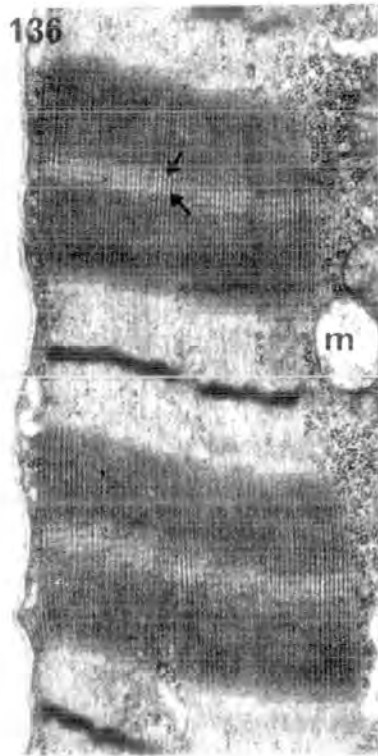
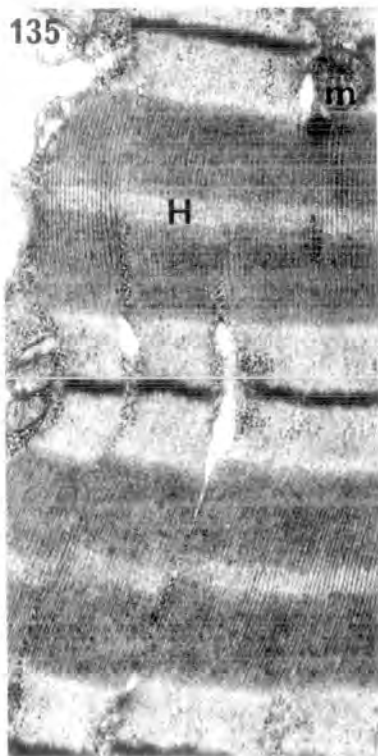
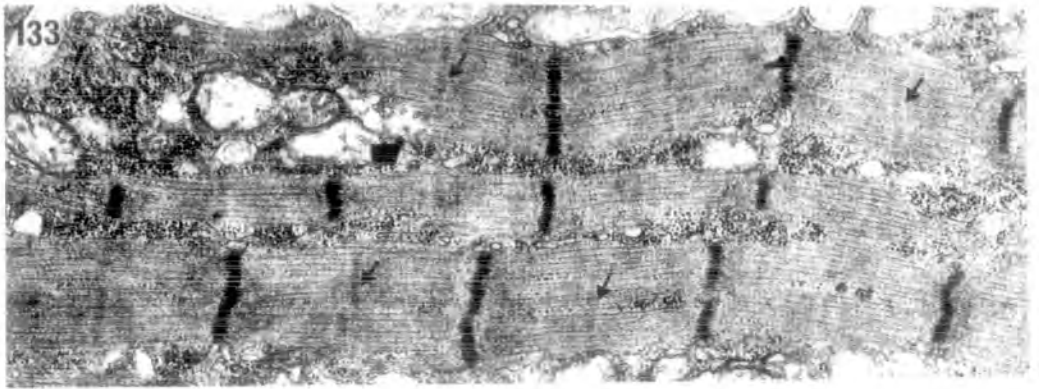
130. Transverse section through the juxta-equatorial region of F2, F3 and F4. Note that the basement membrane (arrows) is confined to the outer surface of the axial bundle. Scale as in fig. 131. x 50,000
131. Transverse section through the juxta-equatorial region of F1 and F3. Basement membrane (arrows) is still confined to the outer surface of the axial bundle. x 50,000
132. Transverse section through the juxta-equatorial region of F1 and F2. Basement membrane is beginning to form on the inner surfaces of the nuclear-bag fibres (single arrows) and appears to stem from the original outer basement membrane (double arrow). Scale as in fig. 131. x 50,000



FIGURES 133-138. The fine structure of intrafusal muscle fibres in developing muscle spindles of rat.

133. Newborn, FHL. Longitudinal section through the polar region of F1. Arrows point to the M line in the centre of the ill-defined H zone.
x 20,000
134. Newborn, FHL. Longitudinal section through the polar region of F2 and F3. Arrows point to M lines. Note the absence of a distinct banding pattern in the myofibrils.
x 20,000
135. 12 DPN. Longitudinal section through the polar region of F1. Note the absence of an M line from the centre of the pseudo H zone. Mitochondria are small and few. x 20,000
136. 16 DPN, PL. Longitudinal section through the polar region of F1. Arrows point to the double M line. Note the small mitochondria and sparse interfibrillar sarcoplasm.
x 20,000
137. 16 DPN, PL. Longitudinal section through the polar region of F2. Arrows point to M lines. Note the abundant interfibrillar sarcoplasm.
x 20,000
138. 16 DPN, PL. Longitudinal section through the polar region of a nuclear-chain fibre. Note the distinct M line (arrows) and large mitochondria.
x 20,000

Scale in fig. 138 refers to all figures.



FIGURES 139-147. The histochemistry of developing extra-fusal muscle fibres in EDL of rat.

Figs. 139-141. Serial transverse sections of EDL of 19.5 DF rat.

139. Alkali pre-incubated ATPase. Arrows point to large myotubes exhibiting a reduced activity. x 900
140. P'ase. Note the small variations in attaining intensity. Arrows point to ATPase-low myotubes. x 900
141. SDH. Note the overall positive reaction of all myotubes. Arrows point to ATPase-low myotubes. x 900

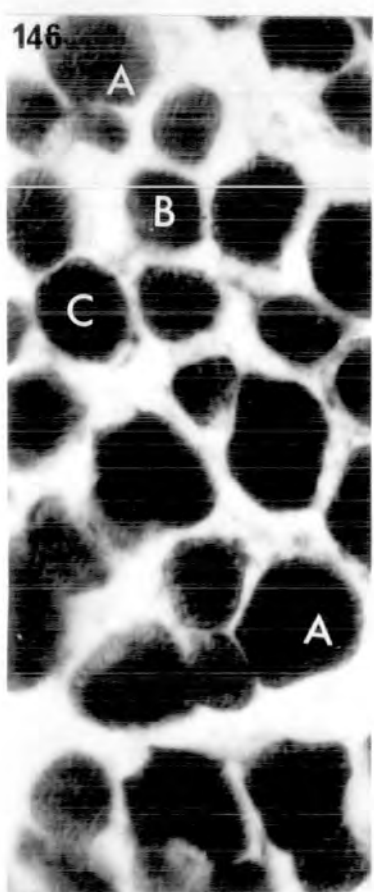
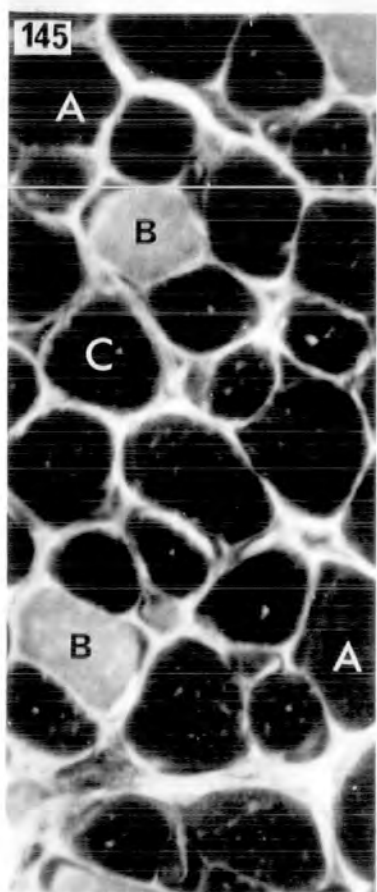
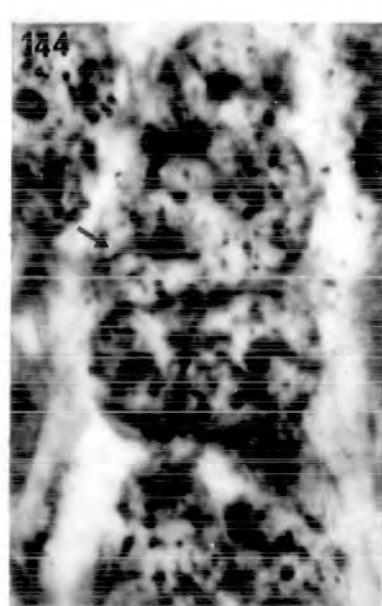
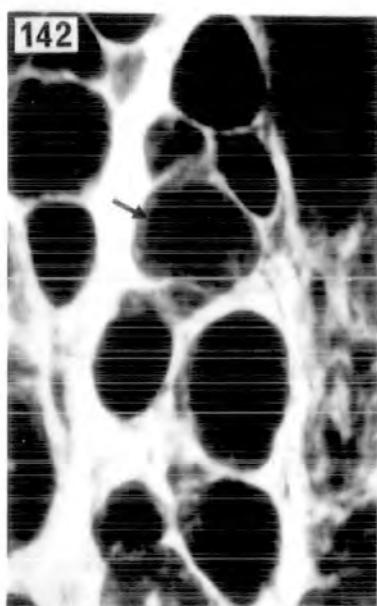
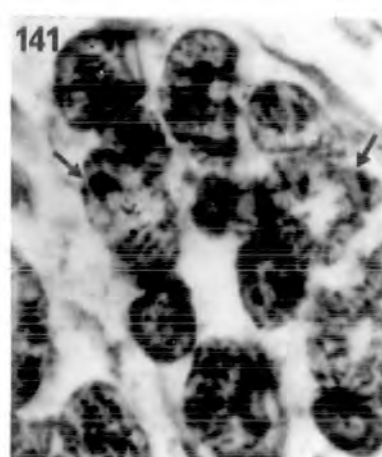
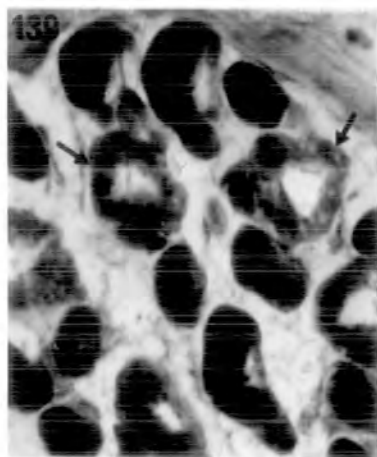
Figs. 142-144. Serial transverse sections of EDL of new-born rat.

142. Alkali pre-incubated ATPase. Arrow points to a large myotube of reduced ATPase activity. x 900
143. P'ase. Arrow points to an ATPase-low myotube, that shows some reduction in P'ase activity. x 900
144. SDH. All myotubes and muscle fibres exhibit equal, positive activity. Arrow points to ATPase-low myotube. x 900

Figs. 145-147. Serial transverse sections of EDL of 8 DPN rat.

145. Alkali pre-incubated ATPase. Note the three types of fibre, differing in diameter and ATPase activity. x 900
146. P'ase. Large A fibres exhibit high activity, whereas B and C fibres exhibit intermediate to low activity. x 900
147. SDH. Large A fibres exhibit low activity compared to types B and C. x 900

Scale on fig. 147 refers to all figures.

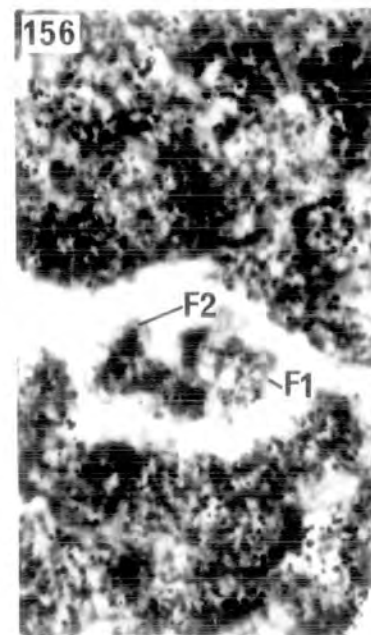
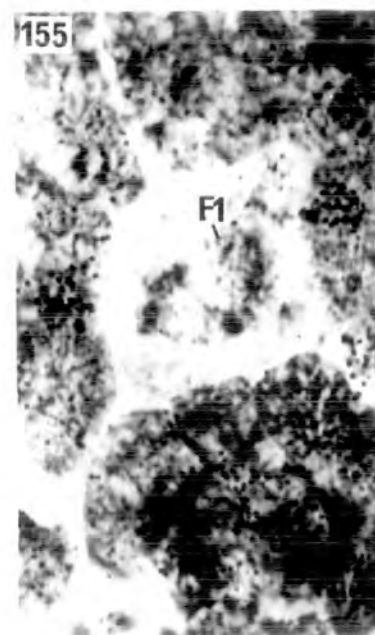
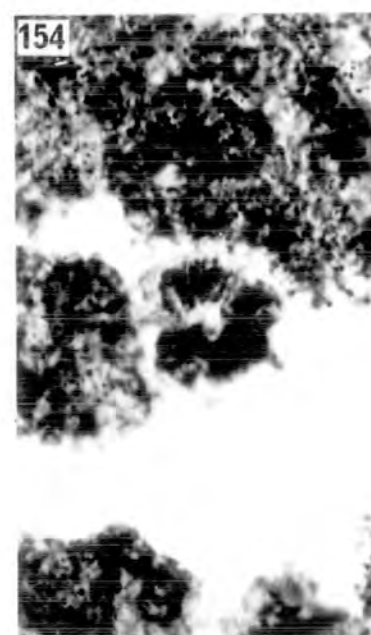
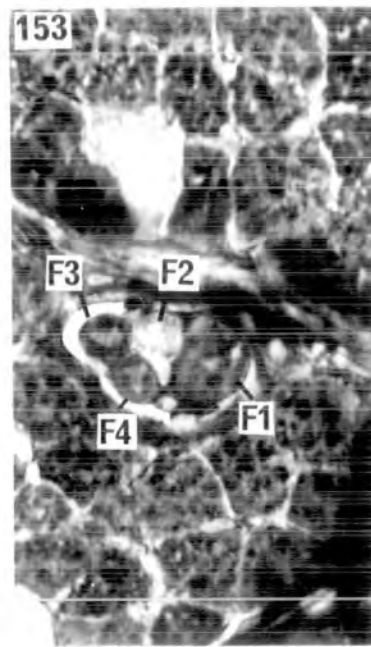
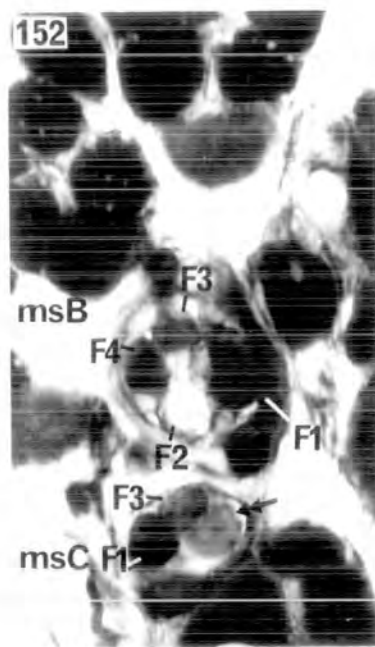
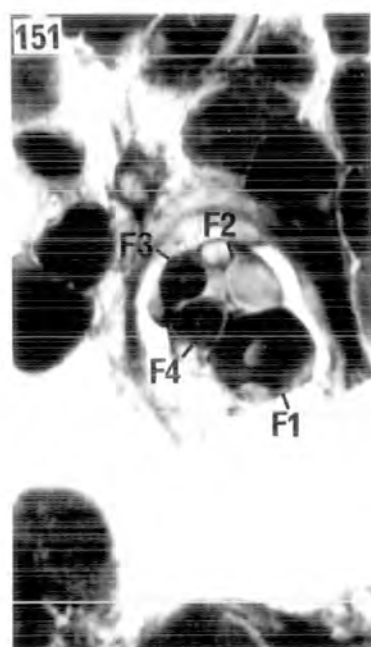
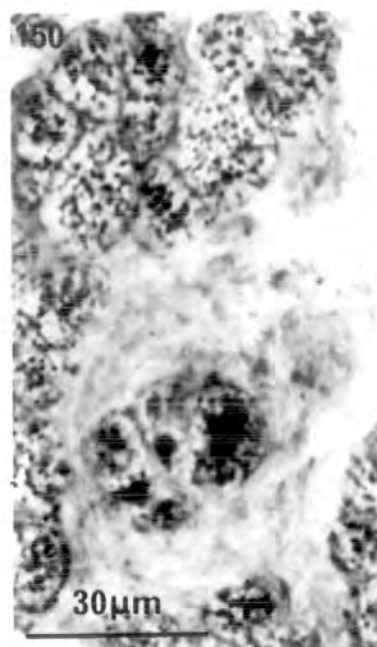
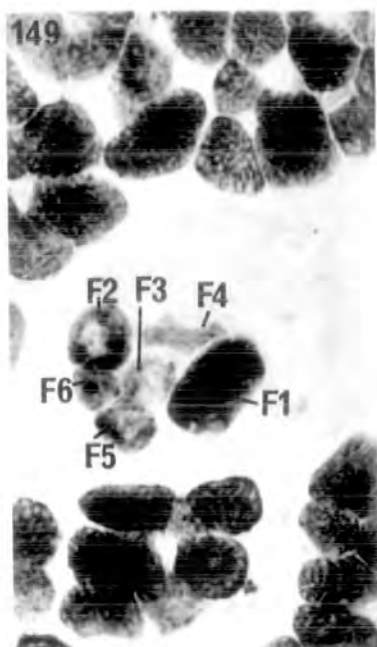


FIGURES 148-156. The histochemistry of developing intra-fusal muscle fibres in PL of rat.

- Figs. 148-150. Serial transverse sections through the juxta-equatorial region of a spindle in 5 DPN rat.
148. Alkali pre-incubated ATPase. Note the equal positive activity of all intrafusal myotubes. x 800
149. P'ase. The large diameter nuclear-bag (F1) exhibits the highest activity, followed by the small diameter bag fibre (F2) and the nuclear-chains (F3-F6). x 800
150. SDH. Note the equal, positive activity of all intrafusal myotubes. x 800

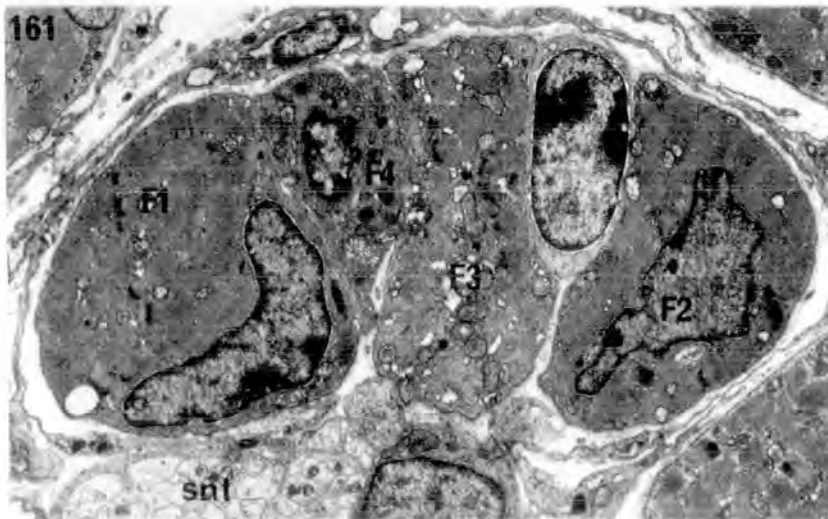
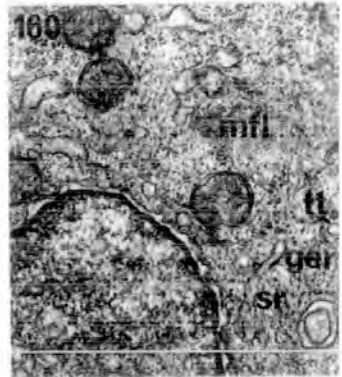
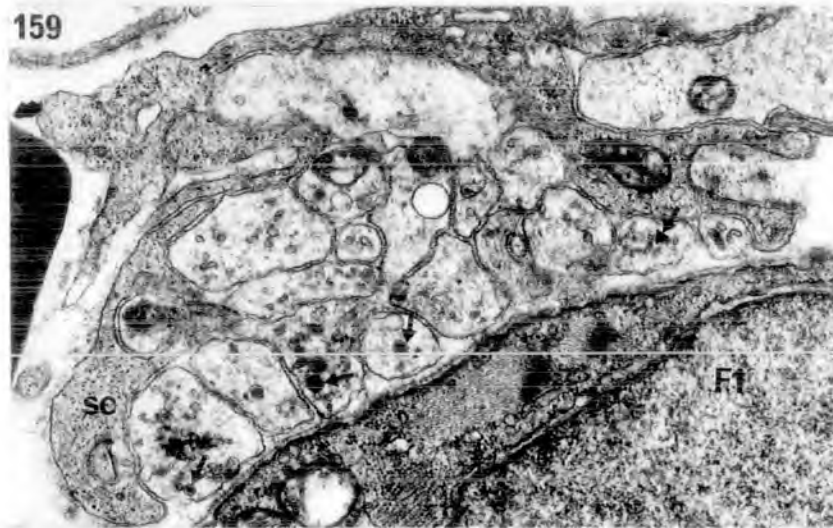
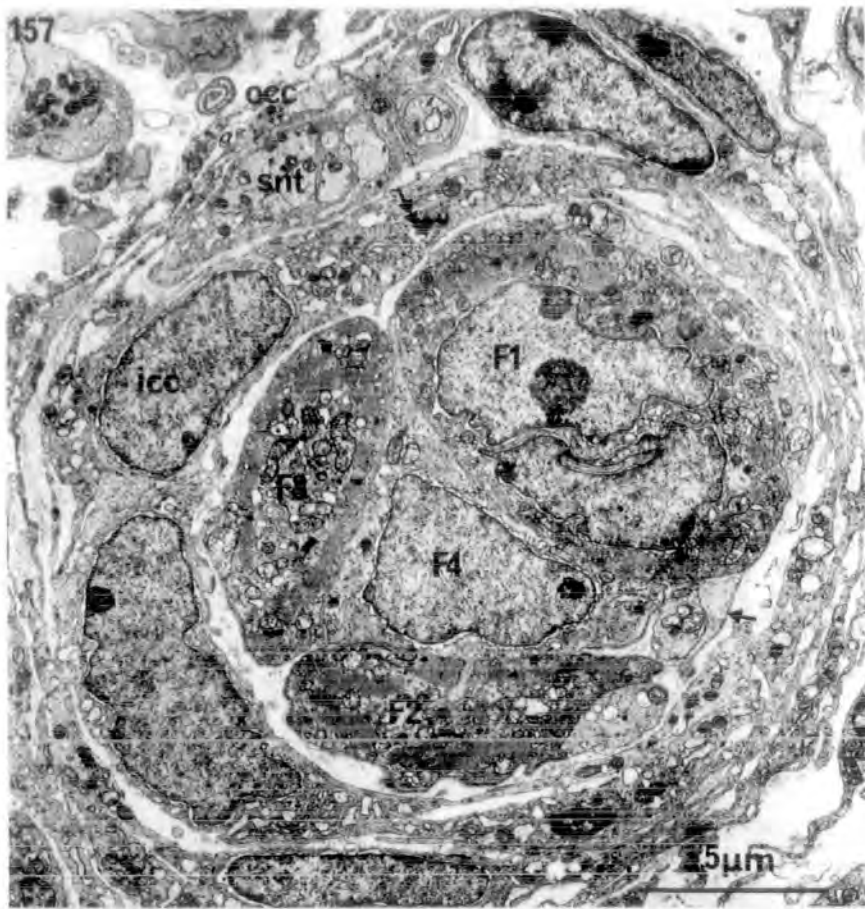
- Figs. 151-156. Transverse sections through the polar region of four spindles in 17 DPN rat.
151. Spindle A. Alkali pre-incubated ATPase. The intermediate bag fibre (F2) exhibits the lowest activity. x 800
152. Spindles B and C. Alkali pre-incubated ATPase. Note particularly the reduced activity of the intermediate bag fibre (double arrow) in spindle C. x 800
153. Spindle D. Alkali pre-incubated ATPase. x 800
154. Spindle A. SDH. Note the high activity of all intrafusal fibres. x 800
155. Spindle B. SDH. The typical bag fibre (F1) exhibits reduced activity. x 800
156. Spindle D. SDH. Note the low activity of the typical bag fibre (F1) compared to the intermediate (F2) and nuclear-chain fibres. x 800

Scale in fig. 150 refers to all figures.



FIGURES 157-162. The fine structure of muscle spindles in FHL of newborn mouse.

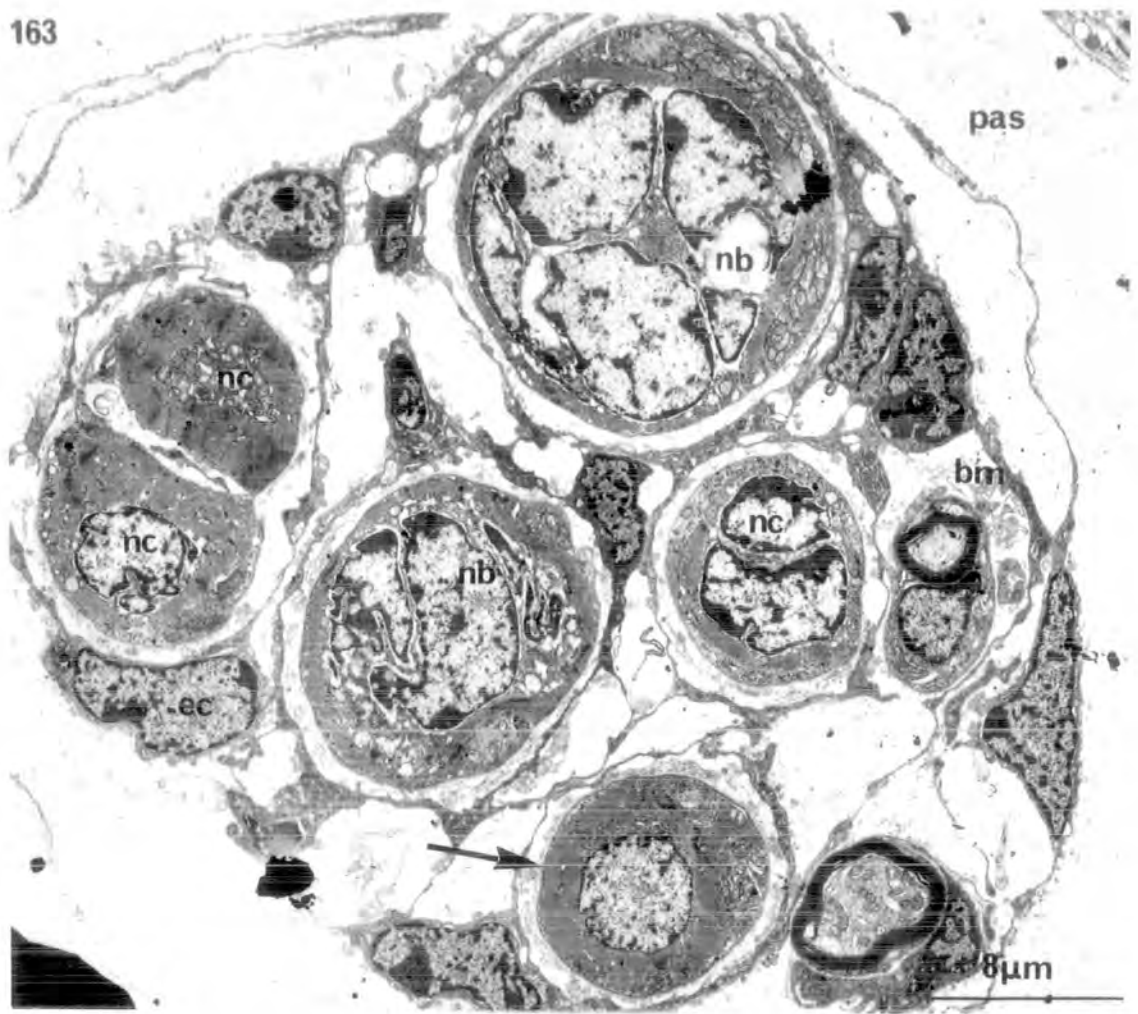
157. Transverse section through the juxta-equatorial region of a spindle. F4 is a newly-formed myotube. Single arrow points to overlapping sensory terminals; double arrow to a cilium in an inner capsule cell.
x 5,000
158. Higher power electron micrograph of the apposed surfaces of F4 and F2, shown in fig. 157. Arrow points to the close association of pseudopodial extensions of F4 with the nuclear envelope of F2. x 20,000
159. Transverse section of polar motor nerve terminal on F1 of a spindle. Single arrows point to dense-cored vesicles; double arrow to a flattened synaptic vesicle. Note the indentations of the post-synaptic sarcolemma. Scale as in fig. 158. x 20,000
160. Transverse section of an immature intrafusal myotube. Scale as in fig. 158. x 20,000
161. Transverse section through the polar region of a spindle. Note the peripheral nucleus in F1, the immaturity of F4 and the bi-lamellate capsule. Scale as in fig. 157. x 5,000
162. Transverse section of an intrafusal myoblast. Arrows point to paired centrioles. Scale as in fig. 158. x 20,000



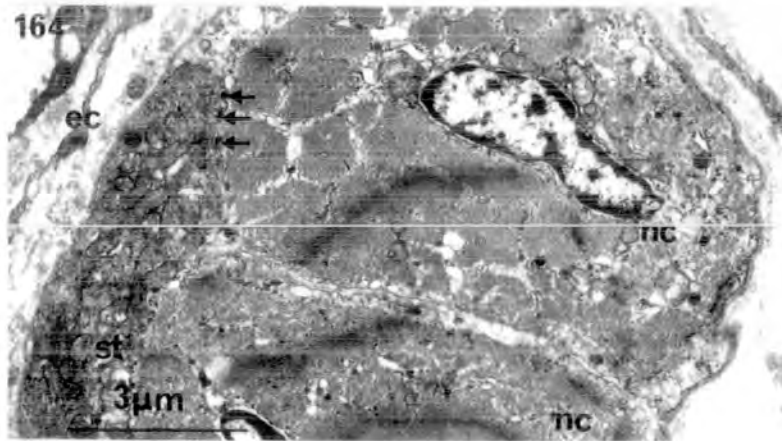
FIGURES 163-166. The fine structure of muscle spindles in FHL of newborn guinea pig.

163. Transverse section through the equatorial region of a spindle. Note the large and small diameter nuclear-bag fibres and three nuclear-chain fibres, two of which are ensheathed by a common basement membrane and endomysial enclosure. Arrow points to an intrafusal muscle fibre of chain equatorial nucleation but which possesses a double M line. x 3,200
164. Higher power electron micrograph of the paired nuclear-chain fibres shown in fig. 163. Note the shared sensory terminal and desmosome-like junctions (arrows). x 8,000
165. Longitudinal section through the polar region of a large diameter nuclear-bag fibre. Arrows point to double M line. x 20,000
166. Longitudinal section of a polar plate terminal. Arrows point to dense-cored vesicles. Scale as in fig. 165. x 20,000

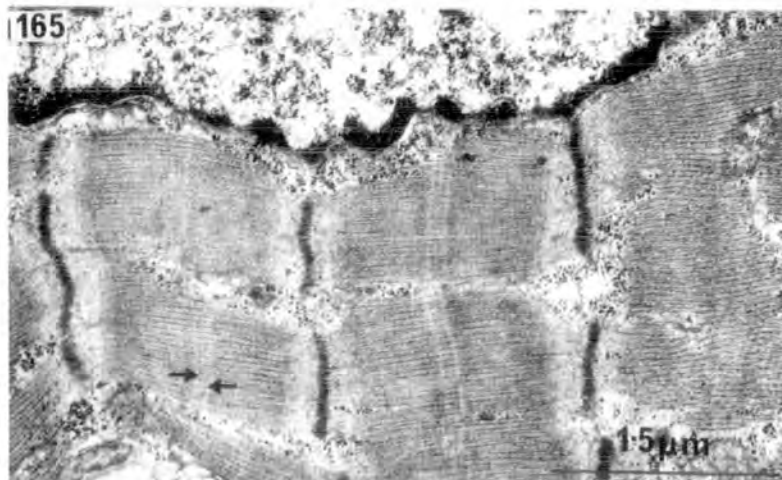
163



164



165



166

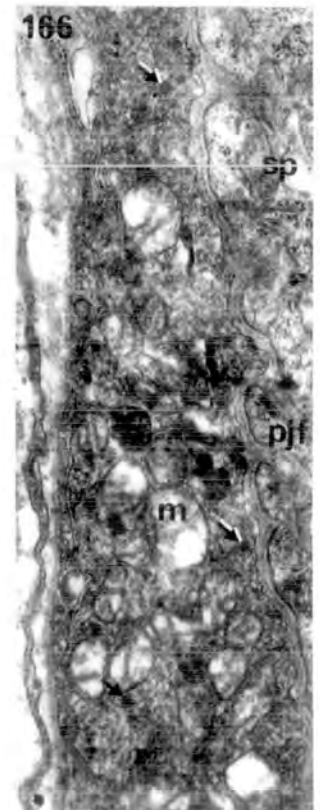


FIGURE 167. Transverse section of normal FHL muscle of 12 DPN rat, at the level of entry of the FHL muscle nerve.

Note the extramuscular, superficial location of the interosseous nerve. Both the FHL and interosseous nerve contain myelinated nerve fibres. Muscle fibres do not vary greatly in diameter. Muscle spindles are ringed.

c.1 μ m thick. Toluidine blue. x 180

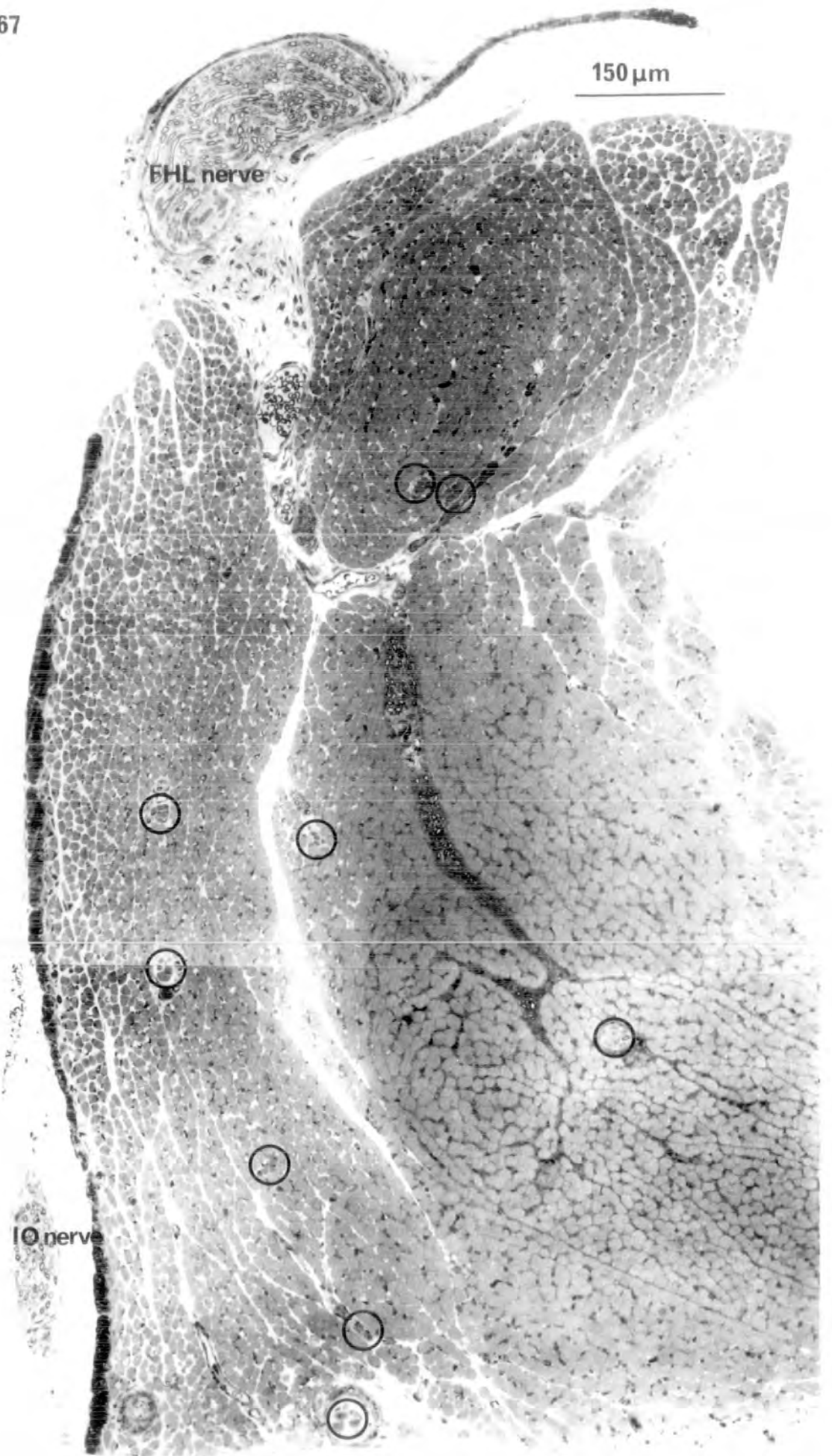


FIGURE 168. Transverse section of FHL muscle of 12 DPN rat, de-efferented at birth, at the level of entry of the FHL muscle nerve.

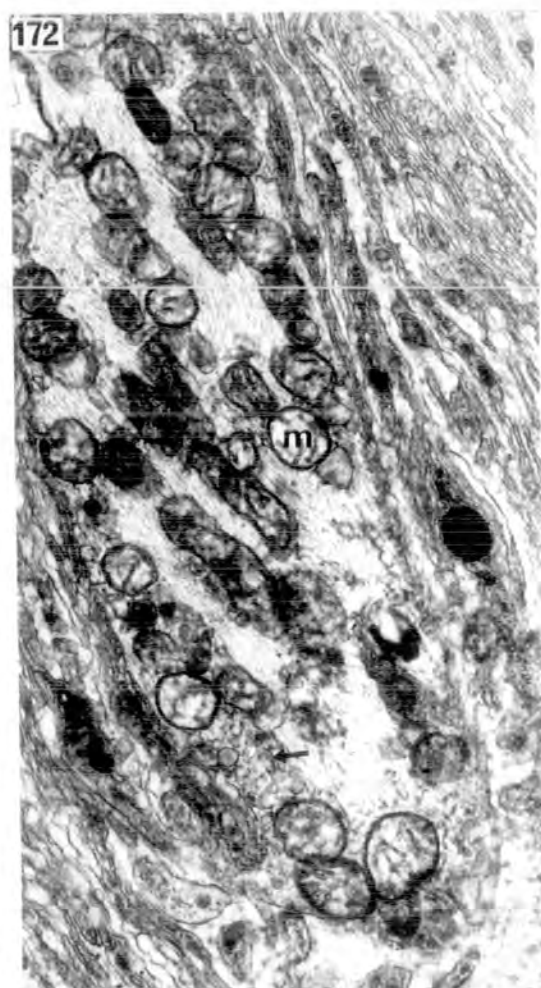
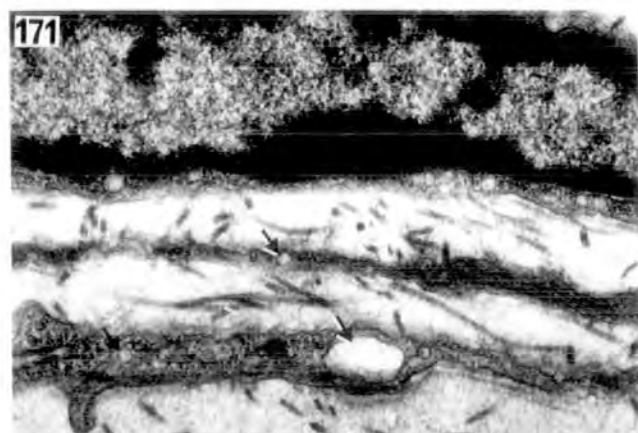
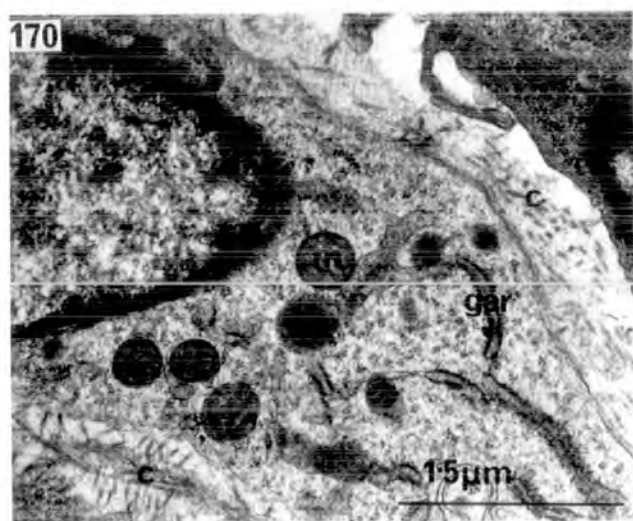
The interosseous nerve is undamaged, containing myelinated nerve fibres. The FHL muscle nerve and intramuscular nerve trunks are extensively damaged, although some axonal regeneration has occurred in the nerve trunk that is ringed. Single arrows point to myotubes. Note the variable diameter of the muscle fibres. Double arrows point to hypertrophied muscle fibres of a re-innervated area. Boxed area contains a re-innervated motor end-plate. Note particularly the absence of muscle spindles.

c.1µm thick. Toluidine blue. x 180



FIGURES 169-172. The fine structure of Pacinian corpuscles in FHL and interosseous membrane of 16 DPN rat, in which the FHL muscle nerve was sectioned at birth.

169. Transverse section through the middle region of a Pacinian corpuscle. Note the central sensory terminal and the bi-lateral arrangement of the inner (1) capsule cells. Arrows point to clefts in the inner capsule cells. Note the difference in shape between middle (2) and outer (3) capsule cells. x 3,200
170. Transverse section of a middle capsule cell. Note the intermeshing collagen fibrils, small mitochondria and abundance of granular ER cisternae. x 20,000
171. Transverse section of an outer capsule cell. Micropinocytotic vesicles (arrows) are the distinguishing feature of this type of cell. Scale as in fig. 170. x 20,000
172. Transverse section of the central sensory terminal. Arrows point to cisternae of smooth ER. Scale as in fig. 170. x 20,000



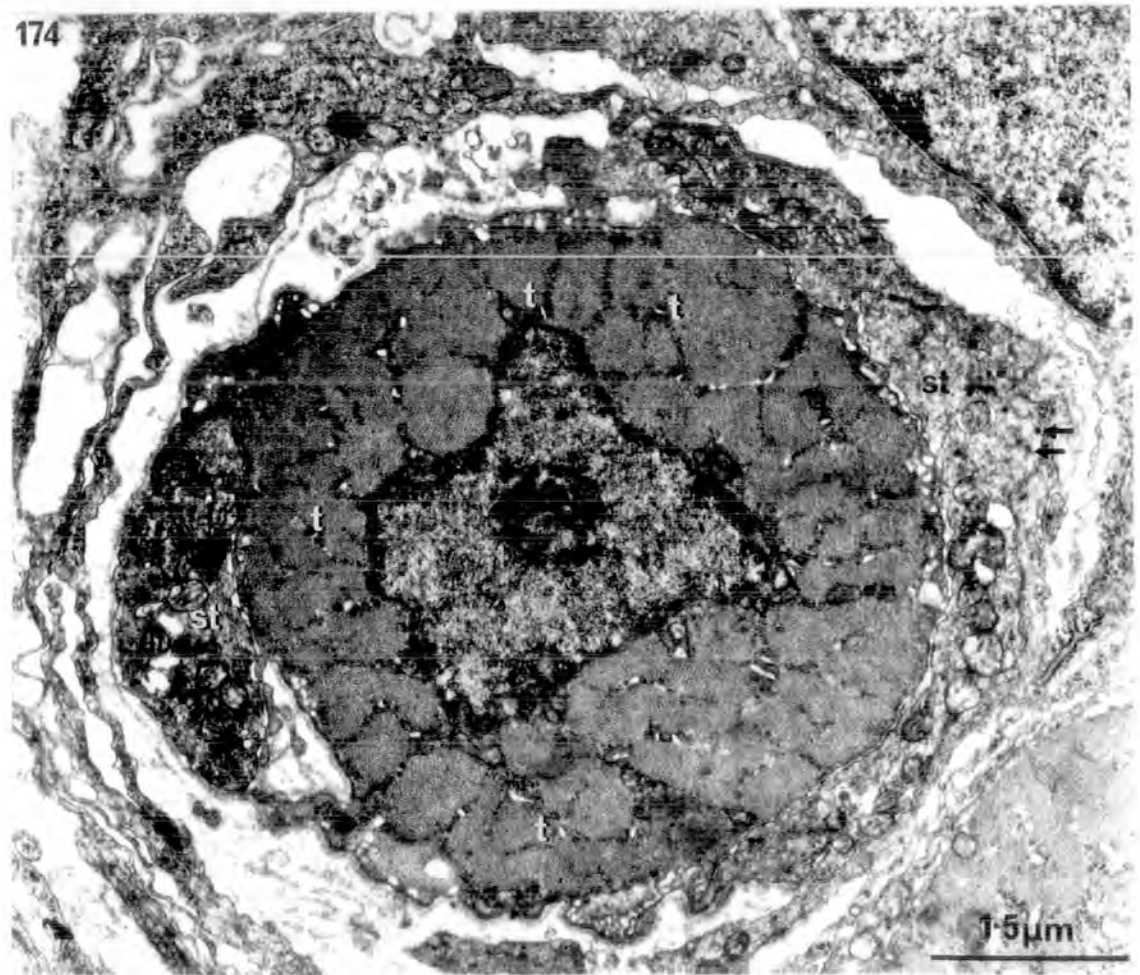
FIGURES 173-174. The fine structure of atypical spindles in FHL of 12 DPN rat, in which the FHL muscle nerve was sectioned at birth.

173. Transverse section through the innervated region. Note the two intrafusal muscle fibres, of large and small diameter, one of which bears sensory nerve terminals. The outer and inner capsule cells are separated by a narrow periaxial space, containing a single vacuolated cell. Note the regenerating axons in the spindle nerve trunk.

x 5,000

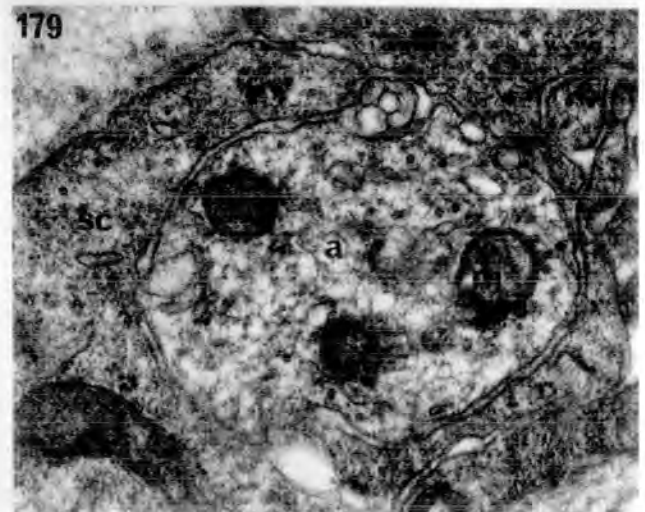
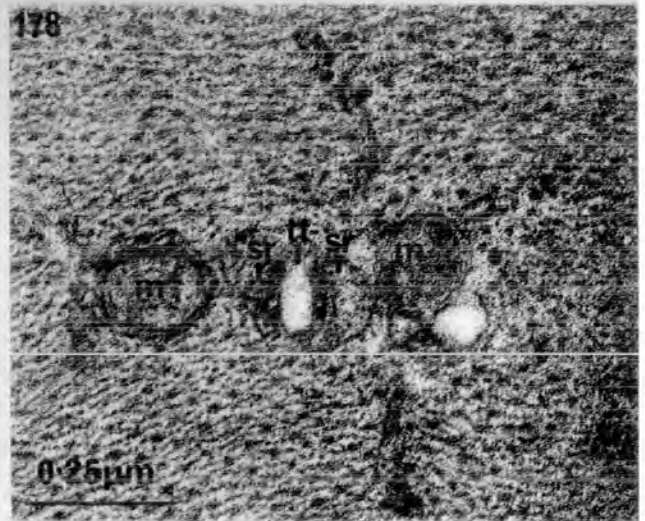
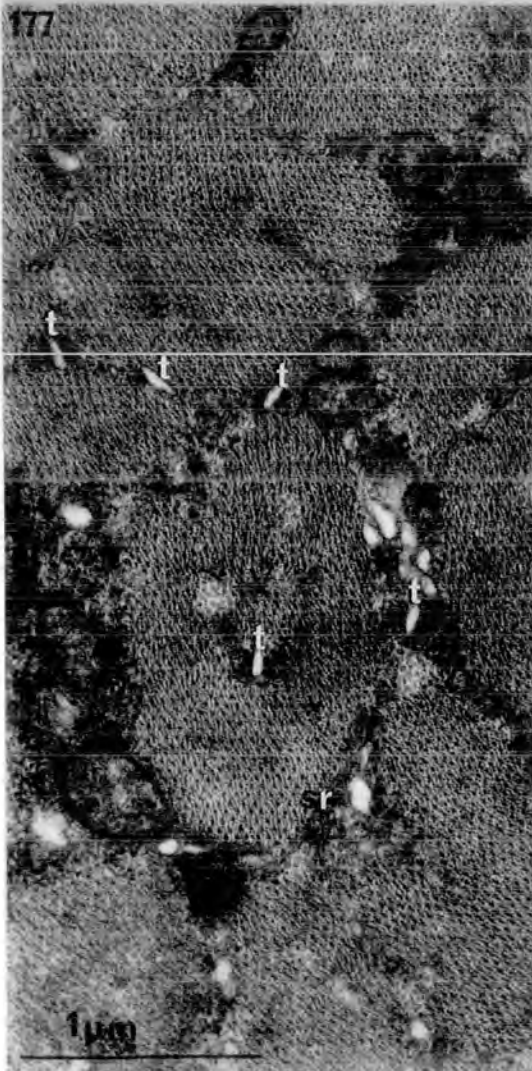
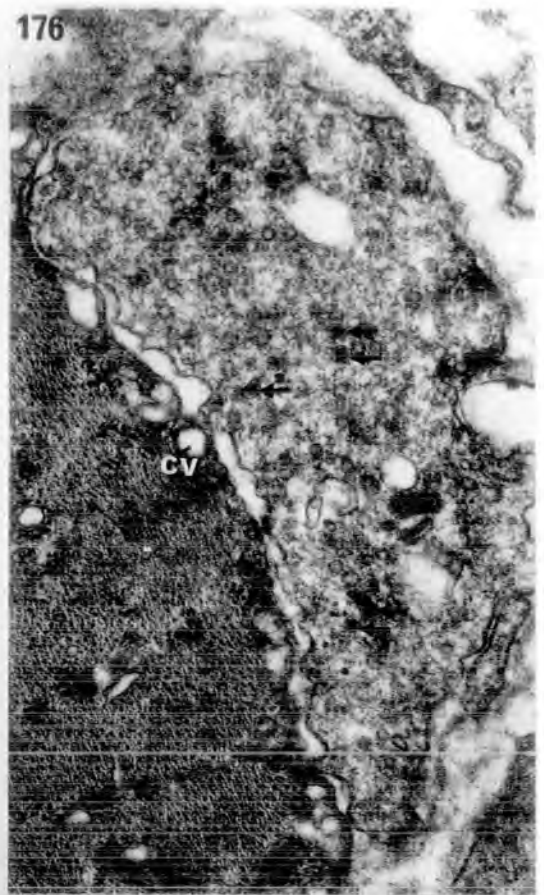
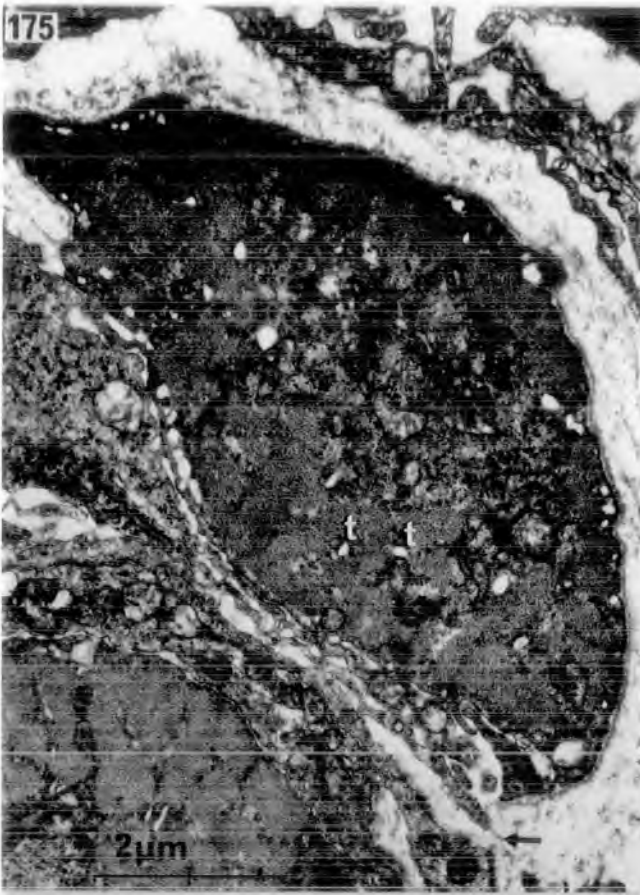
174. Higher power electron micrograph of the large diameter muscle fibre shown in fig. 173. Arrows point to dense-cored vesicles. Note the abundant triads and interfibrillar sarcoplasm.

x 12,600



FIGURES 175-179. The fine structure of atypical spindles in FHL of 12 DPN rat, in which the FHL muscle nerve was sectioned at birth.

175. Higher power electron micrograph of the small diameter muscle fibre, shown in fig. 173. Note the central-core sarcoplasm, the abundance of triads and basement membrane (arrows) that extends over the sensory terminal on the neighbouring muscle fibre. x 12,600
176. Transverse section of a sensory terminal. Arrows point to dense-cored vesicles. Scale as in fig. 177. x 32,000
177. Transverse section through the polar region of an intrafusal muscle fibre. Note the abundance of SR tubules and transversely orientated triads. x 32,000
178. Transverse section of a transversely orientated triad in an intrafusal muscle fibre. x 80,000
179. Transverse section of a regenerating nerve axon in the spindle nerve trunk. Note the absence of myelin. The axon is surrounded by a single Schwann cell. Scale as in fig. 178. x 80,000



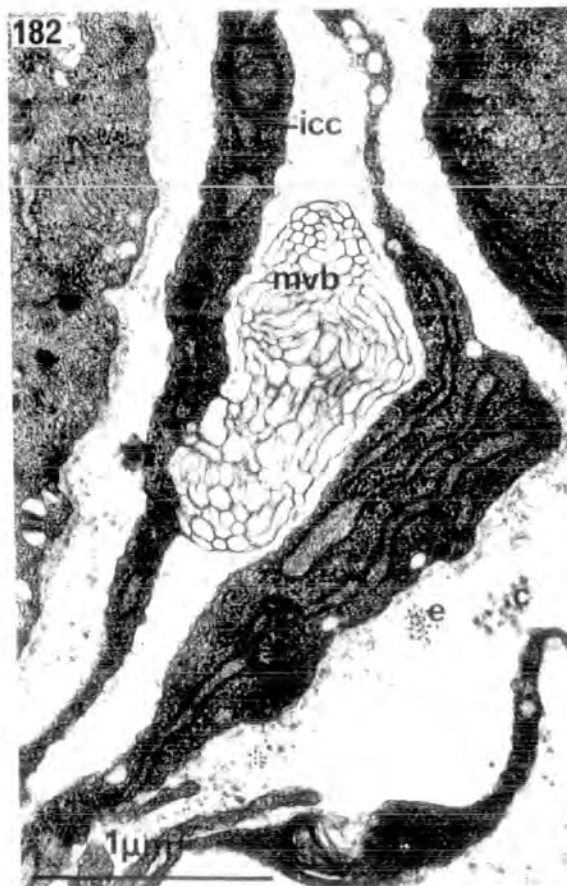
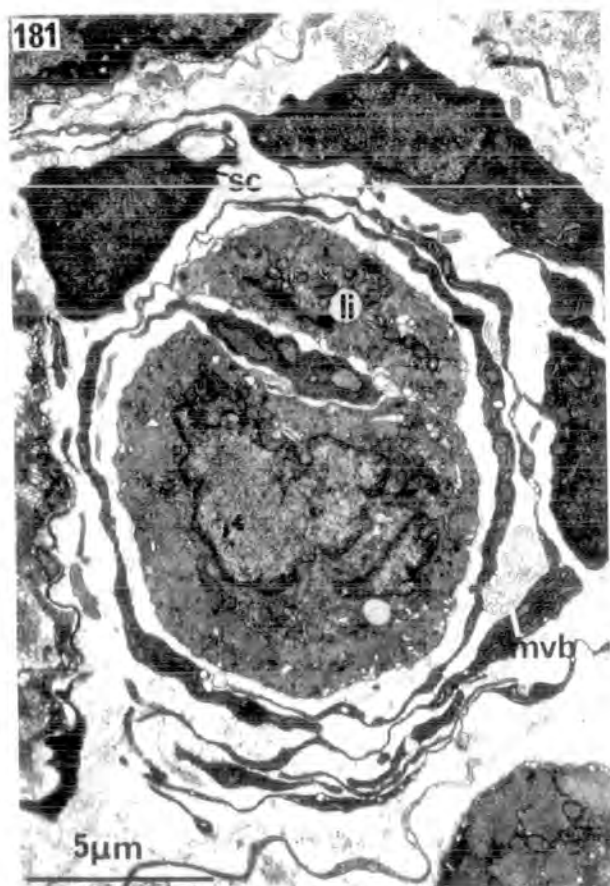
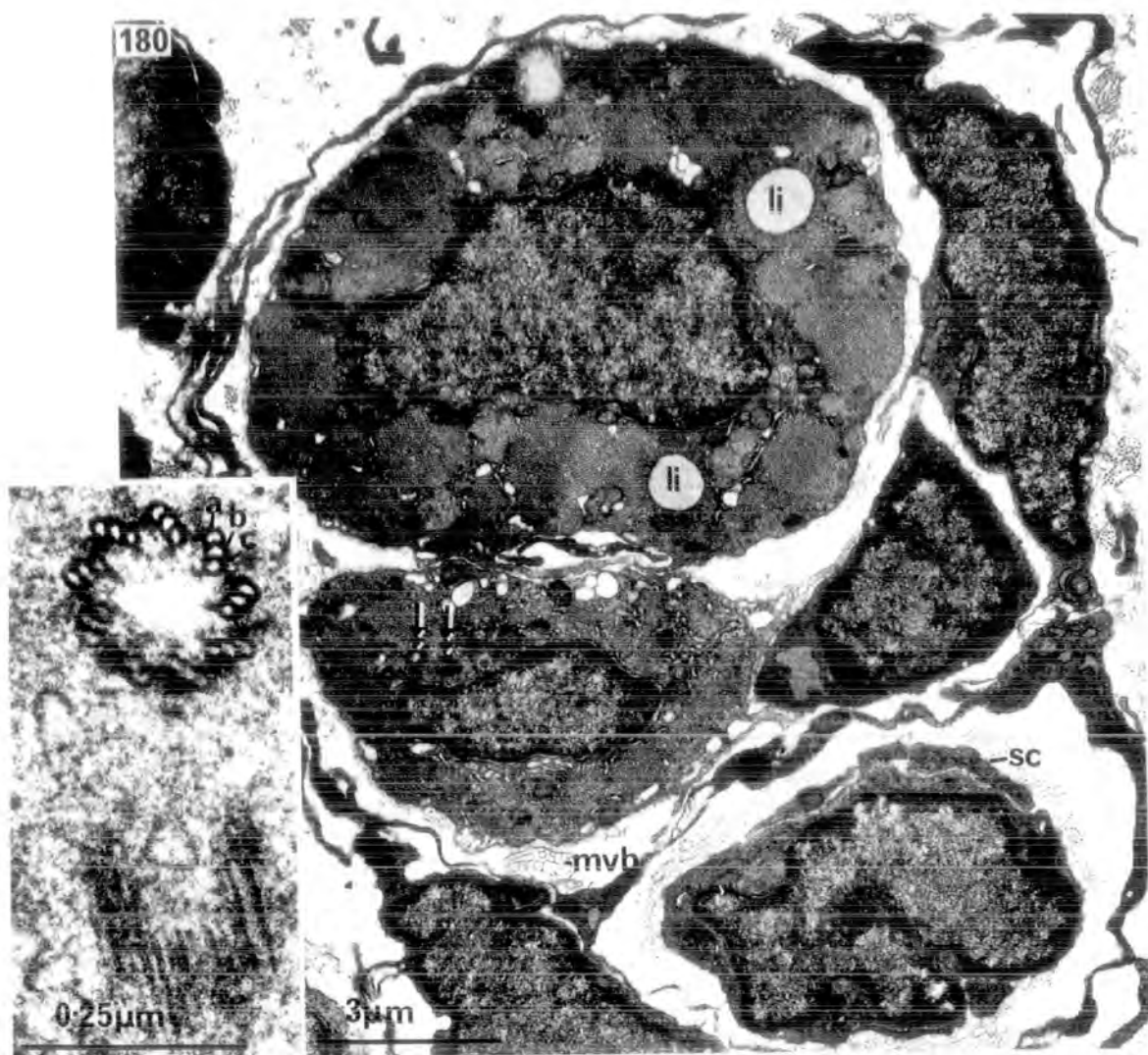
FIGURES 180-182. The fine structure of muscle spindles in FHL of 1 DPN rat, in which the FHL muscle nerve was sectioned at birth.

180. Transverse section through the middle region of a spindle. Both the large and small diameter intrafusal fibres lacked a nuclear bag. Note the paired centrioles (double arrows) in the smaller muscle fibre and the absence of axons from the spindle nerve trunk. x 8,000

Inset. Higher power electron micrograph of the paired centrioles in the small intrafusal fibre. The upper centriole is sectioned transversely, showing the typical arrangement of 9, evenly-spaced triplets (a, b and c) of hollow tubules. x 126,000

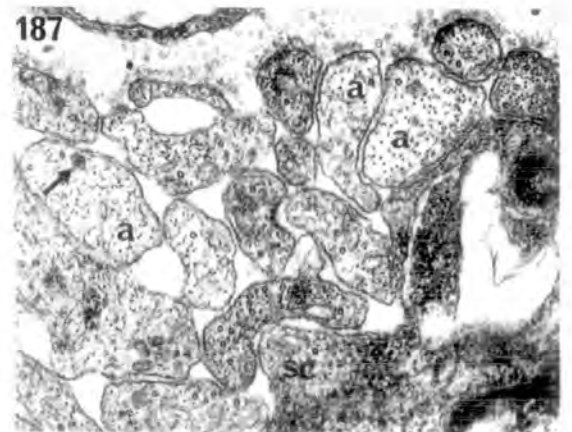
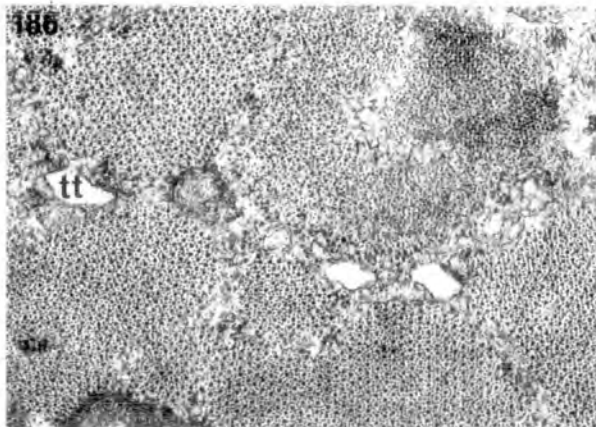
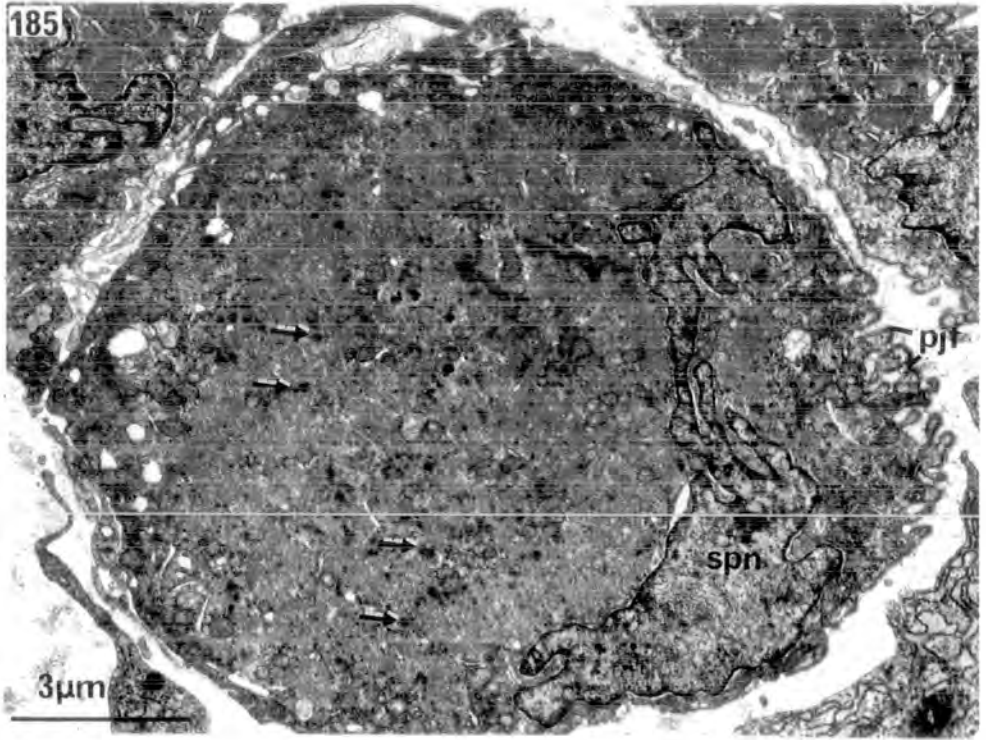
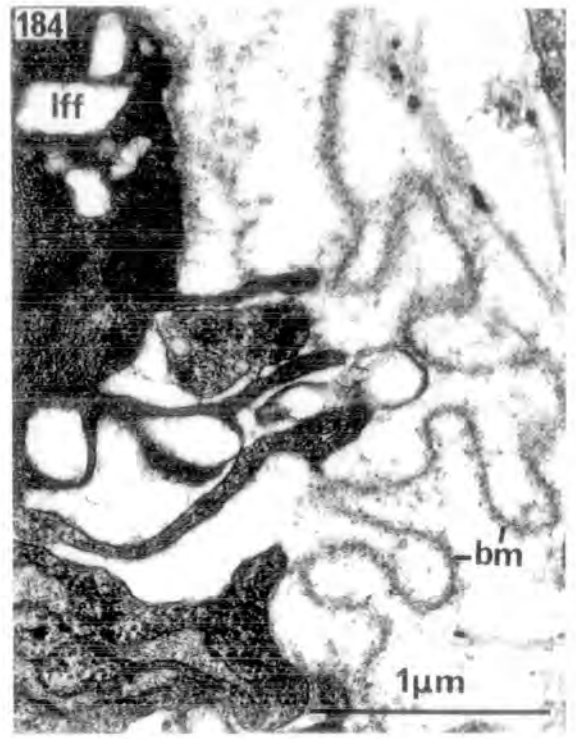
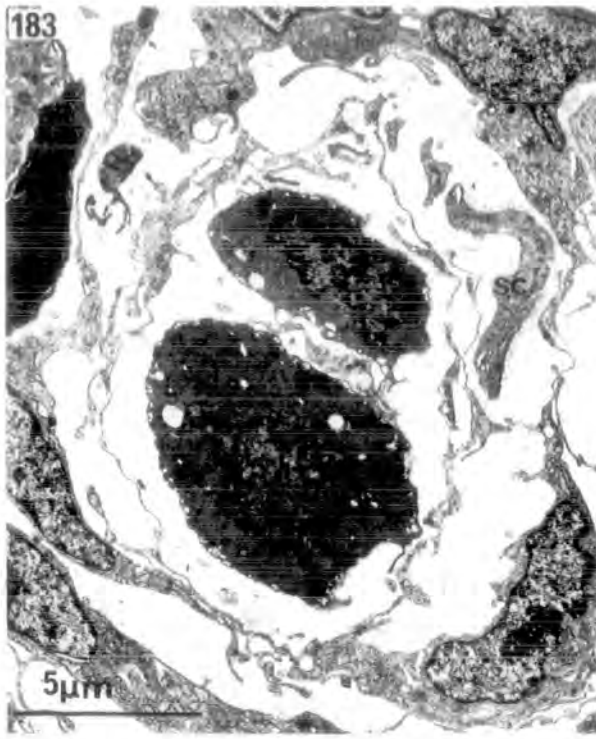
181. Transverse section through the equatorial region of a spindle. Note the aggregation of nuclei in the larger intrafusal muscle fibre, and the absence of axons from the spindle nerve trunk. x 5,000

182. Higher power electron micrograph of an inner capsule cell of the spindle shown in fig. 181. Note the protruding multivesicular body. x 32,000



FIGURES 183-187. The fine structure of muscle spindles, muscle fibres and intramuscular nerve trunks in FHL of 3 DPN rat, in which the FHL muscle nerve was sectioned at birth.

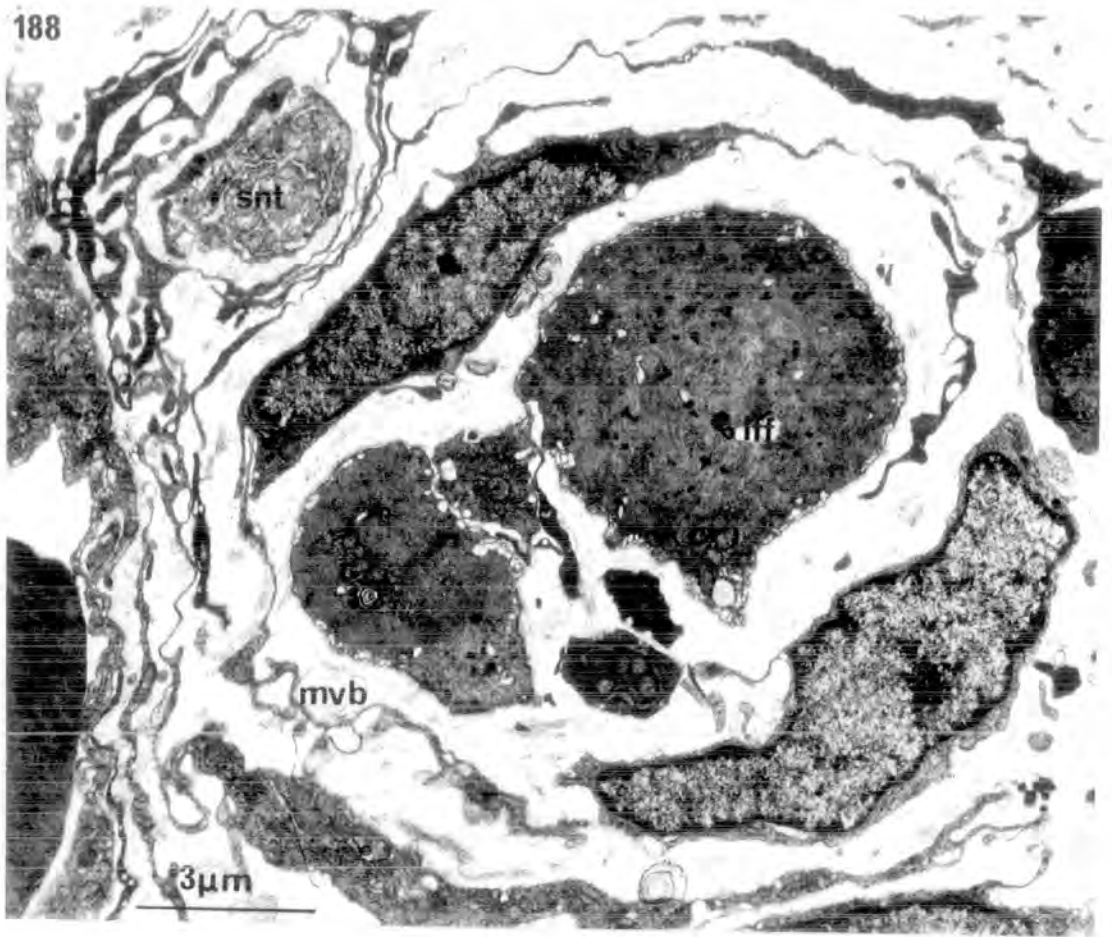
183. Transverse section through the middle region of a spindle. Note the absence of nerve terminals.
x 5,000
184. Higher power electron micrograph of part of the outer surface of the axial bundle of the spindle shown in fig. 183. Note the collapsed basement membrane.
x 32,000
185. Transverse section of a denervated extrafusal muscle fibre, in the region of the motor end-plate. Note the sole-plate nucleus and sarcoplasm, post-junctional folds and absence of nerve terminals. Arrows point to degenerating Z-band material.
x 8,000
186. Transverse section of a denervated extrafusal muscle fibre, showing a normal myofibril architecture. Scale as in fig. 184. x 32,000
187. Transverse section of FHL muscle nerve. Note the numerous small regenerating axons, surrounded by a single Schwann cell, containing numerous neurofilaments and neurotubules. Arrow points to a dense-cored vesicle. Scale as in fig. 184. x 32,000



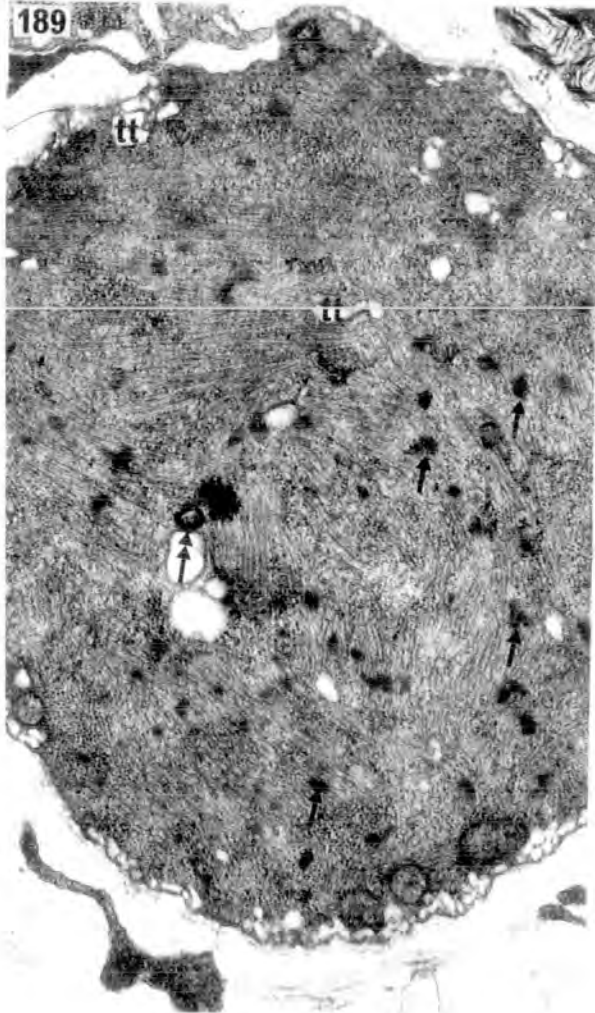
FIGURES 188-190. The fine structure of muscle spindles in FHL of 5 DPN rat, in which the FHL muscle nerve was sectioned at birth.

188. Transverse section through the middle region of a spindle. Note the absence of nerve axons and terminals. x 8,000
189. Higher power electron micrograph of the large intrafusal muscle fibre in the spindle shown in fig. 188. Note the disorganization of the myofibrils and the abundance of T tubules. Single arrows point to degenerating Z bands, double arrow to a myelin figure. Scale as in fig. 190. x 20,000
190. Higher power electron micrograph of the intermediate diameter intrafusal muscle fibre. Note the paucity of assembled myofibrils and numerous branching T tubules. x 20,000

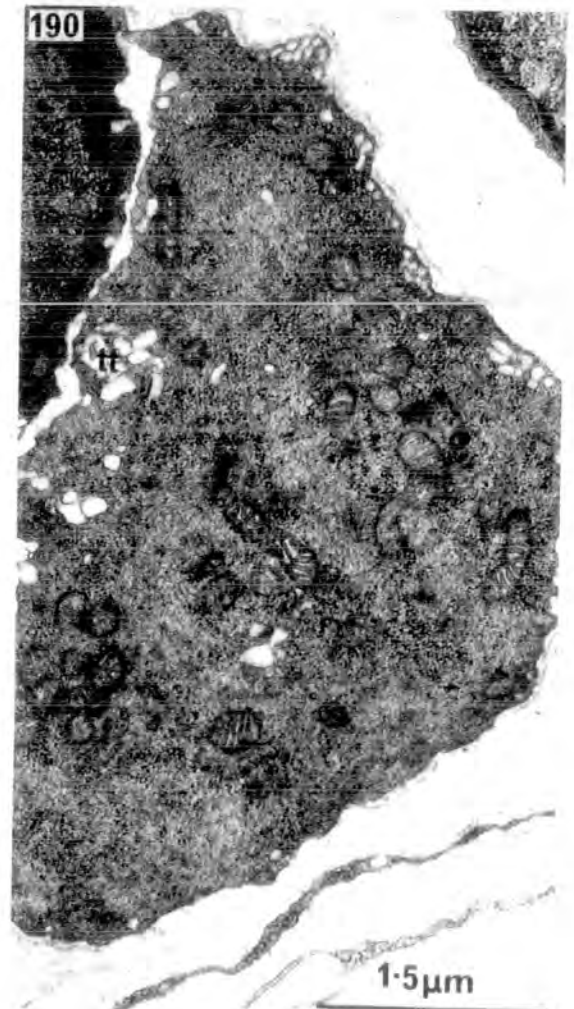
188



189

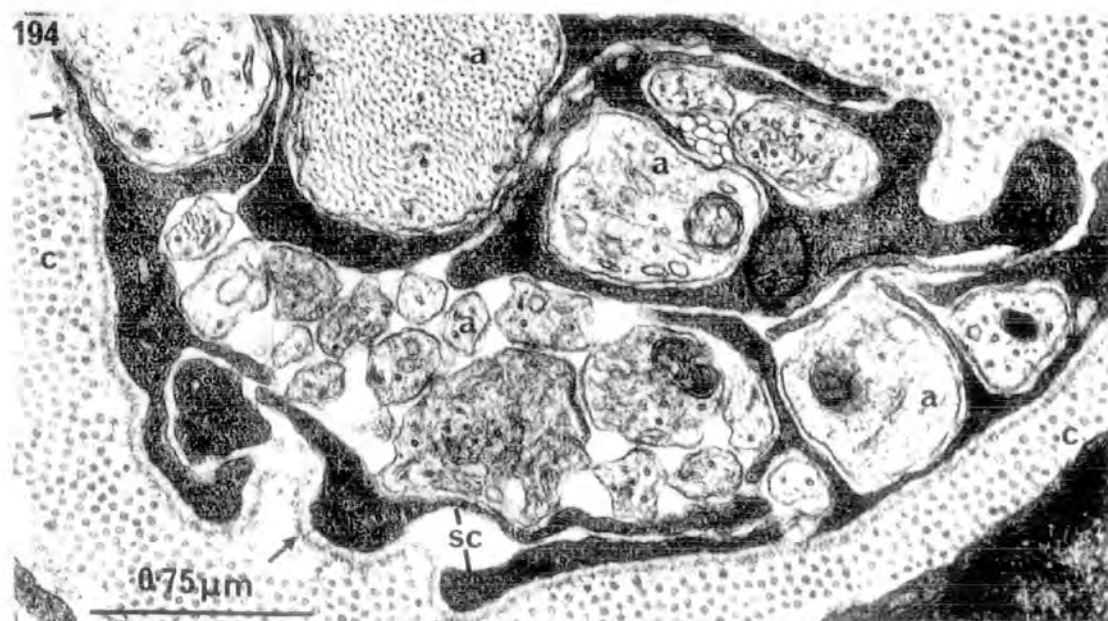
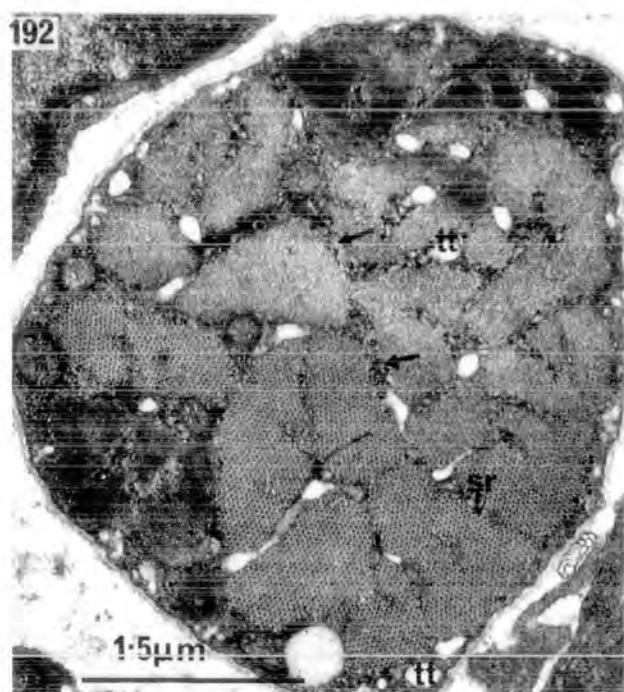
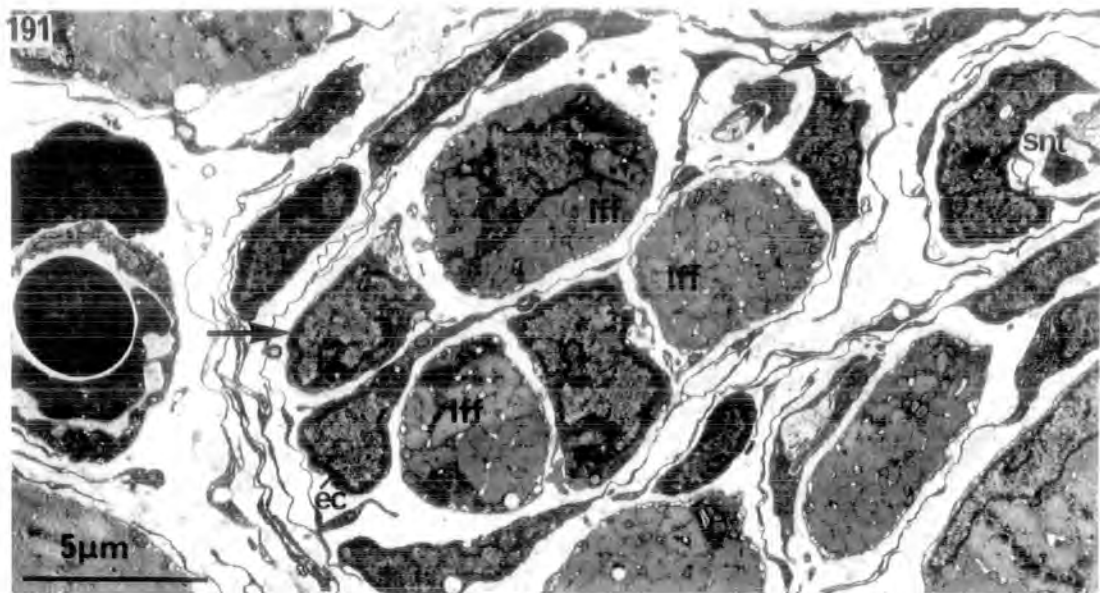


190



FIGURES 191-194. The fine structure of muscle spindles in FHL of 9 DPN rat, in which the FHL muscle nerve was sectioned at birth.

191. Transverse section through the middle region of a re-innervated spindle. All three intrafusal fibres lacked a nuclear bag. Arrows point to regenerating nerve trunks. x 5,000
192. Higher power electron micrograph of the small intrafusal muscle fibre shown in fig. 191. Note the abundance of interfibrillar sarcoplasm (arrows), SR and dilated T tubules.
x 20,000
193. Higher power electron micrograph of a regenerating nerve trunk in the spindle shown in fig. 191. Note the small axons, surrounded by a single Schwann cell. x 25,000
194. Transverse section of a regenerating intramuscular nerve trunk. Note the numerous unmyelinated axons, of varying diameter, that are sub-divided into smaller groups by Schwann cell septa. Arrows point to basement membrane.
x 40,000



FIGURES 195-197. The fine structure of re-innervated muscle spindles in FHL of 12 DPN rat, in which the FHL muscle nerve was sectioned at birth.

195. Transverse section through the middle region of a spindle. Anucleate fragments of three intrafusal muscle fibres (1, 2 and 3), numerous regenerating axons (arrows) and fibroblast-like cells are contained within the multi-lamellate capsule.

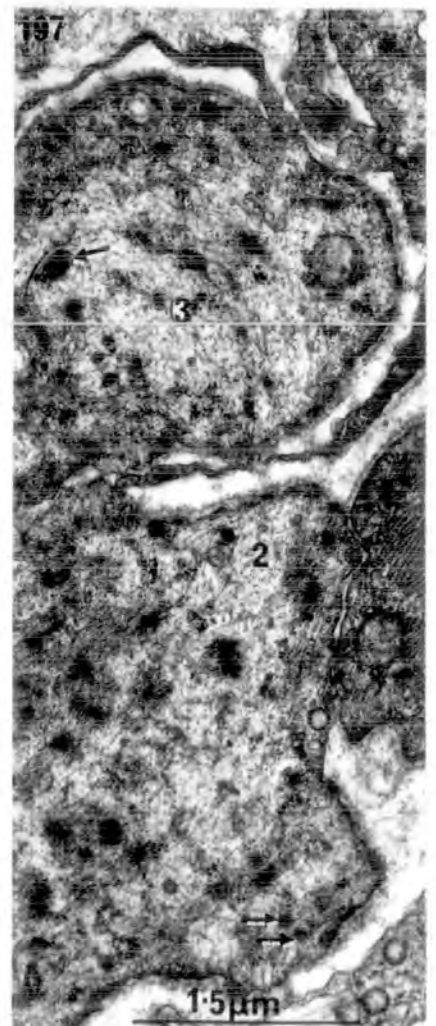
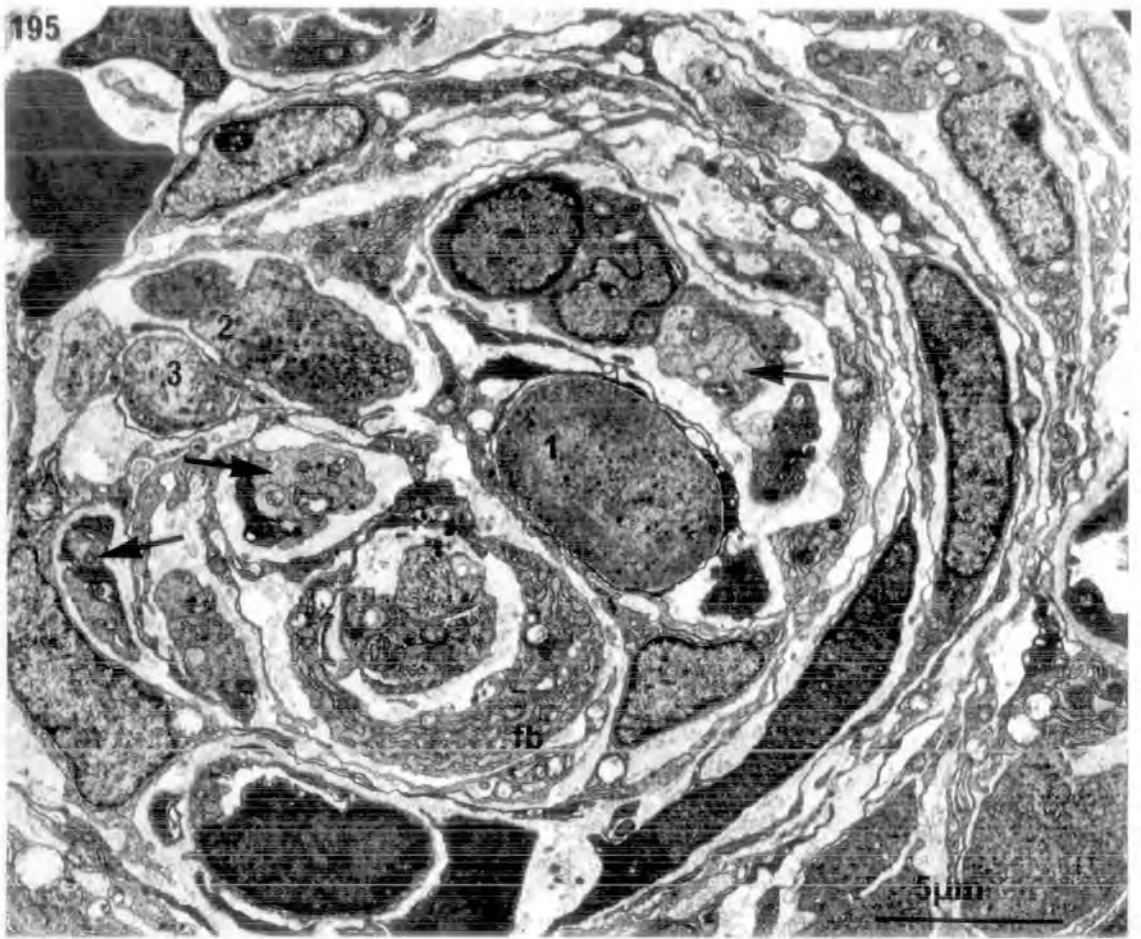
x 5,000

196. Higher power electron micrograph of fibre 1, shown in fig. 195. Note the disorganized myofibrils, degenerating Z bands and dense-bodied lysosomes (arrows). A single myofibril of normal architecture is ringed. Scale as in fig. 197.

x 20,000

197. Higher power electron micrograph of fibre 2, shown in fig. 195. Note the extensive myofibril atrophy. Arrows point to dense-bodied lysosomes.

x 20,000



FIGURES 198-202. The fine structure of re-innervated muscle spindles in FHL of 12 DPN rat, in which the FHL muscle nerve was sectioned at birth.

198. Transverse section through the middle region of the same spindle shown in fig. 195. Note the absence of any muscle component within the well-preserved capsule. Arrows point to regenerating nerve axons. x 5,000
199. Transverse section of a regenerating intracapsular nerve trunk. The axons vary in diameter and are enclosed by a single Schwann cell. x 12,600
200. Transverse section of regenerating FHL muscle nerve. Note the large myelinated axons (arrows) that are surrounded by individual Schwann cells and the groups of small unmyelinated axons that share a Schwann cell. Scale as in fig. 198. x 5,000
201. Transverse section of a regenerating axon in a spindle. Double arrow points to a neurotubule, single arrow to a neurofilament. x 50,000
202. Higher power electron micrograph of a regenerating myelinated nerve fibre, in FHL muscle nerve. x 32,000

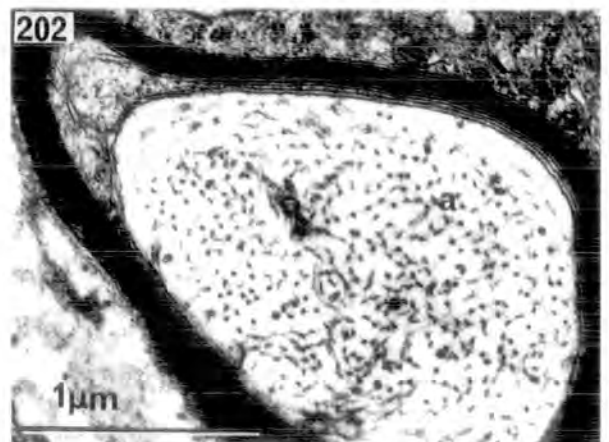
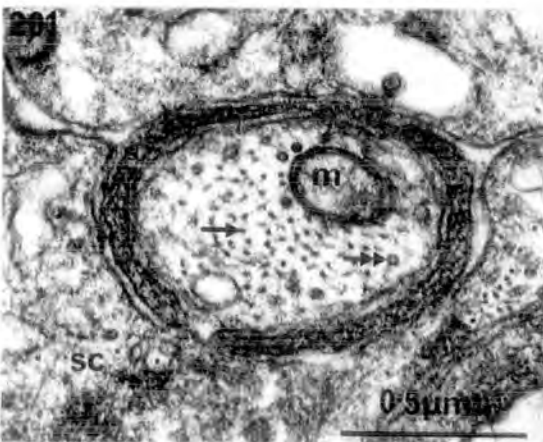
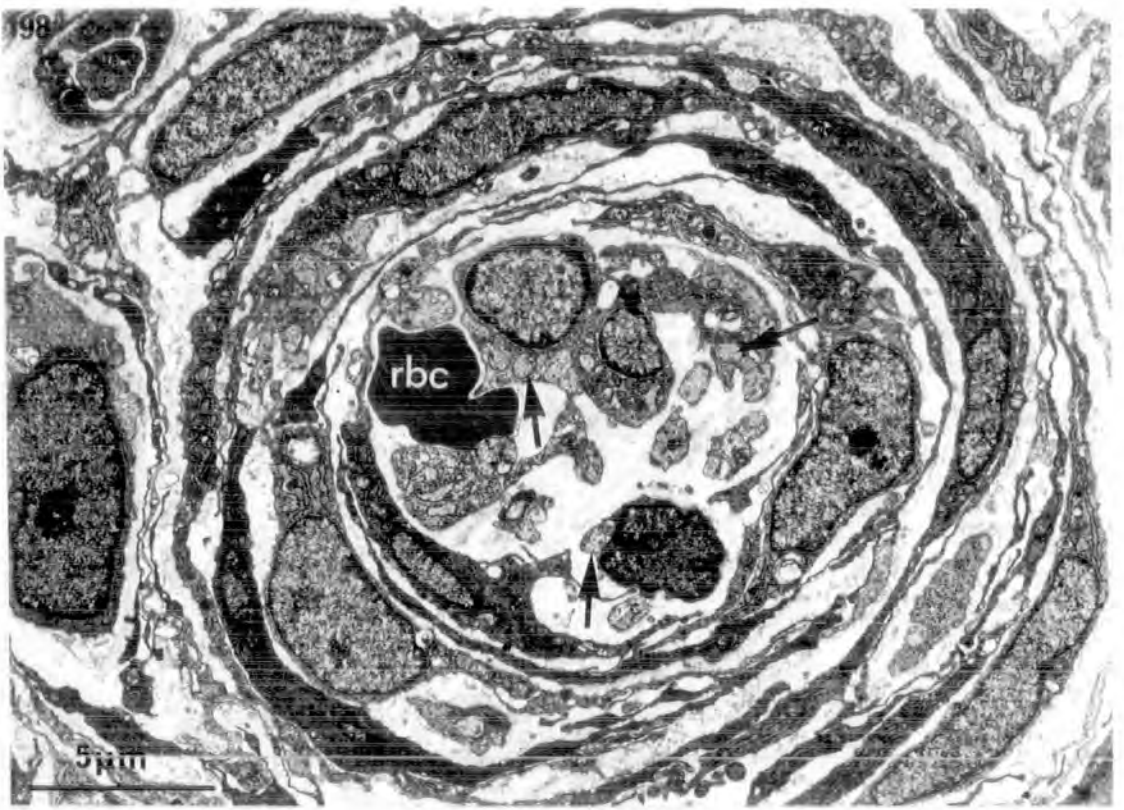


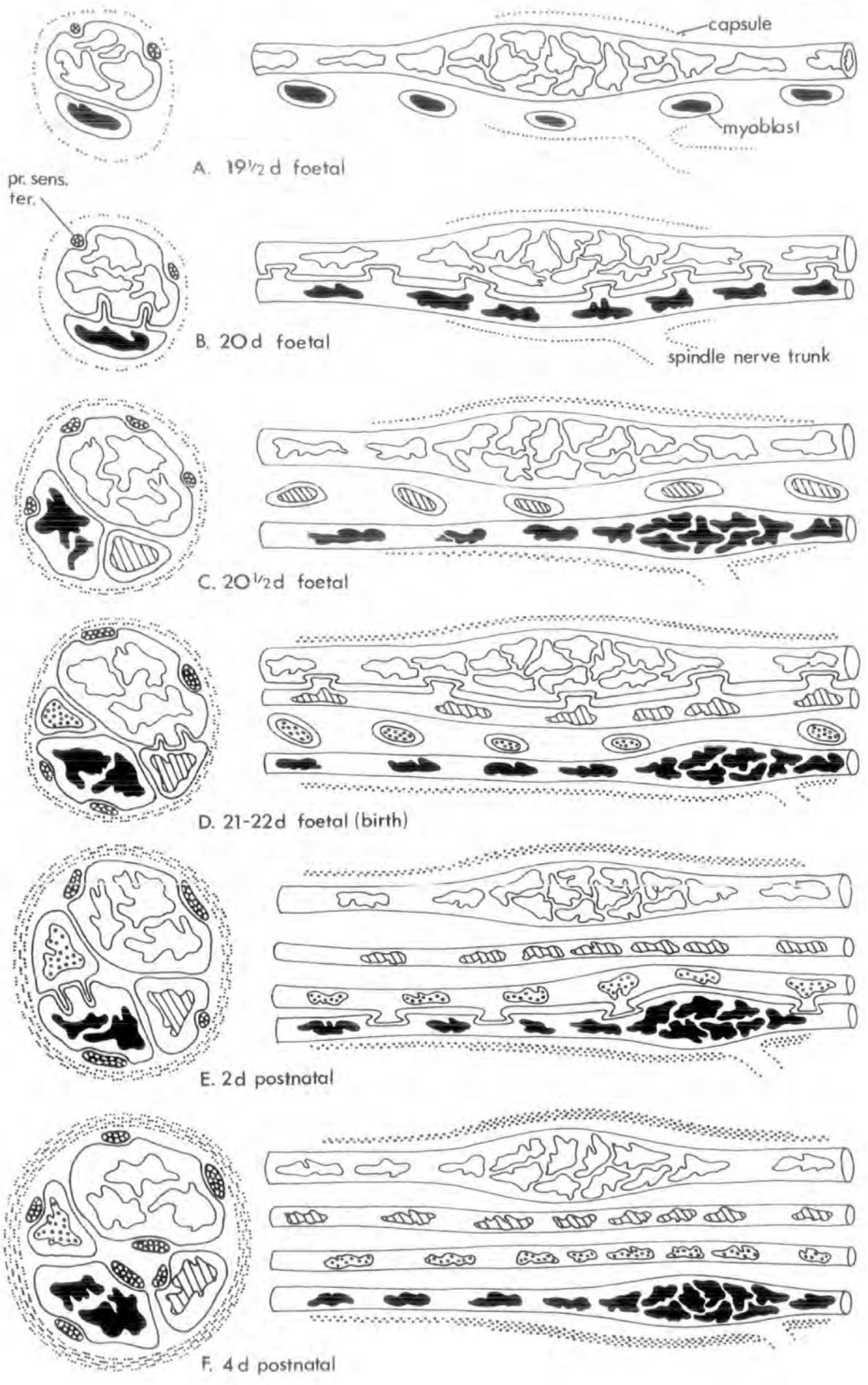
FIGURE 203. Schematic diagrams illustrating the development of muscle spindles in rat.

Diagrams on the left represent transverse sections of spindles at selected developmental stages and those on the right, hypothetical longitudinal sections.

Nuclei in the typical bag fibre (F1) are unshaded; those in the intermediate bag fibre (F2) are black; in the first nuclear-chain fibre (F3) cross-hatched and in the second (F4) stippled.

Pseudopodial apposition between developing muscle fibres is represented by diagrammatic interlocking. The motor innervation is omitted.

pst, primary sensory nerve terminal.



A. 19½ d foetal

B. 20 d foetal

C. 20½ d foetal

D. 21-22 d foetal (birth)

E. 2 d postnatal

F. 4 d postnatal

capsule

myoblast

pr. sens. ter.

spindle nerve trunk

FIGURE 204. Hypothetical model for the formation of nuclear-bag and nuclear-chain fibres, under the morphogenetic influence of primary sensory nerve terminals, in muscle spindles of rat hindlimb shank muscles.

It is proposed that

- i. the influence decreases in strength with the advancement of spindle morphogenesis eg. compare the mid-equatorial influence exerted on F1 at the 19.5 DF stage to that at the 8 DPN-adult stage.
- ii. the influence decreases per unit distance from the first point of contact of the primary axon eg. compare the mid-equatorial and juxta-equatorial influence exerted on F1 at the 19.5 DF stage.

Decreasing sizes of arrowheads represent a decreasing morphogenetic influence.

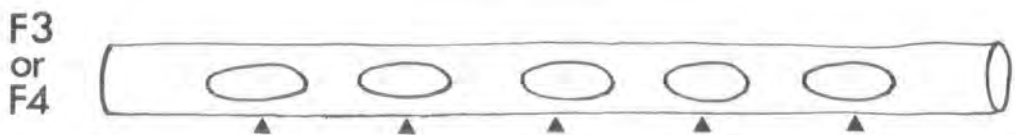
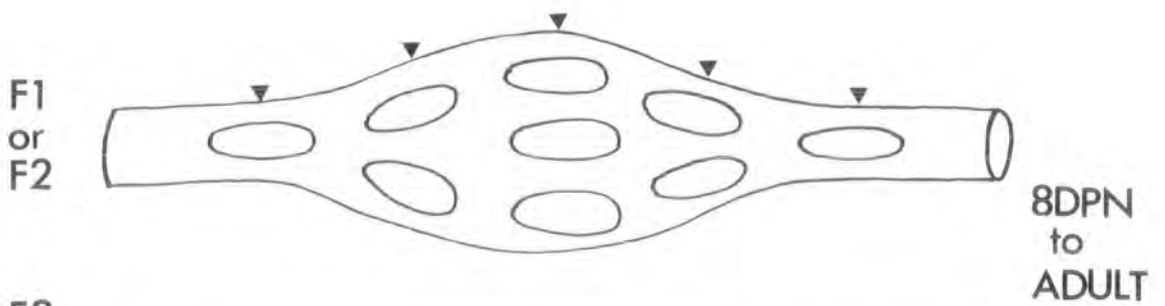
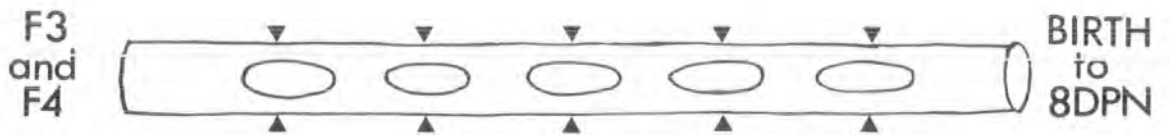
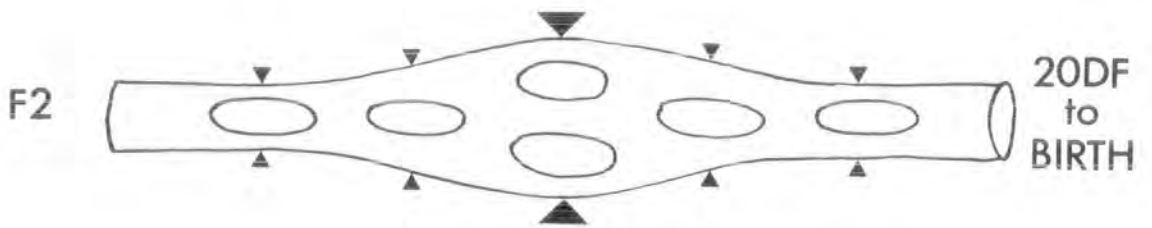
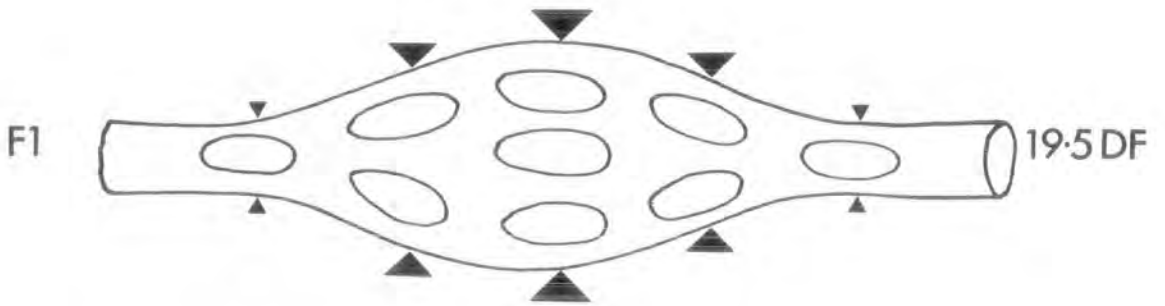


FIGURE 205. Hypothetical model for the formation of nuclear-bag and nuclear-chain fibres in muscle spindles of rat.

- a. Graph illustrating the proposed decrease in strength of the morphogenetic influence, exerted by primary sensory nerve terminals at the mid-equatorial region of developing intrafusal muscle fibres (ordinate), with the advancement of the morphogenetic period (abscissa) in rat hindlimb shank muscle.
- b. Graph illustrating the time of development of intrafusal muscle fibres with aberrant equatorial nucleation in rat hindlimb shank and lumbrical muscles.

In hindlimb shank muscle, the initial contact of the primary axon with two myotubes will lead to the formation of two nuclear-bag fibres of maximum equatorial nucleation. The premature formation of F3 (ie. before birth) will lead to a small aggregation of myonuclei in the nuclear-chain fibre.

The maximum influence exerted during the development of the spindle in rat and guinea-pig lumbrical muscle may only be sufficient to form a small nuclear bag in the first-innervated myotubes (F1 & F2 lumbrical m.).

Nuclei of all intrafusal muscle fibres are black. The morphogenetic period covers the late foetal days (19, 20) and early postnatal days (2, 4, 6, 8, 10) of development. Birth is set at 21 days gestation.

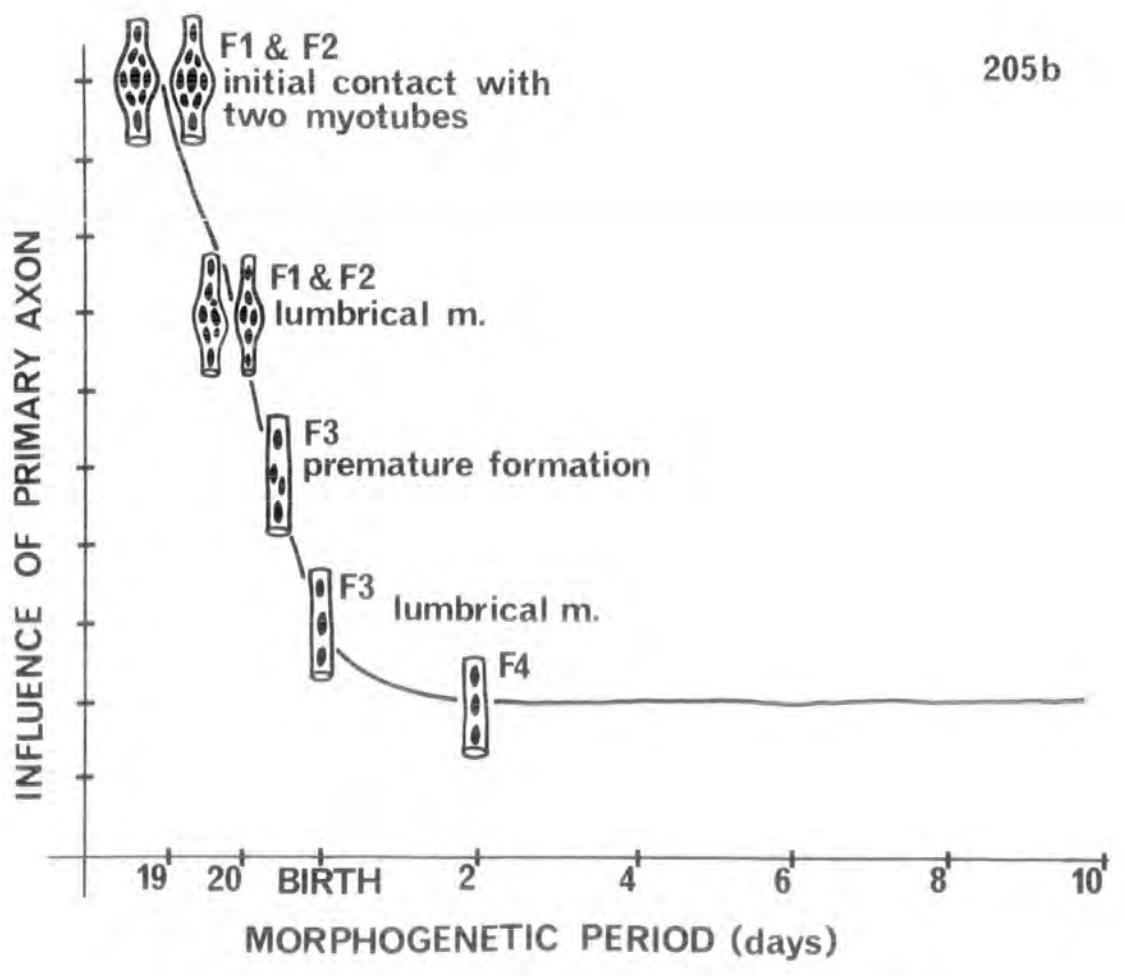
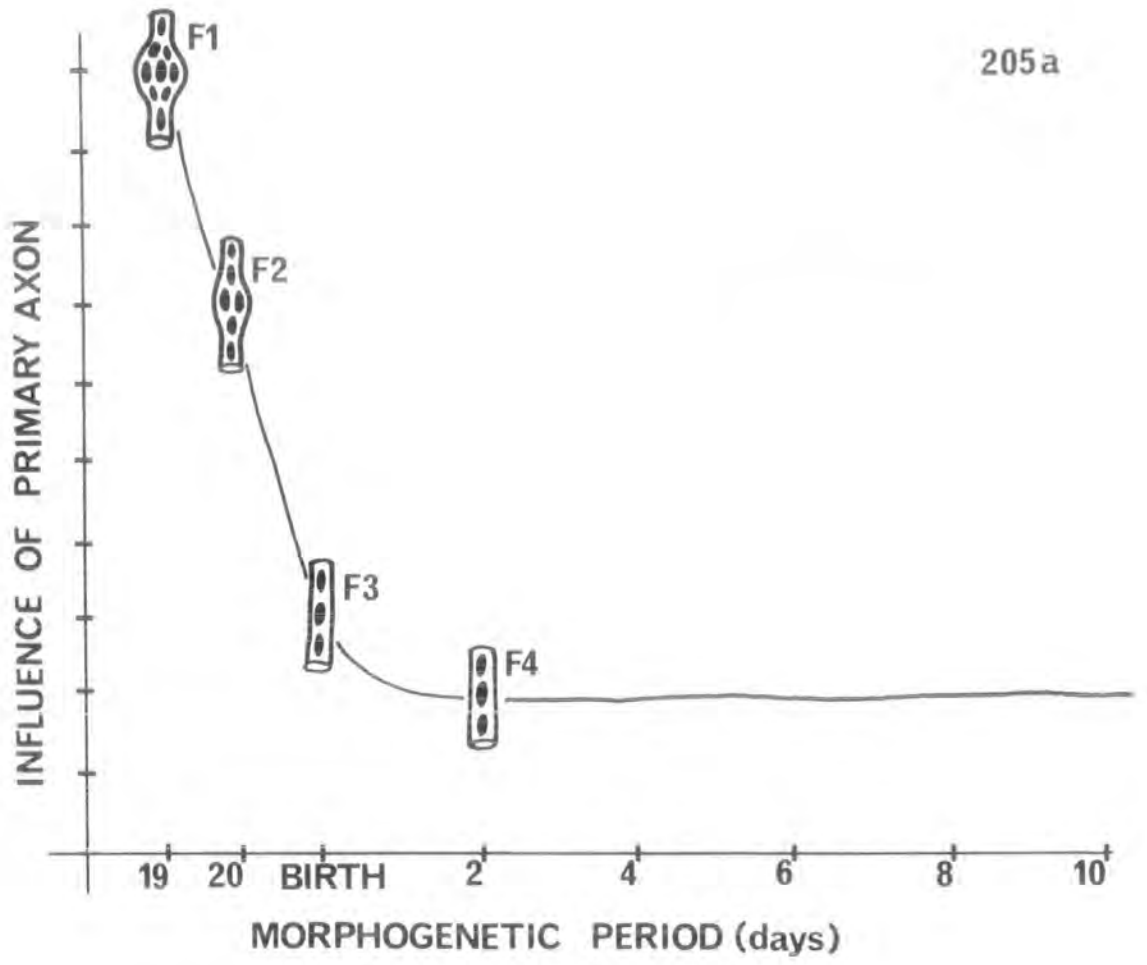


FIGURE 206. Schematic diagram illustrating the proposed role of dense-cored vesicles in the exertion of the trophic influence of sensory and motor nerve terminals, during the development of intrafusal muscle fibres in rat.

It is suggested that the contents of dense-cored vesicles are released by exocytosis at the axolemma and subsequently engulfed by coated vesicles at the sub-terminal sarcolemma (endocytosis). Vacated dense-cored vesicles may then be re-cycled as coated vesicles in the nerve terminal. Both coated and smooth, "synaptic-type" vesicles (sv) may also form spontaneously at the axolemma in sensory nerve terminals.

The trophic influence may be released from the dense-cored coated vesicles by the lysosomal system.

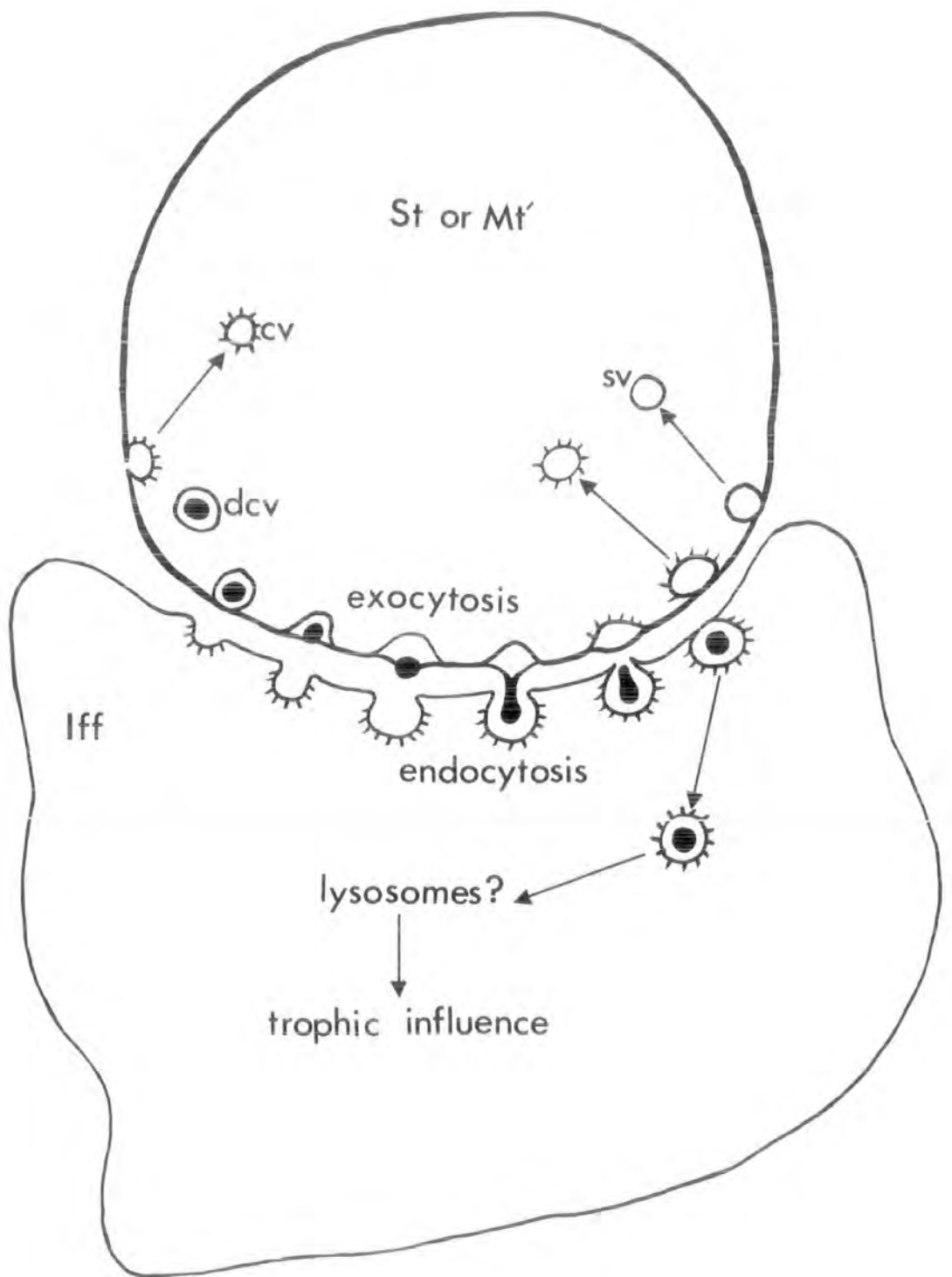


FIGURE 207. Hypothetical model depicting the role of the fusimotor innervation in the determination of the ultrastructural and histochemical variations between intrafusal muscle fibres during development.

Individual diagrams represent transverse sections through the equatorial, juxta-equatorial and polar regions of muscle spindles at selected developmental stages.

It is proposed that at the time of the arrival of the P1 innervation (19.5 DF), only F1 has developed sufficiently to receive the terminals. P2 terminals may innervate both F1 and F2, whereas trail terminals, arriving postnatally, are able to innervate all intrafusal muscle fibres.

Nuclei of the typical bag fibre (F1) are unshaded; in the intermediate bag fibre (F2) black; in the first nuclear-chain fibre (F3) cross-hatched and in the second (F4), stippled.



